On the Neural Mechanism of Flexible Bimanual Movement Control

柔軟な両腕運動制御を実現する計算論的神経機構

Atsushi Yokoi

横井 惇

Division of Physical and Health Education

Graduate School of Education

The University of Tokyo

Acknowledgements

I wish to thank the following people:

- Prof. Dr. Daichi Nozaki, my supervisor and scientific mentor, for providing me an opportunity to touch the spirit of science, and for his continuous support and great patience.
- Dr. Masaya Hirashima, another scientific mentor, for his great technical support and insightful comments regarding my research.
- Profs. Dr. Yoshiharu Yamamoto and Dr. Gentaro Taga for their continuous constructive criticism to improve my research.
- Profs. Dr. Tsukasa Sasaki, Dr. Takashi Eto, and Dr. Yoshiteru Muto for their continuous encouragement.
- Mmes. Megumi Annen, June Naito, and Kanae Abe for their administrative supports.
- Prof. Dr. Stephen Scott and Dr. Isaac Kurtzer at Queen's University and Dr. Andrew Pruszynski at Umeå Univeristy for insightful discussions.
- Dr. Tsuyoshi Ikegami at NiCT, my mentor in science and recreation; Prof. Dr. Atsushi Nakazawa at Hitotsubashi University; and Dr. Akifumi Kishi at New York University, for countless discussions over countless cups of coffee and beer.
- Prof. Dr. Zbigniew Struzik for his critical and encouraging comments.
- Dr. Hiroshi Kadota, Dr. Shoko Kasuga, Dr. Shinya Fujii, Ms. Misato Matamura, and Mr. Shuntaro Sasai for their support.
- Other members and staff of the Division of Physical Health Education (PHE).
- Profs. Dr. Shingo Oda and Dr. Motoki Kouzaki at Kyoto University for encouraging me to enter PHE.
- My family.

Without these people, this work would have been impossible.

Research in this thesis was supported by Japan Society for the Promotion of Science Research Fellowships for Young Scientists.

Original papers

I conducted the research in the present thesis under the supervision of Professor Dr. Daichi Nozaki. I played the major role in most of the research (experimental design, data collection, data analysis, and writing) except for the analytical calculation presented in Appendix 1.

The present thesis is based on three peer-reviewed papers and one peer-reviewed conference proceeding.

1. Yokoi A, Hirashima M, and Nozaki D. Gain-field encoding of the kinematics of both arms in the internal model enables flexible bimanual action. *Journal of Neuroscience*. 31: 17058-17068, 2011.
   (for: Chapter 3 and Appendix 1)

2. Yokoi A, Hirashima M, and Nozaki D. Flexible switching of multiple internal models during bimanual movement. *Sportology*. 1: 41-48, 2011.
   (for: Appendix 2)

3. 横井 惇、平島雅也、野崎大地. 「柔軟な両腕動作制御を可能にする脳内メカニズム」 *Japanese Journal of Biomechanics in Sports & Exercise*. 15(4): 144-154, 2012.
   (for: Chapter 3)

4. Yokoi A, Hirashima M, and Nozaki D. Uncovered hidden ability of nondominant arm for bimanual action. *Proceedings of The Annual Meeting Translational and Computational Motor Control*, 2012.
   (Peer-reviewed abstract: https://sites.google.com/site/acmcconference/)
   (for: Chapter 4)

Table of Contents

List of Figures

List of Tables

Chapter 1

General Introduction

1.1 Motivation: Descartes' other error

The question of how our movement is controlled is relevant to every person, particularly those who are involved in physical education, sports, and rehabilitation, including both trainers and trainees. How does the central nervous system (CNS) control and learn complex movements involving multiple body parts? The simple, but prevalent, approach to examining this question is to deconstruct movements into a set of elementary movements, such as those at the level of single joints or muscles, investigate each of them separately, and then reassemble them. This is known as *reductionism*[1]. The French philosopher René Descartes was one of the pioneers[2] that introduced reductionism to Western society. In his book "*Traité de l'homme*" (1664), he attempted to explain how our body movements are controlled. According to his theory, muscle contraction was the result of *spiritus animalis* (animal spirits), which transferred into the muscle through the nerve fibers originating from the cerebral ventricle (Fig. 1.1).

[1] Such a reductionistic approach is also common in sports training (Finch, 2004).

[2] Although the idea of reductionism itself has existed since the ancient Greeks (e.g., Dēmokritos), Descartes was the first to formally state the idea in his book *"Discours de la méthode"* (1637).

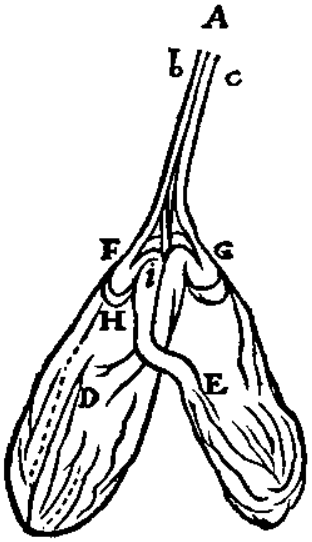

Figure 1.1. An illustration of the eye muscles from Descartes' own sketch.
According to Descartes, descending animal spirits from the cerebral ventricles enter through the nerve fibers (b-F and c-G) and inflate and contract the muscles (D and E). The spirits can also transfer through shunts (D-G, and E-F). If the descending flow of the spirits through b-F is stronger than the shunting flow through E-F, the contraction of muscle D leads to a leakage of animal spirits from muscle E into muscle D, which thus relaxes (or lengthens) muscle E, and vice versa. As a consequence, the eye moves in a certain direction. Adapted from Descartes (1664).

After proposing several explanations about the mechanism of simple muscle contraction (e.g., eye muscles), Descartes clearly stated[3] the following:

> *Now it is easy for you to apply what I have just said of nerve A and the two muscles D and E to all other muscles and nerves; and so to understand how the machine about which I am telling you can be moved in all the ways that our body can, solely by the force of the animal spirits which flow from the brain into the nerves* [in *Treatise of Man* (Descartes and Hall, 1972), p. 29].

[3] Although we can find a description about the mechanism of more complex movement involving multiple muscles and joints, such as the nociceptive reflex, later in his text, Descartes did not describe the detail of *how* the contraction of each muscle should be coordinated in order to generate functional movement (possibly because he did not understand the complexity of multijoint movement, which I will describe later in this thesis).

From this statement, we are able to grasp that he thought that the mechanism of simple muscle contraction was sufficient to understand all movements that we can perform. However, human movement is much more complex than what Descartes thought. For instance, as pointed out by Bernstein, our body is redundant and has many degrees of freedom; thus, there is no unique solution for specifying the configuration of the contraction level for each muscle (or each joint angle) given the position of a fingertip in space alone (Bernstein, 1967). In addition, the motion of a particular joint causes unexpected motion in other joints by interaction torques, which are not present for single-joint movements (e.g.,Hollerbach and Flash, 1982). Furthermore, there are many other problems the CNS must solve to control multijoint movements, such as how different coordinate systems (e.g., Cartesian space and joint or muscle space) are associated with each other and in which coordinate system the movement is planned. These problems become evident only when we consider the movements that require the coordination of multiple joints. Therefore, at least for the control of movements, Descartes clearly made a significant error.

Nearly 350 years after Descartes, we still do not have a unified understanding of how the CNS controls our movement (Wolpert et al., 2011). In the following sections, I summarize the progress of our understanding of the neural control of coordinated movement since Descartes, which progressed from the level of the single-joint (or muscle) to multijoint-limb movement.

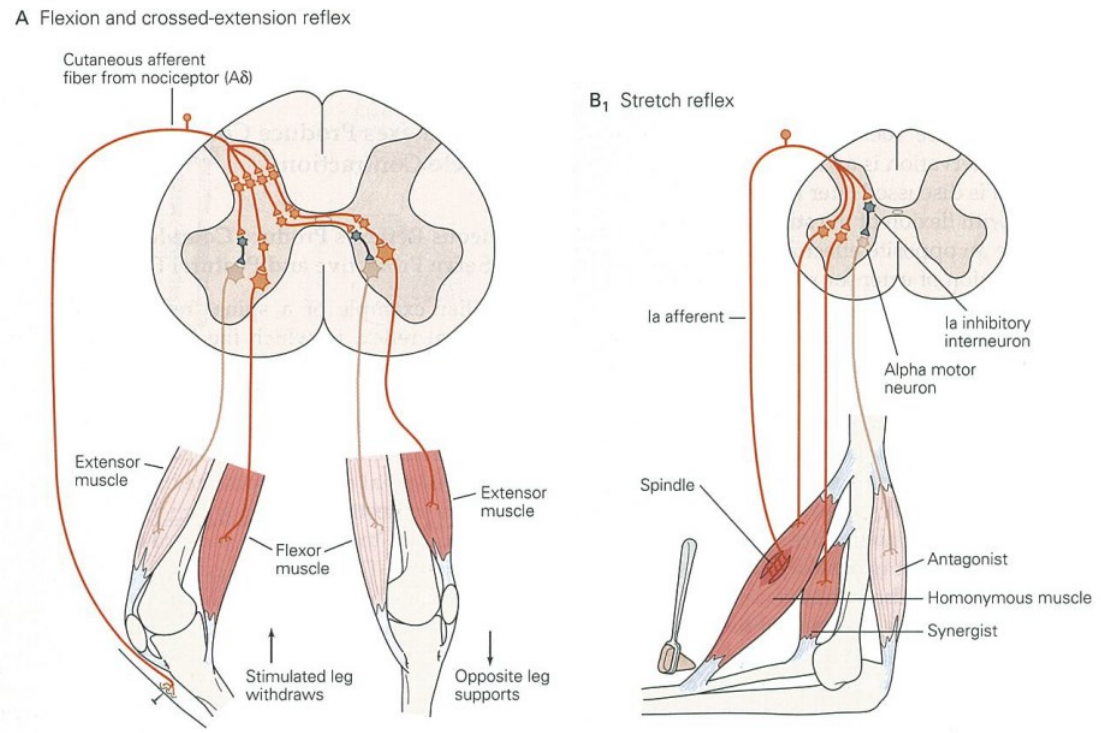

Figure 1.2. Spinal reflex circuit.

Left: Flexion and crossed-extension reflex. *Right*: Stretch reflex and reciprocal inhibition of the antagonist muscle. Inhibitory interneurons are illustrated in blue. Adapted from Kandel et al. (2000), p. 716.

More than 200 years after Descartes[4], Sir Charles Sherrington opened the door for studying the neural control of movement. With a series of electrophysiological recordings of the spinal circuit of decerebrated animals that included demonstration of the reciprocal inhibition of agonist and antagonist muscles around a single joint[5] (Sherrington, 1906), he and his disciples revealed how stereotypic movements, such as reflexes, are controlled entirely within the spinal cord (Sherrington, 1965; Eccles, 1982) (Fig. 1.2). Since Sherrington's study, numerous studies have focused on single joints or muscles in both humans and animals (Eldred et al., 1953; Rack and

[4] For a review of the history of reflex control from Descartes to Sherrington, see Clarac (2005a, b)
[5] Interestingly, the reciprocal innervation of agonist and antagonist muscles was what Descartes had conceptually conjectured in his book (Descartes, 1664).

Westbury, 1969; Marsden et al., 1971, 1972; Nichols and Houk, 1973; Rack and Westbury, 1974; Marsden et al., 1976; Houk, 1979).

Although there were some practical and rational reasons for previous studies to focus on the movement control of single joints or muscles, there were inevitable criticisms. Studying the control of single joints or muscles was essentially insufficient, as I described above, for addressing the various problems that only arise during the coordination of multijoint movements (Hogan et al., 1987). In addition, although some spinal reflexes, such as the scratch reflex, involve the sequential and well-coordinated contraction of multiple muscles that span more than one joint (Sherrington, 1906), it is unclear if similar mechanisms also underlie the control of voluntary movements that are much more complex and flexible than reflexes.

In contrast to the first step made by neurophysiologists, the next step in the study of the control of complex multijoint movements was mainly made by robotic engineers. Because of the emerging demand for machines with limb-like structures in the 1980s, engineers had to face problems that are inherent in learning to control systems with multiple interacting limb segments (Shadmehr and Wise, 2005). Because of the synergistic interactions[6] that occurred between neuroscientists and robotic engineers during the emergence of computational neuroscience (Marr, 1983), studies of how the CNS controls and learns coordinated multijoint movements led to great

[6] Another good example is the theory of feedback control in engineering and the concept of homeostasis described by Claude Bernard during the 19th century.

progress in the examination of the voluntary control of reaching movements of a single upper extremity as a model system (Shadmehr and Wise, 2005; Green and Kalaska, 2011).

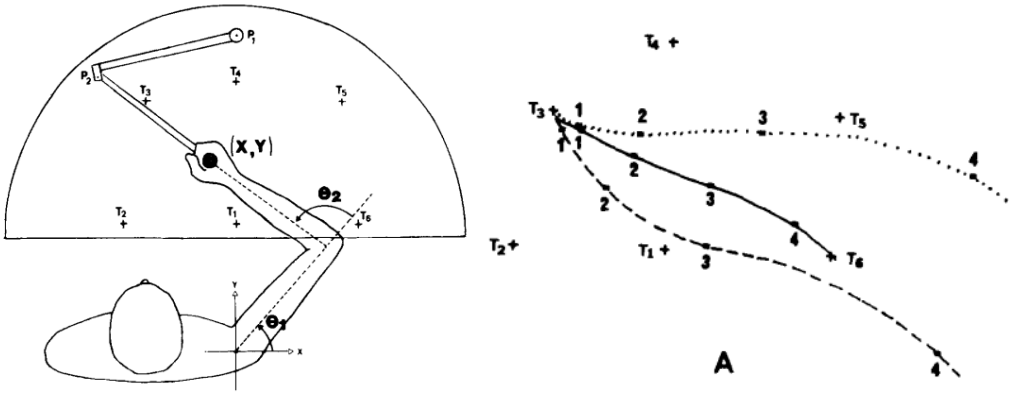

Figure 1.3. The significance of interaction torques.
Left: Experimental setup for the measurement of arm trajectories in a horizontal plane. T1 to T6: Targets for the reaching movement. *Right:* Simulated hand path from T3 to T6. Solid line: Measured trajectory. Dotted line: Simulated hand path after removing the contributions of all velocity terms. Dashed line: Simulated hand path after removing the contributions of all interaction terms. Adapted from Hollerbach and Flash (1982).

For instance, with both human psychophysical experiments and computational analyses, Hollerbach and Flash were the first to describe the significance of compensation of interaction torques during a two-joint reaching arm movement in a horizontal plane (Hollerbach and Flash, 1982) (Fig. 1.3). Subsequently, Bastian and colleagues analyzed the reaching movement of patients with cerebellar ataxia and concluded that the cerebellum plays a crucial role in predicting and compensating for interaction torques (Bastian et al., 1996)[7]. Importantly, the findings of a recent study suggested that elite athletes utilize interaction torques to achieve good performances

[7] Therefore, the clumsiness often seen in the movements of these patients is, at least partly, due to their inability to predict and compensate for interaction torques; thus, from this perspective, Descartes' hypothesis in which he naively extended the idea of single-muscle contraction to all other movements is completely wrong.

(Hirashima et al., 2008).

Besides these examples, there have been multiple lines of evidence on how the CNS controls and learns the reaching movement of a single arm from computational, neurophysiological, and psychophysical perspectives (Shadmehr and Wise, 2005). Among such studies, one influential idea of how the CNS controls movement is that the brain has flexible mapping between the desired movement and the motor commands sent to each muscle, and this is called the internal model (Atkeson, 1989; Kawato and Wolpert, 1998; Wolpert et al., 2011). This concept of an internal model of input-output mapping naturally includes the above discussion of interaction torques; the problem of noisy and delayed sensory feedback, which is inevitable in the biological control of movement; and, furthermore, adaptability to changes in the environment and/or physical properties of our bodies due to various reasons, such as fatigue, aging, or tool use (Franklin and Wolpert, 2011).

One of the most dramatic outcomes of the recent progress in motor control research is the application of neuroprosthetics, which are called brain–computer interfaces or brain–machine interfaces, in humans (Collinger et al., 2012; Hochberg et al., 2012) (Fig. 1.4). By recording and decoding neural activities from certain regions of paralyzed patients' brains, these systems enable them to control a robotic arm in order to move objects, feed themselves, and communicate with the outside world (Green and Kalaska, 2011). Such technique is accomplished by the understanding where in the brain specific information for arm movement control, such as the desired movement

direction, is represented, and by the accumulation of knowledge in controlling the robotic arm to reproduce the intended movement in consideration of the various problems inherent to controlling the multijoint arm.

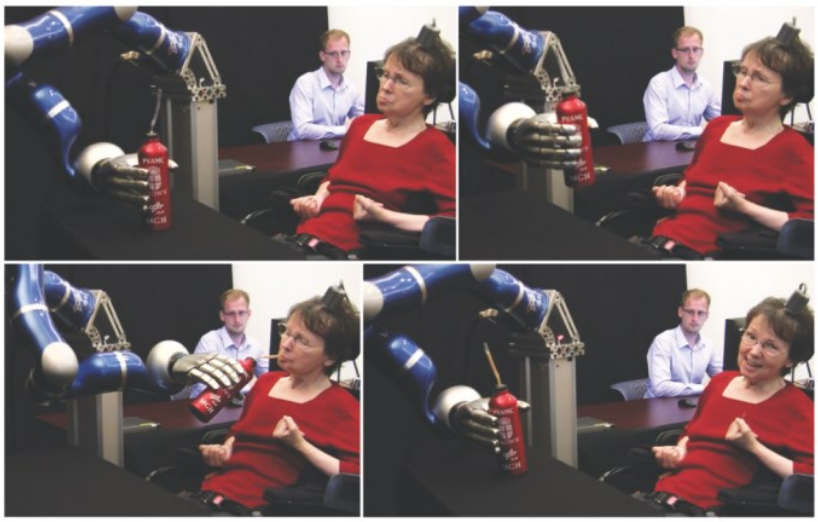

Figure 1.4. Application of the brain–computer interface for a tetraplegic patient.
The first successful trial of a participant trying to use a robotic arm to reach and grasp a bottle, bring it toward her mouth, drink from it, and place the bottle back on the table. Adapted from Hochberg et al. (2012).

However, even with our current understanding of motor control, the same criticism of the studies of single-joint motion from the standpoint of multijoint movement can be applied. There are many more actions that require the coordination of more than one limb under normal conditions[8], and it is unclear if findings that have been acquired through research on the movement of a single arm can be extended to the coordinated movements of entire body parts.

In this thesis, I focused on the coordination between *two arms* (i.e., bimanual coordination)

[8] In Hochberg et al. (2012), a woman with tetraplegia controlled a robotic arm to reach and grasp a bottle and then moved it to her mouth to drink from a straw. However, the ability to unscrew the cap of the bottle with two neuroprosthetic arms remains impossible.

and sought to elucidate how the brain coordinates them. Reducing the problem of coordinated movements in general to the coordination of two arms addresses many important aspects that can be overlooked in single-limb movement studies. Rather, it serves as a good starting point for dealing with coordination in general. As will be described in the following sections, elucidating the problem of bimanual motor control can contribute to the basic theory of motor control, which strongly motivated us to study it. In the next section, I specify the problems to be addressed in the present thesis.

1.2 Specification of the problem

Temporarily and spatially coordinating the motion of two arms is an essential ability in our daily life, and it confers a number of abilities, such as playing musical instruments, opening a bottle of wine, or tool making. To successfully achieve these bimanual actions, a number of hierarchically organized problems need to be solved. First is the problem of *task partitioning*. Given a global task goal, such as playing a C major scale on a violin, the goal should be broken down into specific subtasks for both arms, such as moving a bow and holding down the specific location of a string. The second problem is *role assignment*. Each subtask should be appropriately assigned to each arm according to both internal and external constraints, such as the different abilities of the two arms (e.g., handedness), and the behavioral context. The final problem is the *control of specific arm movements*.

In this problem, each arm should simultaneously achieve each subtask, i.e., two unimanual movements that are performed together. Among these three classes of problems, I will address the last two problems of *role assignment* and the *control of individual arm movements*.

1.2.1 Control of individual arm movements

First, I start with the lowest level of the problem. The primary question is whether we can simply extend the knowledge of the control of single-arm movements to this problem. As expected, the answer is no. In the following section, I describe several reasons for this.

In this stage, each arm should be controlled by taking into account the motion of the opposite arm. Because both arms are physically linked through handheld objects and/or the body, each arm motion can be a perturbation of each other. This means that the same motion of one arm can be exposed to a potentially infinite number of mechanical perturbations that arise from the motion of the opposite arm. How does the motor system solve this problem? Interestingly, this problem poses an important challenge to the recent framework of motor control.

As described in the previous section, earlier works on single-arm reaching movements have suggested that the brain constructs a sensorimotor map between the desired motion and the motor command, called the internal model (Kawato and Wolpert, 1998; Bhushan and Shadmehr, 1999). In addition, it has been suggested that the internal model consists of neural elements that

receive information about the desired motion of the relevant arm and transform it into a motor command (Poggio and Bizzi, 2004). The largest and most implicit assumption is that these neural elements only receive information about the desired motion of the relevant arm. However, during bimanual movements, such as the opening of a jar, interdependence exists between the two arms because they are mechanically coupled through the object and/or body. This fact indicates that the desired motor command that each controller needs to send to each arm is dependent not only on the desired motion of the controlled arm, but also on the desired motion of the other arm. Thus, the mapping of the internal model must mimic that between the desired movement of *both* arms and the motor command to an arm. This raises a serious problem: as long as we assume that the neural elements of the internal model only receive information about the desired movement of one arm, such mapping cannot be constructed. One solution is to assume that the internal model (or elements of it) for one-arm movement receives signals about the desired movements of both arms. However, almost no one has ever addressed this question.

1.2.2 Role assignment for bimanual movements

Once the global goal of a bimanual action is broken down into subtasks, the motor system needs to assign appropriate tasks to each arm, taking into account both external and internal constraints. Generally, we have a strong preference to use one arm over the other arm, and this is called handedness. This is also true, as we know very well, for bimanual movements; the dominant arm

often takes the leading role in a variety of tasks, such as pouring water from a bottle into a glass, whereas the nondominant arm takes a supportive role in those tasks, such as stabilizing the glass. However, depending on the situation, this role assignment may flip. For instance, most of us will hold the bottle with the nondominant hand and the cap with the dominant hand in order to remove it. Then, the subsequent motion will be pouring the bottle of water with the nondominant hand and holding the glass with the dominant hand. Thus, it seems that the two constraints are both taken into account when assigning a specific action to each arm.

The above examples are quite familiar to us. Indeed, many studies have shown that the dominant hand has superior ability over the nondominant hand, e.g., studies of movement accuracy (Woodworth, 1899). Nevertheless, many questions remain unanswered with regard to how the two arms are coordinated. The specific questions/problems are as follows. First, despite observations of hand dominance, we still lack a quantitative and mechanistic understanding of how these differences arise. In addition, whether the abilities of the dominant arm hold during bimanual movements is unclear because these observations were made in unimanual tasks (Annett, 1985; Goble and Brown, 2008). Second, besides the above problems, we lack systematic knowledge of what constitutes the internal and external constraints that have enough power to affect the role-assignment process. Third, how these two constraints are considered in the motor system is still largely unknown. These problems are closely related to the problem of credit assignment or the division of labor in a

redundant and large degree-of-freedom system and, thus, coordinated movement in general (Berniker and Kording, 2008; White and Diedrichsen, 2010).

Taken together, as was stated in the previous section, an understanding of bimanual motor control would make a large contribution to the field of motor control. The studies described here sought to elucidate how the brain solves these problems.

1.3 Overview of studies

In this thesis, I investigate how the brain coordinates two arms. I experimentally examined the ability of each arm to control its movement interacting with the external environment in a variety of situations, such as when an external force is applied to the hands in a bimanual movement context. For this specific aim, I employed a robotic-based virtual-reality system. In this system, a human subject holds the handle of a robotic device called a manipulandum in each hand. Both position encoders and torque motors are implemented in the manipulanda, allowing us to both measure the state of the handle (e.g., position, velocity, force) and feedback the state to the subjects (e.g., applying force to the handle).

The question of how each arm achieves a specific task, taking the motion of the other arm into account, will be addressed in the first study (Chapter 3). I designed a series of experiments to reveal how the movements of both arms are jointly represented in the control process of each arm.

The two major findings of this study are as follows. (1) Information on the motion of both arms is multiplicatively represented in the control process of each arm. (2) Thanks to the multiplicative integration of motion information, human subjects were able to learn complex dynamics that nonlinearly depended on the movements of both arms. The results of this first study provide a convincing example of the motor system's ability to integrate motion of different body parts in a mathematically plausible manner and contribute to an understanding of the process at the lowest level of bimanual movement control (*control of individual arm movements*), which was defined previously.

In the second study (Chapter 4), I address part of the question of the stage of *role assignment*, which was raised previously. A series of experiments was designed to uncover the lateralized ability of the two arms in a bimanual movement context and its possible mechanisms. The two major findings of this second study are as follows: (1) the control process for the nondominant arm encodes movement of the dominant arm in greater accuracy than vice versa and (2) this difference in the encoding of the opposite arm motion in the control process resulted in a greater ability of the nondominant arm to predict the effect of the other arm's motion in bimanual movements. The results of this study demolish the conventional notion of the absolute superiority of the dominant arm and provide a concrete example of the internal constraint of the process of *role assignment* in bimanual movement control with a convincing mechanistic explanation.

What follows in the next chapter (Chapter 2) is a brief summary of earlier studies on the computational approach of motor control and learning that provide a foundation for the present thesis and a short review of earlier studies on bimanual coordination.

Chapter 2

Summary of Earlier Findings

2.1 Introduction

Suppose that you are playing a video game like Street Fighter©. Typically in these kinds of video games, a character's actions (e.g., jumping, kicking, or punching) are controlled by pressing small number of buttons on a controller (e.g., ↑, A, or B buttons) or some combination of them (e.g., →↓↘ + B button). Therefore, it is not surprising that these actions lack flexibility. If you want to more precisely control the character's action, perhaps the most straightforward (and somewhat extreme) way is to independently associate each button with the movement of each joint (or muscle contraction). However, if that is the case, you would be stunned by the more than 300 (or 600) keys on your controller[9] because the human body has ~350 joints (or ~640 muscles)! What makes matters much more complicated is the redundancy in our body. Thus, there is no unique solution to determine, for instance, the position of a fingertip in space. In addition, because the dynamics of a multijoint system are coupled, the motion of a particular joint causes unexpected motion in other joints depending on posture by an interaction torque (Hollerbach and Flash, 1982; Atkeson, 1989). Furthermore, what if there was noise and a delay between a button press and a joint motion (or

[9] A standard computer keyboard has ~100 keys.

muscle contraction)?

In the preceding example of the controller, though the resultant actions are somehow inflexible, the idea itself is not so bad; assuming a small number of elements that send appropriate commands to specific groups of muscles can largely reduce the redundancy in our body and release us from the complex task of controlling each muscle separately. Indeed, it has been revealed that relatively primitive animals, such as frogs, use this strategy (Bizzi et al., 2008). In addition, a recent study suggested that the same strategy is used for relatively automatic movements, such as locomotion, across a variety of species, including humans (Dominici et al., 2011). Therefore, considering that the nervous system is a product of an evolutionary process, our nervous system might take a similar approach for voluntary movement, but, probably does so in a much more sophisticated fashion to achieve greater flexibility.

In this chapter, I review studies on the computational approach in order to understand how the CNS controls voluntary movement. The specific aim of this chapter is to summarize the findings of previous studies on bimanual coordination in light of both the computational approach and specific problems in bimanual movements, which I proposed in the previous chapter. First, I briefly introduce Marr's three levels of computational neuroscience (Marr, 1983) and review several general topics of motor control, such as the concept of the internal model and motor primitives, each of which lies within a separate level of Marr's three levels. Then, I summarize the findings of earlier

studies on bimanual movements from the perspective of the above concepts. Finally, I discuss several unsolved issues for which the studies on bimanual movement presented in this thesis can account.

2.2 Computational approach of motor control and learning

In his memorial book "*Vision*," David Marr (1982) broke down the computational approaches in neuroscience into the three following separate levels of problems: *computational theory*, *representation and algorithm*, and *hardware implementation*. The information processing problems that the brain needs to solve to achieve some specific task, how to solve the problems, and the physical mechanisms that are used to execute algorithms in the brain are described for each level. Marr proposed that although these three levels are loosely coupled with each other, they are relatively independent and can therefore be investigated separately. The aim of computational neuroscience is to understand how the CNS works in all of these levels. In this section, I will briefly summarize the issues of the internal model and motor primitive.

2.2.1 Internal model for predictive motor control

2.2.1.1 Internal model: General description

The concept of the internal model belongs at the level of computational theory. For industrial machines that have much faster and less noisy sensory feedback, pure feedback control, such as

proportional–integral–derivative (PID) control, results in good performance without precise knowledge about the property of the controlled object, even if it is nonlinear (Bennett, 1993). In contrast, when faced with the fundamental problems of biological motor control, such as large noise levels and delays in sensory feedback signals, complex coordinate transformation, and highly nonlinear properties of our body, the brain needs an appropriate model of the physical properties of one's own body and the external environment, and this is called the internal model (Atkeson, 1989; Kawato and Wolpert, 1998; Franklin and Wolpert, 2011) in the context of both *feedforward* and *feedback* control.

Feedforward control, in which the controller programs in advance a set of appropriate feedforward commands for the controlled object in order to achieve a desired outcome, is crucial, especially for rapid movements, such as a golf swing or throwing a baseball, because most of the movement is finished when sensory feedback signals become available. In such cases, an internal model is required to transform desired motion states into appropriate motor commands that can accomplish the desired motion states. Such a class of the internal model is called an *inverse (dynamic) model* (Kawato and Wolpert, 1998; Wolpert and Kawato, 1998). Feedback control, in which feedback sensory signals or differences between the desired and feedback sensory signals are transformed into control commands to the controlled object by the controller, is also essential for our movement. It is obvious that animals cannot deal with sudden unexpected disturbances, such as

encountering obstacles, by only using feedforward control. In addition, as described above, delays in feedback signals make the system with feedback control unstable (Hogan et al., 1987). To cope with this problem, it has been proposed that the brain may use the internal feedback that is generated through a *forward model*, which is similar to the Smith predictor in the engineering field (Miall et al., 1993; Wolpert et al., 1998). The forward model transforms motor commands into predicted sensory states.

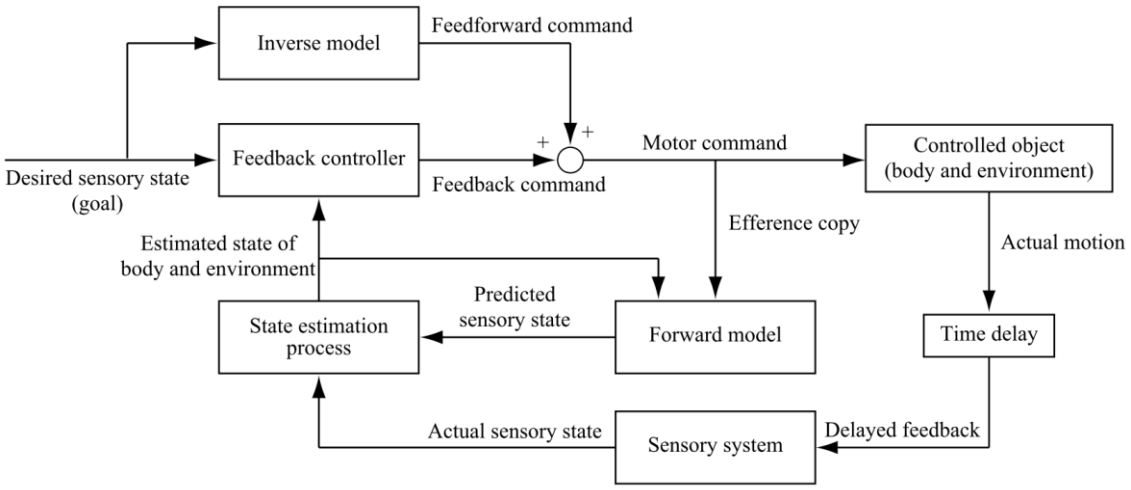

Figure 2.1. Block diagram of motor control.
Current scheme of motor control. Modified from Shadmehr and Krakauer (2008).

In summary, the inverse model, which is a crucial process for feedforward control, transforms the desired sensory states (i.e., result) into motor commands (i.e., cause), and the forward model, which is a crucial process for feedback control, transforms motor commands (i.e., cause) into predicted sensory states (i.e., result). Thus, in a broad sense, these internal models are regarded as *mapping between the desired/predicted sensory state and the motor command*. Another point to note

is that, although the two control schemes (i.e., feedforward and feedback control) have often been studied separately, both contribute to real movements in general (Fig. 2.1).

2.2.1.2 Adaptability of internal models: Behavioral aspect

Another important property required for the internal model is *adaptability*. The physical properties of our body are not static; rather, they change in various time scales. On shorter time scales, for instance, muscle fatigue changes input-output properties, and the use of tools or the holding of objects changes limb dynamics, whereas, On longer time scales, the size and mass of our body dramatically change as we grow from a small child to an adult.

The question of how the CNS constructs a new internal model or modifies the existing one has been studied behaviorally with reaching and pointing movements in various altered environments, such as those involving Coriolis forces (Lackner and Dizio, 1994), viscosity fields (Shadmehr and Mussa-Ivaldi, 1994), or prism glasses (Kitazawa et al., 1995) (for a comprehensive review of this topic, see Shadmehr & Wise, 2005). These studies have often used virtual-reality environments that use robotic devices. In this kind of system, a human subject holds the handle of a robotic arm called a manipulandum that incorporates a position encoder and torque motor, thus allowing experimenters to measure the state of the handle (e.g., position, velocity, and force), and to provide feedback regarding the state to the subjects (e.g., applying force to the handle and presenting visual cursors that represent the position of the handle) (Fig. 2.2).

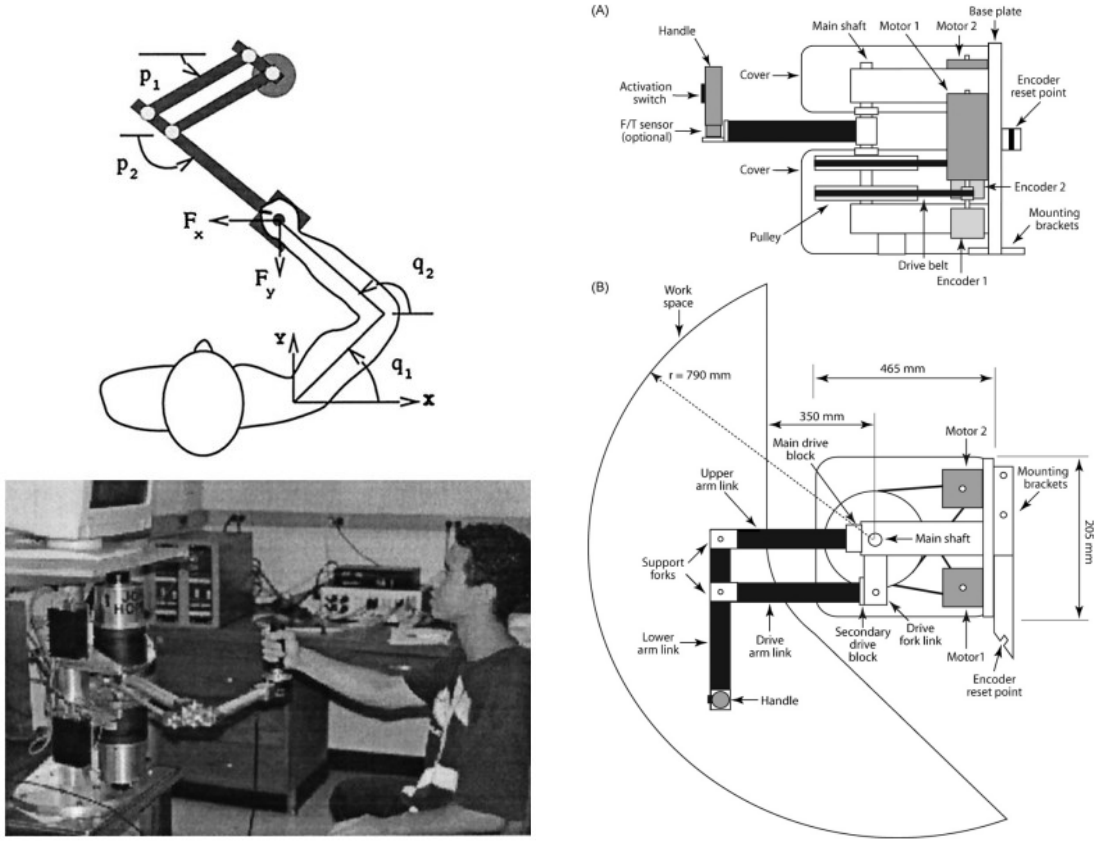

Figure 2.2. Robotic manipulandum for motor research.

Left: Schematic diagram (upper panel) and a picture (lower panel) of a human two-dimensional reaching experiment and the robotic manipulandum used by Shadmehr and Mussa-Ivaldi (1994). *Right*: Anatomy of a similar manipulandum that was developed by Howard et al. Upper: Side view. Lower: Top view. Adapted from Shadmehr and Brashers-Krug (1997) and Howard et al. (2009).

In their pioneering work with this kind of reaching paradigm, Shadmehr and Mussa-Ivaldi (1994) investigated how the internal model for arm reaching adapted to a novel force field that was applied through the handle and how subjects acquired the model of the robotic tool (Fig. 2.3). They instructed the subjects to move a visual cursor from a center position to eight peripheral targets. During the reaching movement, the robot generated a viscous force (i.e., the magnitude of the force was proportional to the velocity of the handle), the direction of which was perpendicular to the motion of the right handle. Before the force field was applied (baseline period), the reach trajectory

was almost straight. At the onset of the force field trials, subjects showed substantial lateral deviations in the reach trajectories because of perturbations that were applied through the handle. However, after a sufficient training period, the reach trajectory became relatively straight, suggesting that the subjects predictively compensated for the force. This was confirmed by *catch trials*, in which the perturbation force was unexpectedly turned off. If the subjects used another more effortful strategy, that is, co-contraction of muscles around the joints, the resultant trajectory showed no difference from that of the baseline period. However, the resultant trajectory was the mirror image of the perturbed one, suggesting modification of the feedforward motor command.

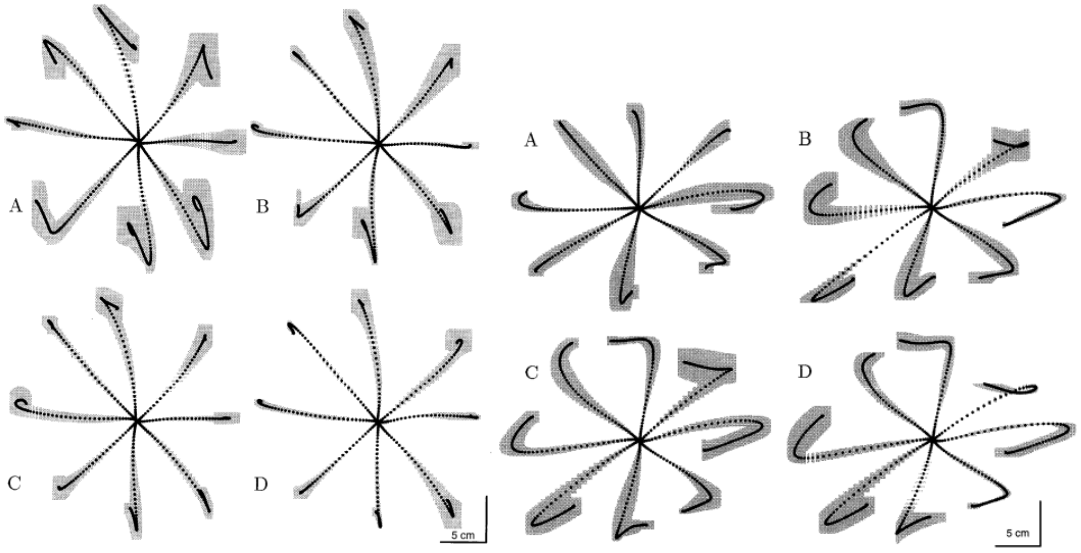

Figure 2.3. Adaptation to novel force fields during reaching movements.
Left: Hand trajectories during force field trials. As training progressed (A to D), the curved trajectories returned to relatively straight ones, like those seen in null field trials. *Right*: Trajectories during catch trials. As training progressed (A to D), the subjects showed curved trajectories that were mirror images of the ones in early training (A in the left panels), suggesting modified feedforward commands to the arm. Adapted from Shadmehr and Mussa-Ivaldi (1994).

Thus, with a relatively short training period, subjects acquired an internal model of the force field (i.e., internal model of the robotic arm) or adapted the existing model to the novel environment. A large number of studies have followed this paradigm to study how humans adapt their internal model to novel environments or construct a new one (Cothros et al., 2006) in various time scales (Smith et al., 2006) and how these memories consolidate across longer time periods (Brashers-Krug et al., 1996; Criscimagna-Hemminger and Shadmehr, 2008). A recent study by Izawa et al. (2011, 2012) demonstrated that both inverse and forward internal models change after adaptation to novel kinematic transformation (Izawa et al., 2012a; Izawa et al., 2012b). The results of these behavioral studies strongly suggest the existence of internal models in the brain and their modification through experience. Then, how are these processes implemented in the brain?

2.2.1.3 Adaptability of internal models: Neural correlates

Several studies have addressed the above question of where internal models are in the brain and how they are modified. Emillio Bizzi and his colleagues were the first to combine the above motor learning paradigm and electrophysiological recording in behaving monkeys to study how neural activation patterns around frontal motor areas change following the adaptation to novel dynamical environments. Through recording from various cortical areas, such as the primary motor (Gandolfo et al., 2000; Li et al., 2001), pre-motor (Xiao et al., 2006), supplementary motor (Padoa-Schioppa et al., 2002; Padoa-Schioppa et al., 2004), and cingulate motor cortices (Richardson et al., 2008), they

found that the population of neurons in these areas show altered activation patterns during both adaptation to the force field and re-adaptation to the original condition (called *washout*), and that there are several types of neurons whose activation patterns change in different phases of adaptation. For example, some group of neurons changed their activity only during the adaptation phase and did not return to the original activation pattern after the washout session, and other groups of neurons exhibited the opposite tendency: the activation pattern only changed during the washout session. These results suggest that the internal model of dynamics control is represented around these cortical areas.

Another line of studies has investigated the role of the cerebellum in motor control and learning. Computationally, the cerebellum was proposed to be an adaptive network, like a perceptron (for review, see Ito, 1989), and this structure was largely thought to contribute to motor control and learning (Wolpert et al., 1998). Several studies have demonstrated that the cerebellum is essential to the modification of simple reflexes and classical conditioning, like the vestibulo-ocular reflex (for review, see Kawato and Gomi, 1992) and eyelid response conditioning (e.g., Kitazawa, 2002). For voluntary movement control, Imamizu et al. demonstrated that the formation of a newly acquired internal model of a tool in the cerebellum (Imamizu et al., 2000). They recorded brain activity by functional magnetic resonance imaging (fMRI) while human subjects learned how to use an experimentally modified computer mouse; the mapping between the motion of the mouse and the

cursor was rotated by certain amount (e.g., 45º). It has also been reported that subjects with cerebellar ataxia show deficits in adapting to novel dynamics and kinematics depending on ataxia severity (Criscimagna-Hemminger et al., 2010; Izawa et al., 2012a), which supports the above notion.

In summary, both frontal motor areas and the cerebellum contribute to the process of motor adaptation. Then, one may be curious about which part of the brain is the neural correlate of the internal model. A recent hypothesis proposed that the internal model and its adaptation process are implemented within the network structure, including both of them (i.e., frontal motor areas and the cerebellum) and many other structures, such as the basal ganglia (Shadmehr and Krakauer, 2008).

2.2.2 Motor primitives: Building blocks for complex movement

The concept of the motor primitive lies between the levels of algorithm and implementation. As described in the previous section, the concept of an internal model specifies the computation(s) that the brain needs to make in order to control voluntary movement, namely, to flexibly construct certain mapping between the desired/predicted sensory state and the motor command. This concept of the motor primitive is one of the candidates for the implementation of an internal model. Because of the complexity and nonlinearity of the dynamics of our body, this map should be highly nonlinear. For

instance, the equation of motion for a two-dimensional arm movement with two degrees of freedom (Fig. 2.4) can be described as follows:

$$\tau_1 = \left(I_1 + I_2 + m_2 l_1 l_2 \cos(q_2) + \frac{m_1 l_1^2 + m_2 l_2^2}{4} + m_2 l_1^2\right)\ddot{q}_1 + \left(l_2 + \frac{m_2 l_1 l_2}{2}\cos(q_2) + \frac{m_2 l_2^2}{4}\right)\ddot{q}_2 - \frac{m_2 l_1 l_2}{2}\sin(q_2)\,\dot{q}_2^2 - m_2 l_1 l_2 \sin(q_2)\,\dot{q}_1\dot{q}_2$$

$$\tau_2 = \left(I_2 + \frac{m_2 l_1 l_2}{2}\cos(q_2) + \frac{m_2 l_2^2}{4}\right)\ddot{q}_1 + \left(I_2 + \frac{m_2 l_2^2}{4}\right)\ddot{q}_2 - \frac{m_2 l_1 l_2}{2}\sin(q_2)\,\dot{q}^2 \quad (2\text{-}1),$$

where τ_1 and τ_2 are the joint torques, q_1 and q_2 are joint angles at the shoulder and elbow, respectively, I_1 and I_2 are inertial moments, m_1 and m_2 are masses, l_1 and l_2 are the lengths of the upper and lower arm segments, respectively, and the dots represent time derivatives. The compact expression of these complicated equations is the following:

$$\boldsymbol{\tau}(t) = D\big(\boldsymbol{q}_d(t), \dot{\boldsymbol{q}}_d(t), \ddot{\boldsymbol{q}}_d(t)\big) \quad (2\text{-}2),$$

where $\boldsymbol{q}_d, \dot{\boldsymbol{q}}_d,$ and $\ddot{\boldsymbol{q}}_d$ are vectors of the desired (or predicted) trajectories of the joint angle, angular velocity, and angular acceleration, respectively. Thus, if we want to move this two-link arm along these desired trajectories, the brain needs to construct this complex, nonlinear mapping. How is this achieved?

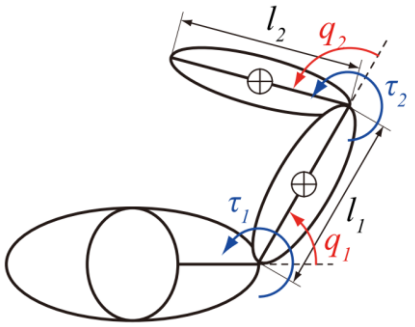

Figure 2.4. Schematic for planer arm reaching.
The system has two degrees of freedom (shoulder and elbow). l_1 and l_2: segment lengths for the upper and lower arms. (q_1, τ_1) and (q_2, τ_2): joint angle and torque at the shoulder and elbow. Circle with a plus sign: position of the center of mass of each segment. Each center of mass is assumed to be located at the center of each segment.

Computationally, the problem of learning (constructing) a map between inputs and outputs can be regarded as a function approximation (Poggio and Girosi, 1990). In this view, the original function $f(\boldsymbol{X})$ is approximated by the approximating function $F(\boldsymbol{W}, \boldsymbol{X})$, where $\boldsymbol{X}$ is an input vector and $\boldsymbol{W}$ is a parameter vector that is estimated (learned) through certain learning algorithms. One classical approximation scheme is the basic function approach, such as the following:

$$F(\boldsymbol{W}, \boldsymbol{X}) = \sum_i^m W_i \Phi_i(\boldsymbol{X}) \quad \text{(2-3)},$$

where $\{\Phi_i\}_{i=1}^m$ is some suitable basic function. Importantly, these classical basic function approaches are closely related to multilayer neural networks (Poggio and Girosi, 1990) and, thus, have some biological plausibility when we think of how these function approximations are implemented in the nervous system. Indeed, in visual systems, there have been numerous examples of neurons that meet the criteria for such basic functions, a certain combination of which can reconstruct the retinal image (Olshausen and Field, 1996). Then, what about motor systems?

2.2.2.1 Motor primitives in the spinal cord

Almost 100 years after Sherrington, a line of electrophysiological studies of the spinal cords of frogs and rats that was conducted by Bizzi and colleagues demonstrated that there are some modules in the spinal cord, the linear combination of which can generate purposeful multijoint leg movements (Fig. 2.5). They have shown that microstimulation of interneuronal circuitry in the lumbar spinal cord of frogs and rats elicits some organized pattern of activity of multiple muscles (Giszter et al., 1993; Mussa-Ivaldi et al., 1994). They have further shown that a linear combination of activity patterns, each of which was separately obtained stimulating a single location of the spinal cord, was quite similar to that obtained by co-stimulating two sites (Mussa-Ivaldi et al., 1994).

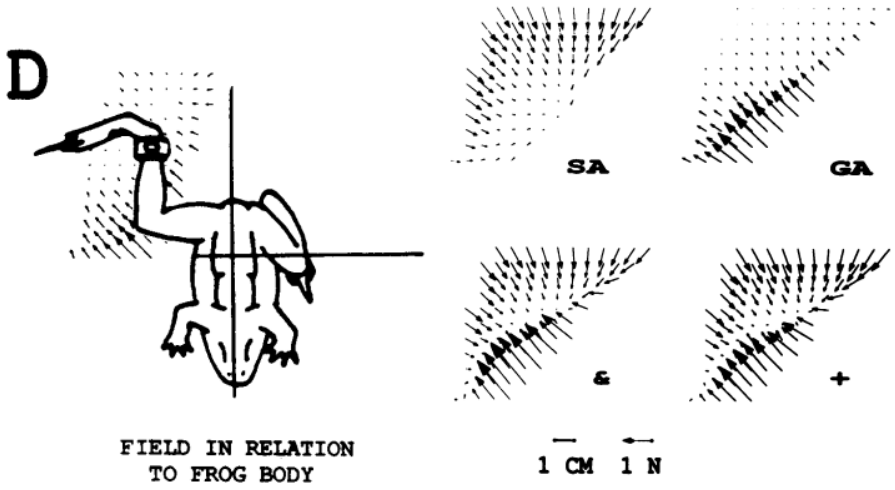

Figure 2.5. Motor primitives in frog spinal cord.
Left: Experimental setup for the measurement of isometric forces in the lower leg of frogs. A force transducer was mounted on the ankle, and endpoint forces were measured in various different postures (indicated as arrows). *Right*: The costimulation of two different sites (indicated as &) evoked quite similar patterns of endpoint forces with linear summation (indicated as +) of the force fields that were evoked following the stimulation of single sites (indicated as SA or GA). Adapted from Giszter et al. (1993) and Mussa-Ivaldi et al. (1994).

Thus, through the linear combination of these spinal primitives, the equation of motion for mapping can be approximated as the following:

$$D\left(\boldsymbol{q}_d(t), \dot{\boldsymbol{q}}_d(t), \ddot{\boldsymbol{q}}_d(t)\right) \approx \sum_{i=1}^{K} c_i \Phi_i \quad (2\text{-}4),$$

where c_i represents a descending supraspinal command and Φ_i is a *primitive* that is a nonlinear function of Eq. (2-3). With this scheme, Bizzi and colleagues were able to reproduce several kinematic features of experimentally observed human upper-limb movements (Mussa-Ivaldi and Bizzi, 2000). In addition, they have found that muscle activity patterns during naturalistic leg movements of behaving frogs and rats, such as swimming and jumping, can be linearly decomposed into a small number of basic patterns (i.e., muscle synergies) that are shared within various other movements (Tresch et al., 1999). Interestingly, the muscle activation patterns evoked by spinal cord microstimulation were qualitatively similar to these decomposed patterns, suggesting that what they found in the spinal cords of frogs and rats was actually a part of the computational building blocks that generate various types of motor actions in behaving animals in the natural environment (for review, see Bizzi et al., 2008). While it seems feasible that these motor primitives within the spinal cord are one of the crucial components of the internal model, there remain several unsolved questions. First, how the nervous system derives the appropriate descending commands to each spinal primitive (i.e., c_i) from a desired movement, which should definitely be generated in higher centers, such as the cerebral cortex, or at least higher than the spinal cord, is unknown. Second, how

these primitives are organized across multiple limbs to generate coordinated motion, in other words, how the activity of primitives that belong to the muscle activation patterns for one limb are adjusted according to the sensory state of other limbs, is unknown.

2.2.2.2 Motor primitives in higher centers

Similar to the spinal primitives, there have been many observations that neurons in motor-related areas in the cerebral cortex show certain patterns of activity during arm movement (Georgopoulos et al., 1982; Kalaska et al., 1989; Cisek et al., 2003; Cisek and Kalaska, 2005). For instance, Georgopoulos et al. (1982) used single-cell recordings of the primary motor cortex of behaving monkeys and identified a group of neurons that exhibited a characteristic firing pattern (Fig. 2.6).

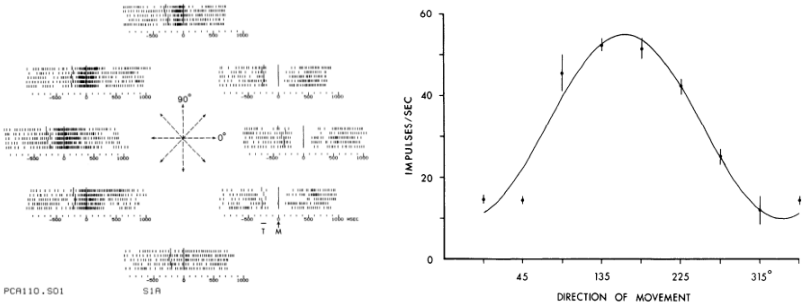

Figure 2.6. Neuronal activity in the primary motor cortex of monkeys during planar reaching movements.

Left: Raster plots from an example neuron of the primary motor cortex as a monkey reached in different directions. *Right*: Average discharge rate of the same neuron plotted against the reach direction. The neuron showed clear cosine tuning (the preferred direction was calculated as 161º). Adapted from Georgopoulos et al. (1982).

The firing frequencies of these neurons were well characterized by unimodal functions, such as the following cosine function:

$$r_i(\theta) = A\cos(\theta - \phi_i) + B \quad (2\text{-}5),$$

where θ is the direction of the reaching movement by the monkey; r_i is the average firing frequency of a cell; ϕ_i is the direction of the reaching movement in which the cell mostly discharged, which is called the *preferred direction* (PD) and which was different for each neuron around 0–360º; A and B are constants; and i is the cell number. They found that the direction a monkey is trying to reach can be reconstructed with the population activity of these neurons with the following equation:

$$\hat{\theta} = \sum_i^N \boldsymbol{w}_i r_i(\theta) \quad (2\text{-}6),$$

where $\hat{\theta}$ and θ are the estimated and original directions of the reaching movement, respectively, and $\boldsymbol{w}_i$ is the unit vector corresponding to the PD of each neuron (Georgopoulos et al., 1986). They concluded that these neurons code the desired kinematics (e.g., movement directions) in a population, and this is called *population coding* (for a review, see (Pouget et al., 2000)). An important point is that cosine and other unimodal functions (e.g., Gaussian functions) can serve as basic functions to approximate nonlinear mapping. Thus, another possible interpretation is that neurons in the primary motor cortex and other areas that show basic function-like activities may serve as nodes to transform the information of desired movements into certain signals in order to organize spinal motor

primitives. In this sense, these neurons can be called cortical (or higher) motor primitives. Recently, Cheung et al. (2009) found that the muscle activation patterns that were decomposed from the arm movements (i.e., muscle synergies) of both the unaffected and affected sides of stroke survivors and found that they were highly similar to each other despite large differences in motor performances between the arms and the various lesion sizes and locations across patients (Cheung et al., 2009b).

Another issue is how the activities of these neurons actually relate to motor behavior. A quite straightforward approach to this question is to stimulate these neurons and see what happens. Typically, a short-duration (30 msec) intracortical microstimulation (ICMS) that consists of 10 pulses at a frequency of 330 Hz evokes brief joint movement or muscle twitches, and this has been used extensively to map the somatotopic representations of the motor cortex (Asanuma and Rosén, 1972; Burish et al., 2008). Using a longer duration of ICMS (500–1000 msec), Graziano and colleagues have reported interesting observations of monkey arm movements that were analogous to the example of spinal motor primitives by Bizzi et al. They observed that stimulations evoked robust arm movements toward specific end positions regardless of the initial arm posture (Graziano et al., 2002; Graziano et al., 2005). In addition, Ethier and colleagues reported that costimulation of the motor cortex of anesthetized cats evoked the linear summation of separately evoked forelimb motions (Ethier et al., 2006). Finally, a recent work demonstrated that the electromyographic (EMG) patterns of hand muscles evoked by long ICMS of motor cortical areas of monkeys were

decomposed into a few basic synergies that showed high similarities to those found in voluntary movements (e.g., reaching and grasping) (Overduin et al., 2008), and these synergies were nonuniformly distributed over the cortical surface (Overduin et al., 2012)[10].

2.2.2.3 Generalization: Behavioral window for motor primitives

The implementation of the internal model through the motor primitives provides a testable hypothesis in terms of motor adaptation. Mathematically, it can be easily shown in Eq. (2-3) that the pattern of learning in W_i is proportional to Φ_i under the assumption of a simple learning algorithm, such as that of a first-order gradient descent. In other words, the pattern of motor learning may reflect how the primitives, Φ_i, represent various movement parameters (e.g., limb velocity and position). Thus, one can estimate the encoding scheme of Φ_i by analyzing how the performance of F changes for new inputs around training data, and this is called *generalization* (Fig. 2.7).

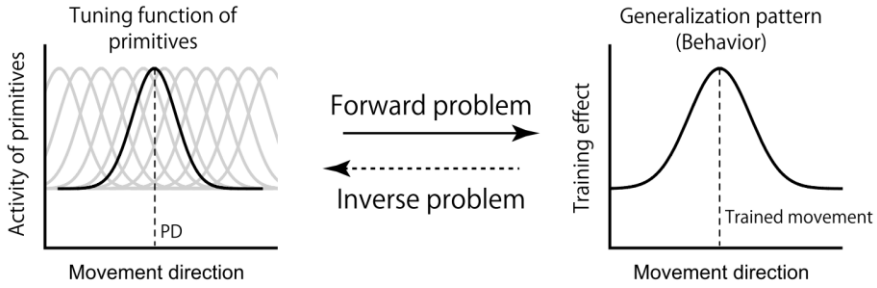

Figure 2.7. Generalization of motor learning and encoding of the motor primitive.
The scheme that the internal models are constructed through the combination of the motor primitives predicts that, under the several assumptions, generalization of motor learning reflects the features of encoding function of the primitives.

[10] While these studies have provided fascinating examples of cortical motor primitives that suggest that a complex arm movement can be evoked through the activity of a specific group of cortical neurons, the interpretation is still under debate. For example, because of the lack of understanding of the effects of a longer ICMS, one cannot conclude whether a small region of motor cortex or a wider network that included the motor cortex was activated through current spreading (Strick, 2002).

By closely analyzing the pattern of how learning that is acquired with a specific movement generalizes to neighboring movement, Shadmehr and co-workers demonstrated how the primitives are tuned to different movement parameters (for a review, see Shadmehr, 2004). For instance, when using the same paradigm as that described in the previous section (Shadmehr and Mussa-Ivaldi, 1994) and the system-identification approach, Donchin et al. (2003) investigated how adaptation to a novel velocity-dependent force field generalizes to different movement directions (Fig. 2.8). They found that the generalization patterns were robust to several different types of novel dynamics (Donchin et al., 2003), and they had similar tuning properties as cerebellar Purkinje cells (Coltz et al., 1999) (Fig. 2.8).

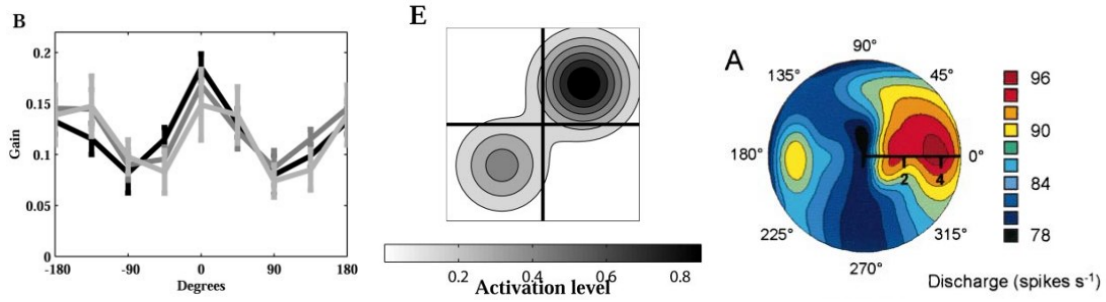

Figure 2.8. Similarity between the estimated encoding pattern of the motor primitive and neuronal discharge patterns.

Left: Generalization pattern of adaptation to a novel force field. The horizontal axis indicates the difference in movement direction between a certain trial and the subsequent trial. The vertical axis indicates how the movement error in the trial affects the subsequent movement in a different direction. *Middle*: Estimated activation pattern of the motor primitive from the generalization data. Horizontal and vertical axes indicate the hand velocity in the x and y directions, respectively. Note that there is the second peak in the opposite direction of the first peak. *Right*: Discharge pattern of a cerebellar Purkinje cell from a monkey performing a planar arm movement with various velocities. Two activation peaks exist in opposite direction. Adapted from Donchin et al. (2003) and Coltz et al. (1999).

Other studies have suggested that these primitives have similar tuning patterns as neurons in the primary motor cortex with respect to their tuning to arm posture and reach direction (Georgopoulos et al., 1984; Hwang et al., 2003).[11]

So far, in this section, I have briefly reviewed the findings of previous studies on the issues of the internal model and motor primitives. Importantly, how the motion states of other limbs affect the state of the internal model (or activity of primitives) for the movement of a particular limb has not yet been investigated because most of the studies reviewed here focused on the movement of a single limb. In the next section, I briefly review the findings of earlier studies on bimanual coordination from this point of view.

2.3 Earlier studies on bimanual movements

As mentioned in Chapter 1, bimanual movement control can be divided into the following three hierarchically organized problems: *task partitioning*, *role assignment*, and *the control of specific arm movements*. In this section, I briefly summarize the findings of earlier studies on bimanual movements according to the above classification, especially for role assignment and the control of specific arm movements, which I aim to investigate in this thesis. I begin with studies that addressed problems that belong to the stage of specific arm movement control. The concepts of the internal

[11] An important point to keep in mind is that, while this approach can explain and predict many aspects of the behavioral data regarding the adaptation to both novel dynamics and kinematics (Shadmehr, 2004; Tanaka et al., 2009), it has little power in localizing the primitives in the nervous system compared to electrophysiological approaches because, in principle, the generalization patterns can contain all possible effects of primitives in different hierarchies of the motor system. I will discuss this point in Chapter 5.

model and motor primitives that I reviewed in the previous section are also helpful in the interpretation of these studies. Then, I review some of the important findings of studies that addressed the problems related to role assignment.

2.3.1 Controlling two arm movements simultaneously

Similar to the control of unimanual movements, which have been intensively studied, bimanual movements are divided into the following two classes of control: *feedforward* and *feedback*. In the very beginning of movements, feedforward control is essential for counteracting the unavoidable noise and delays in sensory feedback signals (~50 msec) because sensory feedback is not available at this period. After sensory feedback is available, feedback control is necessary to counteract unexpected perturbations or environmental changes in some optimal way (e.g., minimizing motor errors and efforts and/or maximizing rewards).

2.3.1.1 Feedforward control during bimanual movements

Traditionally, the feedforward control of bimanual movement has been studied with a class of tasks called voluntary unloading/loading tasks, in which a subject is instructed to maintain the position of his or her arm while taking off (unloading) or putting on (loading) a load that is attached to the arm with the other arm, which is similar to placing a cocktail glass on/off a tray while keeping the tray and other glasses still. In these tasks, predictive muscle deactivations/activations are constantly observed in advance of the onset of unloading/loading and are not observed when the load is taken

off (or put on) by an experimenter (Massion, 1984; Johansson and Westling, 1988; Viallet et al., 1992; Massion et al., 1999), even when the timing is highly predictable (Diedrichsen et al., 2003). These predictive controls are adaptive and are learned by experience (Massion et al., 1999; Morton et al., 2001; Schmitz and Assaiante, 2002; Schmitz et al., 2002). An important feature of this simple bimanual coordination task is that the motor output of one arm is dependent on the active motor plan of the other arm. This idea can be extended to a more mechanistic approach, such as motor control through an internal model. Several recent behavioral studies have begun to examine this point of view (Bays and Wolpert, 2006; Nozaki et al., 2006; Nozaki and Scott, 2009; Howard et al., 2010).

By using robotic devices similar to those used in a study by Shadmehr et al., Bays and Wolpert (2006) studied the acquisition of a novel relationship between two arms (Fig. 2.9). They mimicked a situation in which the subjects manipulate an object that is held in the left hand with the right arm. The goal of the task was to maintain the position of the left handle of the manipulandum within an area that was specified by a visual target presented on a horizontal screen while making out-and-back reaching movements in different directions with the right handle. During the reaching movement, the left robot generated a force with a magnitude that was proportional and perpendicular to the velocity of the right handle. Therefore, the perturbation that the left arm experienced was dependent on the motion state (i.e., speed and direction) of the right arm. Initially, the subjects showed substantial deviation in their left-arm position because of perturbation from the right-arm

motion. However, after about 40 trials of reach, the peak displacement of the left hand was reduced, albeit incompletely, suggesting that the subjects acquired this novel relationship between the motion of the right arm and the force to the left arm (i.e., internal model) and predictively compensated for the perturbation.

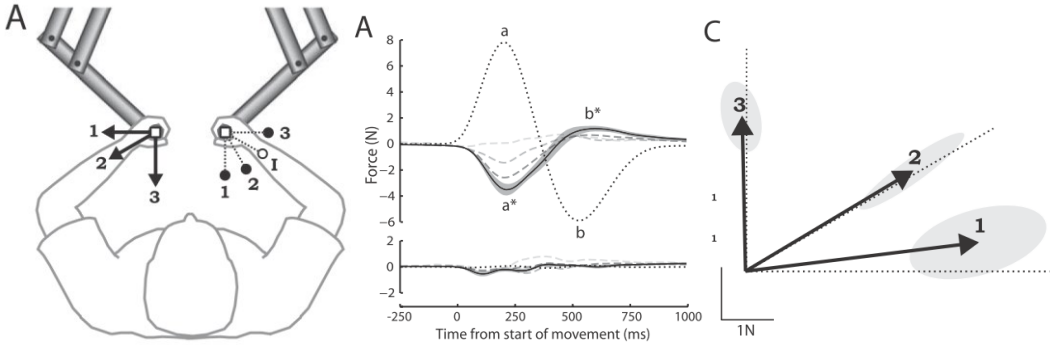

Figure 2.9. Adaptation to a novel bimanual load compensation task.
Left: Experimental setup. Motion of the right handle imposed a force on the left handle perpendicular to the motion of the right handle. The numbered arrows on the left handle indicate the direction of the force when the right handle was moving toward the corresponding target. *Middle*: Force profiles of the left handle perpendicular (top) and parallel (bottom) to the right-hand target direction. The dotted line indicates the mean force that was applied to the left handle in the perturbation trials. The mean force that was generated by the subjects is plotted as dashed lines (light gray: the first clamp trial, mid-gray: 1–10 clamp trials, dark gray: 11–30 clamp trials) and solid lines (31–60 clamped trials) with shaded area (±1 SE across subjects). *Right*: Aftereffect of the left arm averaged across all subjects. The arrows indicate the mean force vectors that were generated in the 31st–60th clamp trials averaged across subjects. The ellipses indicate 95% confidence intervals. Adapted from Bays and Wolpert (2006).

This was confirmed by *clamp trials* in which the perturbation force was unexpectedly turned off and the position of the left handle was clamped to the home position by a virtual spring that was stiff enough to measure the direction and amplitude of the force that the subjects' left arm generated while constraining the handle to the initial position. They observed exactly the same

pattern of compensating force with the velocity of the right handle in the opposite direction to the expected perturbations. This kind of learned predictive compensation was also well modulated by the movement speed of the right arm (Jackson and Miall, 2008). Thus, the findings suggested that the CNS can learn a new internal model of perturbation for the passive left arm that depends on the motion state of the right arm, such as movement speed and/or direction.

At the same time as Bays and Wolpert (2006), Nozaki et al. (2006, 2009) also described this point using a different approach (Fig. 2.10). In their experiment, subjects learned the force field while *unimanually* reaching with their left or right arm. After training, they measured the amount of learning by the catch trial *for both the unimanual and bimanual conditions* and found that only 60–70% of learning was observed in the bimanual condition compared to the unimanual condition. Thus, the motor learning acquired in the unimanual training incompletely transferred to the same arm that was reaching in a bimanual context. In addition, they showed that the opposite was true; the motor learning that was acquired in the bimanual training incompletely transferred to the unimanual context, confirming that the results in the first experiment were not simply due to an increase in attentional demand or caused by the additional motion of the opposite arm. Rather, their results implied that partially different motor memories (i.e., internal models) were involved in the reaching of the same arm depending on the motion state (reaching or not moving) of the opposite arm. Furthermore, they demonstrated that the subjects were able to simultaneously learn opposing force

fields with the same arm movement if they were associated with the two states of the opposite arm (i.e., unimanual or bimanual).

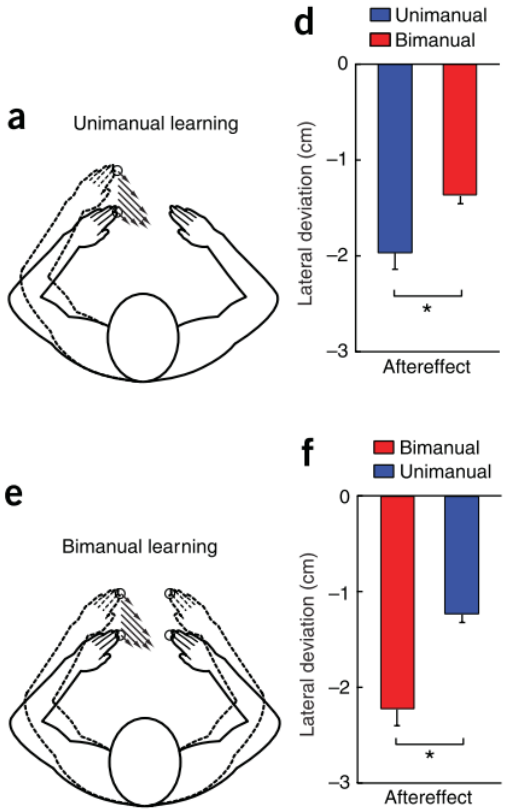

Figure 2.10. Concurrent motion of the right arm modulates the control process for the left arm.

Left: Schematics of unimanual (upper panel) and bimanual (lower panel) training. In unimanual training, subjects tried to reach their left arm in the presence of a force field (indicated as arrows) while maintaining the right arm still. In bimanual training, the subjects reached both arms while the force field was applied only on the left arm. *Right*: Aftereffects for both unimanual and bimanual catch trials for unimanual (upper panel) and bimanual (lower panel) training. Adapted from Nozaki et al. (2006).

These results were well explained by a computational model that introduced the similarity (i.e., overlap) in the internal states of the internal model between bimanual and unimanual reaches (Nozaki and Scott, 2009), suggesting that the contribution of the motor primitives in the internal

model to the motor output of the arm dramatically changed depending on whether the other arm was reaching or at rest. Similarly, Howard et al. (2010) have demonstrated that the opposing force fields can be learned by one arm if they are associated with different movement directions of the opposite arm during bimanual movement (Howard et al., 2010).

In summary, these studies suggest that the motion state of one arm has strong effects on the internal state of the internal model for the other arm, possibly through changing the activation patterns of the motor primitives. However, how the motion states of both arms are integrated in the internal model or in the motor primitives remains completely unknown.

2.3.1.2 Feedback response during bimanual movements

The ability for a rapid motor response to sensory input is necessary to counteract unexpected perturbations or sudden environmental changes. A recent theory of optimal feedback control in biological movement control posits that our nervous system transforms sensory inputs into motor output in an intelligent way to minimize effort and maximize the task goal or reward (Todorov and Jordan, 2002; Shadmehr and Krakauer, 2008; Diedrichsen et al., 2010). The findings of several studies have suggested that in bimanual movement control, similar to the above example of feedforward control, fast feedback responses for the one arm (or finger) can be flexibly triggered from the sensory inputs to the opposite arm (or finger) in a highly task-dependent manner (Ohki and Johansson, 1999; Ohki et al., 2002; Diedrichsen, 2007; Mutha and Sainburg, 2009; Dimitriou et al.,

2012).

For instance, by using an arm reaching paradigm similar to that used by Bays and Wolpert (2006), Diedrichsen (2007) examined how subjects respond to a sudden mechanical perturbation to one arm while simultaneously reaching with both arms in different conditions while the two arms are controlling a single object or two separated objects (Fig. 2.11). In the one-cursor condition, a visual cursor was presented at the average position of the two handles, whereas two cursors were presented for each position of the handle in the two-cursor condition. He found that subjects corrected the movement with both arms in the one-cursor condition, whereas, in the two-cursor condition, the correction was only made for the perturbed arm. Bilateral correction was still observed when visual feedback was occasionally withdrawn, and it was made as early as 190 ms after movement onset, suggesting that proprioceptive input to one arm was sufficient to elicit a bilateral feedback correction. The concept of signal-dependent noise in the motor command, the variance of which increased proportionally to the size of the command (Harris and Wolpert, 1998), predicts that it was more effective in the single-cursor condition for correcting movement error that was caused by the error from one arm than with both arms, likely because sending a larger corrective command to one arm may be subject to larger variability compared with smaller commands to both arms. Indeed, simulation with an optimal feedback control model closely matched the behavioral data.

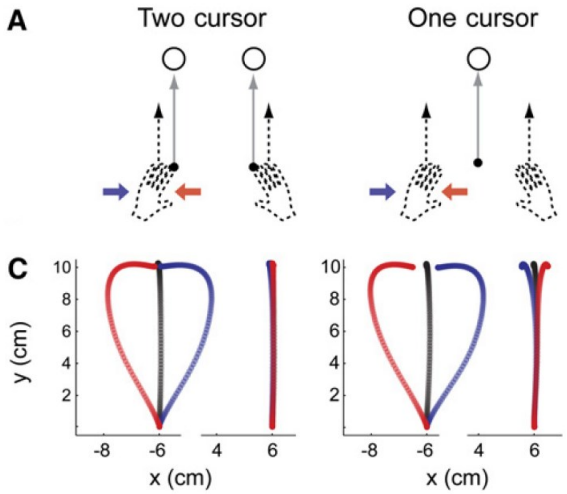

Figure 2.11. Fast task-dependent feedback during bimanual movements.
Upper: Subjects were asked to reach both arms to move visual cursors (presented as filled circles) to targets (presented as open circles). In the two-cursor condition, a visual cursor was presented for each hand. In the one-cursor condition, the cursor was presented at the averaged position of both hands. One of the hands was perturbed with either a leftward (red) or rightward (blue) force field. *Lower*: Hand paths for each condition (left: two cursor, right: one cursor). The black trajectories show the data for the unperturbed trial. Adapted from Diedrichsen (2007).

Several years later, findings of several studies that analyzed the muscle stretch reflex suggested that the type of motor response observed by Diedrichsen (2007) might be mediated by fast involuntary processes, such as reflexes. Mutha and Sainburg (2009) and Dimitriou et al. (2012) demonstrated that long-latency stretch reflexes are modulated in a similar manner to what was observed by Diedrichsen (2007); namely, it depends on whether subjects are controlling single objects or two independent objects with two arms. For example, in the recent work by Dimitriou et al. (2012), subjects were asked to maintain the position of two handles of robotic manipulanda in two conditions. In the first, the handles were linked through a virtual horizontal bar, and the task was to maintain the tilt of the bar, just like balancing a loaded tray (Fig. 2.12). In another (control)

condition, the subjects were asked to separately maintain the positions of two small bars for each handle. In the control condition, stretch reflexes were only elicited in the muscles of the perturbed arm. However, in the single-bar condition, long-latency reflexes were also elicited for the muscles of the unperturbed arm in the direction that compensated for the change in the orientation of the virtual bar, despite that the muscles of the unperturbed arm were *not* stretched at all. In addition, when perturbations were applied to both arms in the same direction, which did not change the orientation of the virtual bar, the amplitudes of the long-latency reflexes were attenuated compared to those observed for responses to the same perturbation in the control condition.

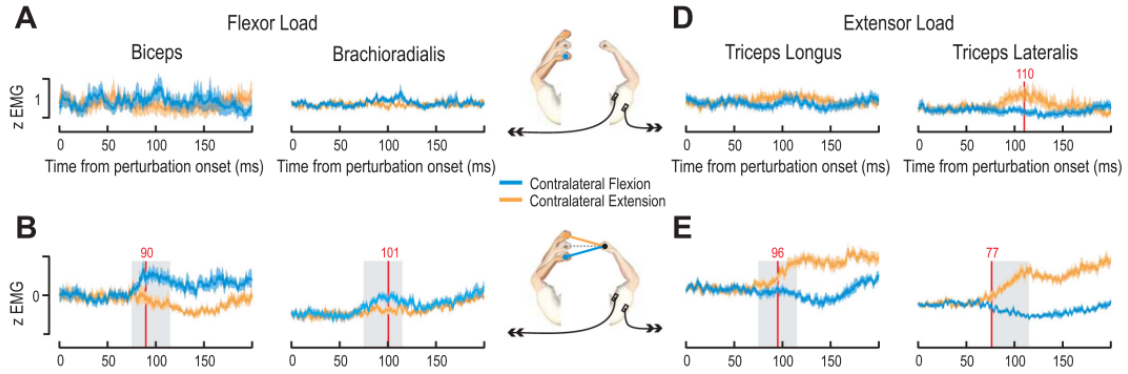

Figure 2.12. The long-latency reflex of a limb is modulated by sensory input from the opposite limb and task constraint.

Graphs: *z*-standardized EMG from the right upper arm muscles (biceps, brachioradialis, triceps longus, and triceps lateralis). *Schematics*: Subjects were asked to maintain the position of each handle. Mechanical perturbation (either extension or flexion) was applied to the left arm in randomly chosen trials. *Upper panels*: When two hands controlled separate objects, the right arm muscles were insensitive to left arm perturbation. *Lower panels*: In contrast, when two hands controlled a single object, the long-latency reflex of the right arm was elicited by left arm perturbation. Adapted from Dimitriou et al. (2012).

In summary, these results suggested that rapid motor responses (e.g., long-latency stretch reflexes) in one arm are intelligently controlled by integrating the sensory states of both arms and the

task variables. Recently, the long-latency reflex has been considered a candidate for the physiological foundation of the theory of optimal feedback control in biological movement (Scott, 2003), which suggested that it is mediated by cortical circuits that involve the primary motor cortex (Pruszynski et al., 2011). How the sensory information for both arms is integrated in the forward internal model, which is considered a crucial component for feedback control, remains elusive.

2.3.2 Assigning tasks between two arms

Most of our daily bimanual movements are asymmetric, and the hands play complementary roles in achieving a common task goal. For example, even writing consists of two different roles: writing and holding/manipulating pages (Guiard, 1987). Compared to studies on the control of specific arm movements during bimanual movements, little attention has been paid to the process of role assignment during bimanual movement. In the following section, I briefly summarize the findings of studies related to this topic according to the basic constraints that constitute the process of role assignment during bimanual movements.

2.3.2.1 Internal constraints for bimanual role assignment

Differences in the abilities of two upper limbs (i.e., hands and arms) in various aspects of motor control is known as *handedness*, and it is a strong constraint on determining role assignment during bimanual movements. A common belief is that the dominant limb is more skilled than the nondominant limb in every aspect of sensorimotor ability, such as movement accuracy (Woodworth,

1899). Indeed, superiority of the dominant limb has been intensively studied with various manual tasks, including a peg-moving task (Annett, 1985), a dot-filling task (Tapley and Bryden, 1985), a finger-tapping task (Peters and Durding, 1978), an aiming task (Flowers, 1975; Todor and Kyprie, 1980), and a maximum-grip force task (Petersen et al., 1989; Crosby et al., 1994; Armstrong and Oldham, 1999). A number of hypothetical mechanisms that account for the superiority of the dominant hand-hemisphere system in the manual performance of different tasks have been proposed, such as differences in the movement planning process (Todor and Kyprie, 1980; Carson et al., 1993; Elliott et al., 1995; Mieschke et al., 2001) or the utilization of sensory signals for correcting movement errors (Flowers, 1975; Todor and Doane, 1977; Todor and Cisneros, 1985; Carson et al., 1993; Roy et al., 1994). In a recent study, Berniker and Kording (2008) proposed that, compared to the dominant arm, the nondominant arm has large uncertainties in the state estimation process (Berniker and Kording, 2008). From the perspective of Bayesian information integration, they argued that larger uncertainty in the nondominant arm clearly explains previous observations about the asymmetrical transfer of motor learning between the dominant and nondominant arms (Dizio and Lackner, 1995; Criscimagna-Hemminger et al., 2003; Wang and Sainburg, 2004).

In contrast, a recent approach by Sainburg and colleagues attempted to rethink the common master-slave perspective between dominant and nondominant hands/arms (for a review, see (Sainburg, 2010)). In a series of reaching paradigm experiments, they proposed that the two

arm-hemisphere systems are specialized for different aspects of the motor control process rather than for the absolute superiority of one side. For example, in a study by Duff and Sainburg (2007), subjects were asked to make fast center-out reaching movements with either the dominant or the nondominant arm (Duff and Sainburg, 2007). In certain trials, an inertial mass was attached to the arm as a perturbation. They found that the final position error was comparable between dominant and nondominant arms in late phases of the perturbation trials, while the initial direction error was significantly smaller in the dominant arm. Subsequent catch trials demonstrated that the dominant arm exhibited larger aftereffects than the nondominant arm, suggesting that the dominant arm adapted to the inertial mass and was therefore able to predictively compensate for intersegmental dynamics. However, it has also been suggested that the nondominant arm showed small adaptation to the inertial mass, and it had to make more of an effortful solution.

They concluded that the dominant arm-hemisphere system is more specialized for the coordination of limb dynamics, such as predictively compensating for interaction torques and achieving a less curved trajectory during movements, and that the nondominant arm-hemisphere system is more specialized for controlling limb impedance, such as maintaining the stable position of a limb and achieving similar end-point accuracies as the dominant arm. Similar results have been reported by others (Schabowsky et al., 2007). They argued that such a specialized ability of the nondominant arm for impedance control is beneficial for bimanual object manipulation, such as with

tool making (Sainburg, 2010). Furthermore, they argued that observations of the motor performances of unilateral stroke patients support this view, and the motor performance of limbs on the intact side show some impairments in abilities that are associated with the function of the lesioned hemisphere (Schaefer et al., 2007).

Taken together, it seems plausible that these differently specialized abilities between the two arm-hemisphere systems may contribute to the assignment of different roles (i.e., performing tasks and doing nothing) to the two systems, at least for unimanual tasks (i.e., hand selection). The remaining substantial question to be asked is whether these differences in the motor-control strategies between the two arm-hemisphere systems that were measured in unimanual tasks are also expressed during bimanual tasks. Considering that there are dense connections between both hemispheres through a large bundle of axons called the corpus callosum (CC), a simple linear summation (or pure parallel expression) of two specialized functions during bimanual movements is unlikely.

2.3.2.1 External constraints for bimanual role assignment

Although the internal constraints described above are likely to play a dominant role in most cases, role assignment may be a much more flexible process than we expect from the consistent, habitual assignment of two roles in daily life. A line of recent studies from Roland Johansson's laboratory has demonstrated that these seemingly habitual role assignments can flip depending on the spatial

congruency between manual actions and their consequences (Johansson et al., 2006; Theorin and Johansson, 2007, 2010). In addition, they found that prefrontal and posterior parietal network activation was involved in this process, suggesting the requirement of higher cognitive processes to resolve competition between the two potential roles for both hands in bimanual object manipulation. The basic paradigm of their experiment is shown in Fig. 2.13.

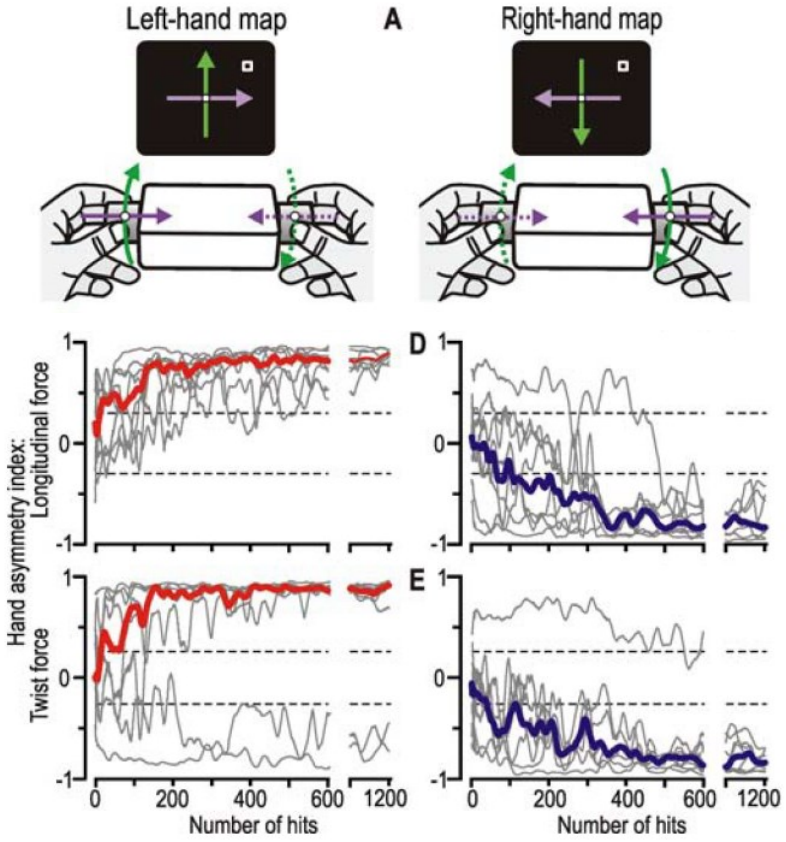

Figure 2.13. Flexible role assignment during bimanual object manipulation.
Upper: Schematics for two-task mappings. Subjects were asked to track a visual target (not shown) moving randomly with a cursor (white dot). In the left-hand map, counterclockwise/clockwise torque on the left knob was translated as upward/downward motion of the cursor, and compressing/pulling force was translated as rightward/leftward motion of the cursor. This relationship was reversed in the right-hand map. *Middle and Lower*: Time courses of the hand asymmetry index (red: right-hand map, blue: left-hand map). +1 and -1 indicate complete left-hand and right-hand mapping, respectively. Adapted from Johansson et al. (2006).

Subjects held small knobs that were attached to both ends of a custom-built manipulandum with the thumb and two fingers (index and middle finger) of both hands. Force transducers were implemented in the knobs, and longitudinal forces and twist forces were continuously monitored and transformed into the x and y positions of the visual cursor, respectively (i.e., pulling or pushing to move the cursor horizontally and twisting to move the cursor vertically). The subjects were asked to move the cursor and track a randomly moving target by maintaining the position of the manipulandum. Note that in order to maintain a stable position of the manipulandum, two complementary roles need to be assigned to the hands so that one hand is the prime actor that manipulates the position of the visual cursor while the other hand acts as a stabilizer with an output that matches the force that the prime actor produces but in the opposite direction. Each subject experienced two types of mapping according to the relationship between cursor motion and force direction, and these were presented in random order. In the right-hand map, the pulling force was converted to a rightward motion of the cursor and a clockwise twist force that was applied between the hands was converted to an upward motion of the cursor, which made it more congruent for the right hand to control the cursor. The left-hand map produced the opposite scenario, and it was more natural for the left hand to control the cursor.

Interestingly, although the subjects had no prior knowledge about the type of mapping, they selected the prime-actor hand for the movement, which was consistent with the mapping. The

hand that the subjects assigned as the prime actor was assessed by calculating the correlation coefficient between the applied force and the motion of the manipulandum and the EMG signals because larger and faster muscle activations of the prime-actor hand moved the manipulandum in a consistent way. This was also confirmed by the measurement of corticospinal excitability with transcranial magnetic stimulation (TMS) that was applied to each side of the primary motor cortex. The magnitude of the TMS-evoked EMG (MEP) of the hand muscles was consistent with the correlation analysis (i.e., MEP was larger in the muscles of the prime-actor hand) (Johansson et al., 2006). These data suggested that the brain assigns an appropriate role to each hand to maximize task performance because spatial incongruency between visual stimuli and action deteriorates task performance, such as in the Simon task (Simon and Wolf, 1963) or the Eriksen flanker task (Eriksen, 1995).

In an fMRI study, several brain regions areas, such as the right dorsolateral prefrontal cortex (dlPFC), the bilateral dorsomedial prefrontal cortices (dmPFC), the posterior parietal cortex (PPC), and the right inferior parietal lobule (IPL), have been shown to be engaged in the process of bimanual role assignment (Theorin and Johansson, 2010). Especially, the dlPFC and the IPL are known to have a functional connection with this activity (Fincham et al., 2002; Dosenbach et al., 2006), and they constitute part of the executive control network (Seeley et al., 2007; Sridharan et al., 2008; Habas et al., 2009), which is considered important in decision-making or response-selection

processes that are based on sensory information. Importantly, the prefrontal cortex, including the dlPFC, is considered crucial for resolving competition between potential action plans (Casey et al., 2000; Egner and Hirsch, 2005; Cisek, 2008; Coulthard et al., 2008). Lesions in these areas affect the action-selection process (Cisek, 2008; Coulthard et al., 2008). A recent study that applied TMS to the PPC demonstrated the reversal of habitual hand choice during a unimanual reaching task (Oliveira et al., 2010).

Taken together, these results suggest that role assignment during bimanual movement is a dynamic decision process in which the optimal roles are selected for each limb from potential action/hand pairs that integrate both bottom-up (i.e., internal constraints) and top-down (i.e., external constraints) information, and brain networks involving the PPC and frontal cortex play an important role in this process.

2.4 Summary

In this chapter, I briefly summarized the findings of earlier studies on the computational approach to voluntary movement control and bimanual movement control. In order to cope with the fundamental problems of biological motor control, such as large noise levels and delays in sensory feedback signals, the brain constructs a map between the desired/predicted sensory state and the motor command. These internal models are highly adaptive to changes in the physical properties of both

the environment and one's own body. The nervous system may implement this adaptive mapping through a flexible combination of the activity of a set of neural elements, called the motor primitive. The motor primitive may exist throughout the sensorimotor transformation pathway, which includes the cerebral cortex and the spinal cord. Such a scheme can predict that the generalization of motor learning may reflect the possible encoding of motor primitives, and, so far, there has been good agreement between predictive models and behavioral data.

With respect to the stage of the control of specific arm movements, several previous studies on bimanual movements have suggested that the internal model for an arm can utilize information about the motion of the other arm. When assigning two different roles to two arms, the brain selectively enhances the optimal hand/role pairs from competing choices by taking into account both internal constraints, such as handedness, and external constraints, such as the spatial congruence of motion. Recent ideas about handedness involve the view that two hand/arm-hemisphere systems are specialized for complementary functions, rather than the concept that the dominant hand/arm-hemisphere system has absolute superiority in all aspects of movement control. Dynamic interactions within the executive control network, including the prefrontal and posterior parietal cortices that flexibly coordinate these constraints may underlie the flexible role-assignment process during bimanual action.

The remaining issues are as follows. First, although it has been suggested that the internal model for one arm is capable of utilizing the motion state of the other arm in order to learn about the mechanical perturbations, how this ability can be explained at the level of the motor primitive and how information about motion of the relevant arm and that of the other arm are integrated within the internal model (or primitives) is largely unknown. Second, whereas specialized motor control functions for two arm-hemisphere systems have been suggested, such observations were made in a unimanual context. Whether these characteristics of two arms are also expressed during bimanual movements is unclear. Third, how these specialized functions in two arms are explained at the level of the motor primitive is also unknown. These issues are addressed in the studies presented in this thesis. In Chapter 3, I address the first issue of how motion information from both arms is represented in the internal model.

Chapter 3

Gain Field Encoding of the Kinematics of Both Arms in the Internal Model Enables Flexible Bimanual Action

3.1 Abstract

Bimanual action requires the neural controller (internal model) for each arm to predictively compensate for mechanical interactions resulting from movement of both that arm and its counterpart on the opposite side of the body. Here, we demonstrate that the brain may accomplish this by constructing the internal model with primitives multiplicatively encoding information from the kinematics of both arms. We had human participants adapt to a novel force field imposed on one arm while both arms were moving in particular directions and examined the generalization pattern of motor learning when changing the movement directions of both arms. The generalization pattern was consistent with the pattern predicted from the multiplicative encoding scheme. As proposed by previous theoretical studies, the strength of multiplicative encoding was manifested in the observation that participants could adapt reaching movements to complicated force fields depending nonlinearly on both arms' movement directions. These results indicate that multiplicative neuronal influence of the opposing arm's kinematics on the internal models enables the brain to control

bimanual movement by providing great flexible ability to handle arbitrary dynamical environments resulting from the interactions of both arms.

3.2 Introduction

One of the unsolved problems in motor control science is how the brain orchestrates the movement of multiple body parts as a unified action (e.g., bimanual movement). Previous studies of unimanual reaching movement have suggested that the brain accomplishes flexible movements by constructing an "internal model" of the dynamic properties of the body and the environment (Kawato, 1989; Bhushan and Shadmehr, 1999). It was also suggested that humans build these internal models through a flexible combination of motor primitives encoding the desired arm's kinematics (Thoroughman and Shadmehr, 2000; Donchin et al., 2003; Sing et al., 2009). However, this powerful scheme is not directly compatible with control of bimanual movement. When we perform bimanual movements such as manipulating an object, every movement of each arm disturbs the other arm because the dynamics of both arms are coupled through the object and the person's body. Therefore, the desired motor command for each arm cannot be determined solely by the state of the arm itself, which may not be explained by the conventional scheme of primitives. One solution is to assume that an additional neuronal process adjusts the motor command by estimating the interaction;

however, this may create another question regarding how this additional process is implemented in the brain.

An alternative is to assume, as we have done here, that the primitives of the internal model encode not only the desired kinematics of the relevant arm, but also those of the opposite arm. This proposal is based on recent reports that distinct internal models can be constructed depending on the opposite arm's kinematics (Nozaki et al., 2006; Nozaki and Scott, 2009; Howard et al., 2010). According to this assumption, the process of constructing an internal model for one arm with primitives can be formulated as $\hat{f} = \boldsymbol{w}^{\boldsymbol{t}}\boldsymbol{g}(\boldsymbol{x}_r, \boldsymbol{x}_l)$, where $\hat{f}$ is a force output, $\boldsymbol{w} = (w_1, w_2, \cdots)^t$ is a weight vector, and $\boldsymbol{g} = (g_1(\boldsymbol{x}_r, \boldsymbol{x}_l), g_2(\boldsymbol{x}_r, \boldsymbol{x}_l), \cdots)^t$ is a vector whose elements represent the output of each primitive; $\boldsymbol{x}_r$ and $\boldsymbol{x}_l$ represent the kinematics of the right and left arm, respectively.

From this viewpoint, the brain's ability to accomplish flexible bimanual movement can be regarded as the ability to construct flexible force output by combining the primitives. How, then, should the primitives encode both arms' kinematics? Previous theoretical works (Pouget and Sejnowski, 1997; Salinas and Sejnowski, 2001) have provided a clue. They proposed that neurons encoding 2 inputs, x_1 and x_2, multiplicatively [$\boldsymbol{h}(x_1, x_2)$; "gain-field" encoding (Andersen and Mountcastle, 1983; Andersen et al., 1985)] work as a set of basis functions enabling downstream neurons to construct the arbitrary output function $y(x_1, x_2) = \boldsymbol{w}^{\boldsymbol{t}}\boldsymbol{h}(x_1, x_2)$. This close similarity to the current problem led us to further hypothesize that multiplicative encoding of both arms'

kinematics in the primitives enables the brain to create an arbitrary force output. We tested this hypothesis by examining the generalization pattern of motor learning (Shadmehr and Mussa-Ivaldi, 1994; Thoroughman and Shadmehr, 2000; Donchin et al., 2003; Hwang et al., 2003; Sing et al., 2009), which should reflect the encoding structure in the primitives (Hwang et al., 2003; Wainscott et al., 2005).

3.3 Materials and Methods

Participants. Thirty-six healthy right-handed volunteers (aged 18–31 years; 12 women) participated in our study after providing written informed consent. All experimental procedures were approved by the ethics committee of the Graduate School of Education, The University of Tokyo.

General task settings. The participants were asked to make simultaneous center-out bimanual reaching movements (Fig. 3.1*A*), with a movement amplitude of 8 cm and a duration of 400 ms, holding the handles of 2 robotic manipulanda (Phantom 1.5 HF; SensAble Technologies, Woburn, MA, USA). Throughout the experiment, the position of each handle was always visible as a white cursor (diameter = 6 mm) on a horizontal screen over the handles. The movements of the handles were constrained to a virtual horizontal plane implemented by a simulated spring (1.0 kN/m) and dumper (0.1 N/(m/s)). Wrist braces were used to reduce unwanted wrist movements. The

participants' upper arms were supported by arm slings to reduce fatigue and allow maintenance of a constant arm posture.

Initially, the participants were required to move each cursor into its home position (diameter = 10 mm; the distance between the starting positions was 20 cm). After a 2-s holding time, a gray target (diameter = 10 mm) appeared for each hand in each position. The "go" cue, a color change and "beep" sound, was provided after a further random holding time (1–2 s). A warning message was presented on the screen if the movement speed of either handle was above ("Fast") or below ("Slow") a target range of 376 ± 56.4 mm/s. At the end of each trial, the handle of each manipulandum automatically returned to its home position. The motion data for each manipulandum were recorded at a sampling rate of 500 Hz. The data for the handle velocity and force were low-pass filtered using a fourth-order Butterworth filter with a cutoff frequency of 8 Hz.

Evaluation of motor performance. We had participants adapt to a novel force field during bimanual reaching movements (Fig. 3.1*B*; see the following sections for further details). To quantify the degree of motor adaptation when changing movement directions of both arms (See Fig. 3.1*B* for the definition of "movement direction"), we employed the "error clamp" method (Scheidt et al., 2000; Smith et al., 2006; Sing et al., 2009). During error-clamped trials, the trajectory of the handle was

constrained to a straight line toward the target by a virtual "channel" (Fig. 3.1*B*) in which any motion perpendicular to the target direction was constrained by a 1-dimensional spring (2.5 kN/m) and damper (25 N/ms^{-1}). This method enabled us to measure directly the lateral force exerted toward the "channel"; the difference between this lateral force at the peak velocity and that from the baseline session was used as the aftereffect of learning. To quantify performance in trials where the error-clamp method was not adopted (e.g., trials in the training phase), we quantified the lateral deviation of each handle trajectory at the peak velocity from a straight line between the starting position and target.

Experiments 1 and 2. Experiments 1 and 2 (N = 8 apiece) were designed to investigate how the adaptation of one arm (left arm in Exp. 1 and right arm in Exp. 2) to a novel force field acquired while reaching both arms forward was transferred to the same arm when the movement directions of both arms were changed (8 directions for the trained arm, and 6 directions for the opposite arm, i.e., 48 (= 8 × 6) combinations; Fig. 3.1*C*). Participants also performed unimanual reaching movements in 8 directions.

The experiment was composed of 280 trials in the baseline session, 80 trials in the training session, and 463 trials in the testing session. Experiments 3–5 also consisted of these 3 sessions (Table 3.1). During the baseline session, each pattern of 56 combinations of movement directions for

both arms (48 and 8 bimanual and unimanual movement patterns, respectively) was performed in a randomized order within each cycle; thus, every movement configuration was performed in a single cycle. The first 112 trials were composed of null force field trials, and the subsequent 168 trials were composed of error-clamped trials. During the training session, participants moved both arms forward and a velocity-dependent rotational force field was applied on one arm as $\boldsymbol{f} = \boldsymbol{B}\boldsymbol{v}$, where $\boldsymbol{f} = (f_x, f_y)^t$ is the force to the handle of the trained arm ([N]), $\boldsymbol{v} = (v_x, v_y)^t$ is the velocity of the handle ([ms^{-1}]), and $\boldsymbol{B}$ is the viscosity matrix ([N/ms^{-1}]). To cancel out the biomechanical effect of the force direction, the direction was reversed for half of the participants, as $\boldsymbol{B} =$ [0 -10; 10 0] or $\boldsymbol{B} =$ [0 10; -10 0]. During the testing sessions, besides the force field trials with both arms reaching forward, every other trial was a catch trial (error-clamped trials), allowing quantification of the aftereffects of the training trials. The order of the 56 movement patterns was randomized within each of the 4 cycles.

Experiment 3. In Experiments 1 and 2, only one movement configuration was adopted for the training. Experiment 3 was designed to examine how participants adapt to a force field when they are trained at multiple movement configurations and how the learning effect can be generalized to the other movement configurations. We also used the data to evaluate how accurately the mathematical models identified in Exp. 1 (described later) can predict the aftereffects.

Ten participants trained with the same force field used in Experiment 1 for 4 different movement combinations: (θ_r, θ_l) = (0º, 0º), (0, 180), (180, 0), and (180, 180) (Fig. 3.1*D*). The direction of the force field was reversed between the parallel [(θ_r, θ_l) = (0º, 0º), (180, 180)] and opposite [(θ_r, θ_l) = (180º, 0º), (0, 180)] movement patterns. The experiment consisted of 192 trials for the baseline session, 160 trials for the learning session, and 399 trials for the testing session (total = 751 trials). In the baseline session, 64 movement patterns (8 directions for each arm: θ_l = -135, -90, -45, 0, 45, 90, 135, 180 [º] and θ_r=-135, -90, -45, 0, 45, 90, 135, 180 [º]) were adopted. Subsequent to the 64 null force field trials, 128 error-clamped trials were performed for the baseline session (2 cycles). After the learning session of 4 movement patterns (40 cycles), in the testing session, the force field trials of the 4 movement patterns and catch trials (i.e., error-clamp trials) of the 64 movement patterns (Fig. 3.1*D*) were performed alternately (3 cycles). Movement patterns were performed in a randomized order within a single cycle for all sessions.

Experiments 4 and 5. Experiments 4 and 5 were designed to investigate if participants could adapt their arm movements to more complicated dynamic force fields that change nonlinearly with the kinematics of both arms. The participants (N = 5 for each experiment) attempted to adapt their left arm movement to a velocity-dependent rotational force field, the magnitude of which depended nonlinearly on the movement directions of both arms as $\boldsymbol{f}_{\exp 4} = \cos(\theta_l - \theta_r)\boldsymbol{Bv}$ (Experiment 4)

and $\boldsymbol{f}_{\exp 5} = \cos(\theta_l + \theta_r)\boldsymbol{Bv}$ (Experiment 5). The direction of the force fields was reversed for 2 of 5 participants. Regarding $\boldsymbol{f}_{\exp 4}$, the relative difference in the movement directions between both arms determines the direction of the force field. As long as the movement directions of both arms are the same in the extrinsic workspace, the direction of the force field to the left arm is identical; the force direction reverses when both arms move in the opposite direction. On the other hand, in $\boldsymbol{f}_{\exp 5}$, as long as the movements of both arms are mirror symmetric (i.e., the same direction with respect to the joint or intrinsic workspace), the direction of force field to the left arm is identical; however, this force reverses direction when both arms move in the opposite direction in the intrinsic workspace.

The experiments consisted of 144 trials for the baseline session, 960 trials for the learning session, and 192 trials for the testing session (total = 1296 trials). Participants were asked to reach in 16 movement configurations (θ_l = -90, 0, 90, 180 [°] and θ_r= -90, 0, 90, 180 [°]) for all sessions. In the baseline session, the error-clamped trials were randomly conducted once every 3 trials (3 cycles). In the learning session (40 cycles), 16 movement patterns were randomly performed within each cycle; to effectively promote learning, the number of trials with force was twice that of trials with null force. In the testing session, in addition to the force field trials performed the same as in the training session, catch trials (error-clamped trials) were performed once in every 4 trials (3 cycles), and the order of the movement patterns was randomized within each cycle.

Theoretical background. We modeled the motor learning process using the state space model (Thoroughman and Shadmehr, 2000; Donchin et al., 2003; Wainscott et al., 2005; Lee and Schweighofer, 2009; Nozaki and Scott, 2009), consisting of N primitives that encode the movement directions of both arms as $g(\theta_r, \theta_l)$, where θ_r and θ_l are the movement directions of the right and left arms, respectively (Fig. 3.3*A*). The output force created by the internal model can be represented by a linear summation of the outputs of primitives as:

$$\hat{f}^{(i)} = \left[\boldsymbol{w}^{(i)}\right]^t \boldsymbol{g}(\theta_r^{(i)}, \theta_l^{(i)}) \tag{3-1}$$

where i is the trial number, and $\boldsymbol{g}(\theta_r, \theta_l) = [g_1(\theta_r, \theta_l), g_2(\theta_r, \theta_l), \cdots, g_N(\theta_r, \theta_l)]^t$ and $\boldsymbol{w} = [w_1, w_2, \cdots, w_N]^t$ are column vectors whose elements represent the output and weight of each primitive, respectively.

A state space model of the motor adaptation to the force field f can be represented as:

$$e^{(i)} = d(\theta_l^{(i)})(f^{(i)} - \hat{f}^{(i)}) \tag{3-2}$$

$$\boldsymbol{w}^{(i+1)} = \alpha \boldsymbol{w}^{(i)} + e^{(i)} K \boldsymbol{g}(\theta_r^{(i)}, \theta_l^{(i)}) \tag{3-3}$$

where e is the movement error, $d(\theta_l)$ is the compliance that depends on the movement direction of the trained arm (here, we assumed that the left arm is trained), and α and K are constants representing, respectively, the spontaneous loss of memory and the update rate to the error.

From Eqs. (3-1)-(3-3), the weight vector after sufficient training of a constant force field f is obtained as:

$$\boldsymbol{w}^t = \frac{Kd(\theta_l) f \boldsymbol{g}(\theta_r,\theta_l)^t}{1-\alpha+Kd(\theta_l)\boldsymbol{g}(\theta_r,\theta_l)^t \boldsymbol{g}(\theta_r,\theta_l)}. \quad (3\text{-}4)$$

When movement directions of both arms are changed by $\Delta\theta_r$ and $\Delta\theta_l$, the force output (i.e., aftereffect) is represented as: $\hat{f}(\theta_r + \Delta\theta_r, \theta_l + \Delta\theta_l) = \boldsymbol{w}^t \boldsymbol{g}(\theta_r + \Delta\theta_r, \theta_l + \Delta\theta_l)$. Thus, the function of how the training effect is transferred from (θ_r, θ_l) to $(\theta_r + \Delta\theta_r, \theta_l + \Delta\theta_l)$ is represented by:

$$\Phi(\Delta\theta_r, \Delta\theta_l) = \frac{\hat{f}(\theta_r+\Delta\theta_r,\theta_l+\Delta\theta_l)}{\hat{f}(\theta_r,\theta_l)} = \frac{\boldsymbol{g}(\theta_r,\theta_l)^t \boldsymbol{g}(\theta_r+\Delta\theta_r,\theta_l+\Delta\theta_l)}{\boldsymbol{g}(\theta_r,\theta_l)^t \boldsymbol{g}(\theta_r,\theta_l)}. \quad (3\text{-}5)$$

Decomposition of the generalization function. If the primitives encode the movement directions of both hands multiplicatively as: $g_j(\theta_r, \theta_l) = r_j(\theta_r) l_j(\theta_l)$, when N is sufficiently large (N is assumed to be a square number), and $l_j(\theta_l)$ and $r_j(\theta_r)$ have translational symmetry with respect to j and are distributed uniformly on the (θ_r, θ_l) plane, then $\boldsymbol{g}(\theta_r, \theta_l)^t \boldsymbol{g}(\theta_r + \Delta\theta_r, \theta_l + \Delta\theta_l) \approx \frac{1}{N}\sum_{j=1}^{\sqrt{N}} r_j(\theta_r)\, r_j(\theta_r + \Delta\theta_r) \sum_{j=1}^{\sqrt{N}} l_j(\theta_l) l_j(\theta_l + \Delta\theta_l)$. Thus, the transfer function is:

$$\Phi(\Delta\theta_r, \Delta\theta_l) = \Phi(\Delta\theta_r, 0)\Phi(0, \Delta\theta_l). \quad (3\text{-}6)$$

On the other hand, if the primitives encode the movement directions of both hands additively as: $g_j(\theta_r, \theta_l) = r_j(\theta_r) + l_j(\theta_l)$, then

$$\boldsymbol{g}(\theta_r, \theta_l)^t \boldsymbol{g}(\theta_r + \Delta\theta_r, \theta_l + \Delta\theta_l) = \sum_{j=1}^{N} \left[r_j(\theta_r) + l_j(\theta_l)\right]\left\{\left[r_j(\theta_r + \Delta\theta_r) + l_j(\theta_l)\right] + \left[r_j(\theta_r) + l_j(\theta_l + \Delta\theta_l)\right] - \left[r_j(\theta_r) + l_j(\theta_l)\right]\right\}.$$ Thus, the transfer function is:

$$\Phi(\Delta\theta_r, \Delta\theta_l) = \Phi(\Delta\theta_r, 0) + \Phi(0, \Delta\theta_l) - 1. \quad (3\text{-}7)$$

It should be noted that previous work (Wainscott et al., 2005) obtained theoretically similar

relationships [Eqs. (3-6) and (3-7)] in the generalization function calculated from the trial-by-trial changes in the aftereffects.

Estimating the function of the primitives. Here, we assume that the encoding function can be represented by a Gaussian function. In the case of multiplicative and additive encoding, the primitive can be represented, respectively, as:

$$g_j(\theta_r, \theta_l) = \left\{a_r \exp\left[\frac{-(\varphi_{rj}-\theta_r)^2}{2\sigma_r^2}\right] + b_r\right\}\left\{a_l \exp\left[\frac{-(\varphi_{lj}-\theta_l)^2}{2\sigma_l^2}\right] + b_l\right\} \qquad (3\text{-}8)$$

and

$$g_j(\theta_r, \theta_l) = a_r \exp\left[\frac{-(\varphi_{rj}-\theta_r)^2}{2\sigma_r^2}\right] + a_l \exp\left[\frac{-(\varphi_{lj}-\theta_l)^2}{2\sigma_l^2}\right] + b \qquad (3\text{-}9)$$

where $a.$ and $b.$ are constants, and $\varphi.$ indicates the preferred direction.

Substitution of Eqs. (3-8) or (3-9) into Eq. (3-5) yielded the theoretical transfer function

$$\Phi(\Delta\theta_r, \Delta\theta_l) = \frac{\left\{{a_r}^2\sigma_r \exp\left[-\frac{(\Delta\theta_r)^2}{4\sigma_r^2}\right] + 2\sqrt{2}a_r b_r \sigma_r + 2\sqrt{\pi}b_r^2\right\}\left\{{a_l}^2\sigma_l \exp\left[-\frac{(\Delta\theta_l)^2}{4\sigma_l^2}\right] + 2\sqrt{2}a_l b_l \sigma_l + 2\sqrt{\pi}b_l^2\right\}}{\left\{{a_r}^2\sigma_r + 2\sqrt{2}a_r b_r \sigma_r + 2\sqrt{\pi}b_r^2\right\}\left\{{a_l}^2\sigma_l + 2\sqrt{2}a_l b_l \sigma_l + 2\sqrt{\pi}b_l^2\right\}} \qquad (3\text{-}10)$$

for the multiplicative encoding case, and

$$= \frac{\sqrt{\pi}{a_r}^2\sigma_r \exp\left[-\frac{(\Delta\theta_r)^2}{4\sigma_r^2}\right] + \sqrt{\pi}{a_l}^2\sigma_l \exp\left[-\frac{(\Delta\theta_l)^2}{4\sigma_l^2}\right] + 2a_r a_l \sigma_r \sigma_l + 2\sqrt{2\pi}a_r b\sigma_r + 2\sqrt{2\pi}a_l b\sigma_l + 2\pi b^2}{\sqrt{\pi}{a_r}^2\sigma_r + \sqrt{\pi}{a_l}^2\sigma_l + 2a_r a_l \sigma_r \sigma_l + 2\sqrt{2\pi}a_r b\sigma_r + 2\sqrt{2\pi}a_l b\sigma_l + 2\pi b^2} \qquad (3\text{-}11)$$

for the additive encoding case.

In order to estimate the parameters in the primitives (Eqs. (3-8) and (3-9)), the data of

motor learning transfer when changing the movement direction of one arm in Exp. 1 (i.e., $\Phi(\Delta\theta_r, 0)$ and $\Phi(0, \Delta\theta_l)$) were fitted by a Gaussian function:

$$\Phi = c \exp\left(-\frac{\Delta\theta^2}{2\sigma^2}\right) + d, \qquad (3\text{-}12)$$

using the method of least squares. Then, the parameters of the primitives (Eq. (3-8) or (3-9)) were estimated by comparing the parameters of Eq. (3-12) with Eq. (3-10) or (3-11).

Estimating the parameters α and K. The trial-dependent changes in movement error when a constant force f is imposed for only a particular movement combination (θ_r, θ_l) is:

$$e^{(n)} = \frac{K[d(\theta_l)]^2 f \boldsymbol{g}^t \boldsymbol{g}}{1-\alpha+Kd(\theta_l)\boldsymbol{g}^t\boldsymbol{g}}[\alpha - Kd(\theta_l)\boldsymbol{g}^t\boldsymbol{g}]^{(n-1)} + \frac{(1-\alpha)d(\theta_l)f}{1-\alpha+Kd(\theta_l)\boldsymbol{g}^t\boldsymbol{g}}, \qquad (3\text{-}13)$$

where $\boldsymbol{g}$ is the abbreviation of $\boldsymbol{g}(\theta_r, \theta_l)$. We estimated the values of K by fitting the trial-dependent changes in the training phase with Eq. (3-13). The value of α was set to 0.996 in advance, adopted for the slow process of motor learning (Smith et al., 2006). We ignored the contribution of the fast process because a relatively high number (500 - 1000) of training trials were performed in our experiments.

Simulation of state space model. The simulations of Experiments 1, 3, 4, and 5 were performed 100 times each using Eqs. (3-1)–(3-3) with the identified primitive [i.e., Eq. (3-8) for the multiplicative

model or Eq. (3-9) for the additive model]. The task schedule was randomized for the 100 simulations, and the output data were averaged. The initial condition was $\boldsymbol{w} = \mathbf{0}$.

Statistics: Experiments 1 and 2. To determine the effect of the movement of the opposite arm on the aftereffects, a one-way repeated-measures ANOVA with factors of the opposite-arm movement direction (6 directions) was performed for the data obtained when the trained arm was moving in the original direction. A post-hoc multiple comparison test (Tukey-Kramer) was then performed to explore differences in the aftereffect among 6 movement directions of the opposite arm.

To test which encoding scheme, additive or multiplicative, was more likely, we compared the actual aftereffects and the artificial aftereffects constructed based on each encoding scheme. More specifically, to construct the artificial data of the generalization curve $\bar{f}(\theta_r, \theta_l)$, the aftereffects obtained when only the movement direction of the trained arm was changed (8 data points, i.e., $\hat{f}(0, \theta_l)$) were shifted as $\bar{f}(\theta_r, \theta_l) = \hat{f}(0, \theta_l) + \hat{f}(\theta_r, 0) - \hat{f}(0,0)$ for additive encoding or multiplied as $\bar{f}(\theta_r, \theta_l) = \hat{f}(0, \theta_l)\hat{f}(\theta_r, 0)/\hat{f}(0,0)$ for the multiplicative encoding model. We used 13 aftereffects [i.e., $\hat{f}(0, \theta_l)$ and $\hat{f}(\theta_r, 0)$] to predict the other 35 aftereffects using both multiplicative and additive models. Then, the sums of the squared residual errors between the predicted and actual aftereffects of those 35 data points were calculated for each participant; the

data of the multiplicative and additive models were subsequently compared using one-way repeated-measures ANOVA with factors of model type.

Statistical analysis: Experiments 3, 4, and 5. To evaluate how accurately the model predicted the actual aftereffects, we performed linear regression between the aftereffects obtained experimentally ($\hat{f}_{\mathrm{exp}}$) and those predicted by the model ($\hat{f}_{\mathrm{mdl}}$) as $\hat{f}_{\mathrm{exp}} = \beta_1 + \beta_2 \hat{f}_{\mathrm{mdl}}$ [the number of data was calculated as movement configurations × participants; i.e., 640 (64 × 10) for Exp. 3 and 80 (16 × 5) for Exp. 4 and 5]; the correlation coefficient (R^2), intercept (β_1), and slope (β_2) were also calculated. Since the β_1 and β_2 may differ by participant, we checked the validity of the regression by performing linear regression with a linear mixed model: $\hat{f}_{\mathrm{exp}} = \beta_1 + \beta_2 \hat{f}_{\mathrm{mdl}} + b_1 + b_2 \hat{f}_{\mathrm{mdl}} + \varepsilon$, where the b_1 and b_2 are random effects (participant) of the intercept and slope, respectively. Since the inclusion of the random effects did not significantly improve the regression in Experiments 3–5 ($P > 0.05$ by the likelihood-ratio test), we adopted a simple linear model.

3.4 Results

Experiment 1: Effect of motor learning transfer when changing each arm's movement direction

This experiment was designed to investigate how the adaptation of the left arm to a novel force field acquired while reaching both arms forward was transferred to the same arm when the movement directions of both arms were changed (8 directions for the trained arm and 6 directions for the opposite arm, i.e., 8 × 6 = 48 combinations; Fig. 3.1*C*) and when the movement was performed unimanually (8 directions). With the training, the lateral deviation of the left handle at the peak velocity gradually decreased (Fig. 3.2*A*). After the 80 training trials, we performed catch trials at every other trial. The lateral movement deviation of trials immediately following the catch trials was not significantly different from those of the last 10 trials of the training phase ($P = 0.5633$ by *t*-test; Fig. 3.2*A*). This indicated that catch trials using the error-clamped method did not deteriorate the motor learning performance, and confirmed the validity of conducting the catch trials so frequently. The adaptation of the trained hand did not seem to influence the untrained hand. There was no significant lateral deviation throughout the experiment (Fig. 3.2*B*, *t*-test with Bonferroni correction for 4 bins of 20 trials), which is consistent with the results of recent studies showing that there is no influence of the perturbation to one arm on another hand when 2 cursors are appropriately presented for both arms (Diedrichsen, 2007).

First, we demonstrated how the movement direction of each arm influenced motor learning transfer. Figure 3.2 indicates the aftereffects when the movement direction of the trained arm (Fig. 3.2*C*) or the opposite arm (Fig. 3.2*D*) was changed while maintaining the movement direction of the other arm in the original trained direction. When the movement direction of the trained arm was altered, the aftereffect gradually decreased as the movement direction deviated more from the original direction, converging monotonically to 0 when the angular difference was greater than 90º (Fig. 3.2*C*, *E*). Figure 3.2*E* also shows the generalization pattern observed in the unimanual movement. The amplitude of the generalization function decreased during the unimanual movement, demonstrating the partial motor learning transfer from bimanual to unimanual movement, which was reported in previous studies (Nozaki et al., 2006; Nozaki and Scott 2009). In contrast to previous studies (Donchin et al., 2003), a bimodal generalization pattern was not observed; the aftereffects for an angular difference of 180º were not significantly different from those of 90º.

A similar decay pattern in the aftereffect was observed when the movement direction of the opposite arm was changed (Fig. 3.2*D*, *F*). However, unlike the pattern for the trained arm (Fig. 3.2*C, E*), the aftereffects decayed to approximately 61.7 ± 16.5% (mean ± SD) of the aftereffect of the original direction (Fig. 3.2*F*). The movement directions of the opposite (right) arm significantly affected the aftereffect ($F_{5,35}$ = 16.3, $P < 0.001$ by one-way repeated measures ANOVA), and a post-hoc test revealed significant differences for several movement directions (0º vs. [30º, ±60º, or

±180º], 30º vs ±180º, and -30º vs [±60º or ±180º]), indicating that the aftereffect was a smooth function of the movement direction of the opposite arm and that the movement direction of the opposite arm smoothly interferes with the internal model.

The generalization pattern is considered to reflect the possible encoding pattern of the kinematics in the primitives of the internal model (Thoroughman and Shadmehr, 2000; Donchin et al., 2003; Hwang et al., 2003; Poggio and Bizzi, 2004; Sing et al., 2009). The generalization pattern observed when changing the opposite-arm movement direction suggests that the primitives also encode neuronal information that changes smoothly with the kinematics of the opposite arm.

The generalization curves (Fig. 3.2*E, F*) were fitted well by the Gaussian function (Eq. (3-12)): The variance explained by this model was high (R^2 = 0.85 and 0.94 for $\Phi(0, \Delta\theta_l)$ and $\Phi(\Delta\theta_r, 0)$, respectively). From the estimated parameters (c, d, and σ) summarized in Table 3.2, we calculated the concrete encoding function for the additive and multiplicative encoding models [Eqs. (3-8) and (3-9)] (Fig. 3.3*A, B*). The parameters are also shown in Table 3.2.

Experiment 1 and 2: Whole generalization pattern

We trained the identified multiplicative and additive models with the task of Experiment 1. Both models exhibited almost identical generalization patterns in $\Phi(\Delta\theta_r, 0)$ and $\Phi(0, \Delta\theta_l)$ but predicted completely different patterns of generalization when the movement directions of both arms were simultaneously changed (Fig. 3.3*C, D*). As expected from Eqs. (3-6) and (3-7), the

multiplicative encoding model predicted the change of the amplitude of the generalization curves, and the additive model predicted the upward or downward shift of the curves (Fig. 3.3*C, D*).

Although the additive model predicted negative learning transfer when the movement configurations were more different from the training configuration, this was not indicated in the actual data (Fig. 3.4*A*). In contrast, the actual data appear to support the prediction made using the multiplicative model (Fig. 3.4*A*). To statistically test which model explained the actual data more accurately, we predicted the aftereffect data of 35 movement configurations from those of 13 movement configurations using both additive [Eq. (3-8)] or multiplicative [Eq. (3-9)] models. The residual sums of squares between the actual and predicted aftereffects of both models were then statistically compared by one-way repeated-measures ANOVA. We found a significant main effect of model ($F_{1,7} = 21.96$, $P < 0.005$) for Experiment 1. In Experiment 2 in which the right arm was trained, we also found a significant main effect of model ($F_{1,7} = 9.03$, $P < 0.05$, Fig. 3.4*B*), suggesting that the multiplicative model explains the data more accurately than the additive model.

Experiment 3: Generalization of motor learning performed in multiple movement configurations

In Experiments 1 and 2 in which only one movement configuration was used for the learning of a force field, the generalization patterns to the other movement configurations were not localized around the movement configuration for the training, but were elongated along the axis of the

opposite arm's movement direction (Fig. 3.4). With this generalization pattern, when participants tried to learn different force fields simultaneously with different movement configurations, the training effects obtained with training movement configurations should influence each other and create a particular generalization pattern. Experiment 3 aimed to examine this issue and determine how accurately our multiplicative encoding model identified above in Exp. 1 (Table 3.2) could predict the global motor learning pattern.

Figure 3.5*A* shows the generalization pattern measured for 64 different combinations of movement directions (8 directions for each arm) when the training was performed at movement configurations of (0, 0), (0, 180), (180, 0), and (180, 180). The participants exhibited significant aftereffects at these 4 points ($P < 0.001$ by *t*-test with Bonferroni correction), and the training effect gradually decayed around the training configurations This pattern was quite similar to that predicted by the multiplicative model (Fig. 3.5*B*). Linear regression between the predicted and actual aftereffects produced an R^2 value of 0.38 ($P < 0.001$); in addition, the intercept and slope of the regression line were close to 0 (-0.01 ± 0.03) and 1 (1.03 ± 0.05), respectively (mean ± SD). These results suggest that without altering the parameters of the multiplicative model identified in Exp. 1, the model accurately predicted not only the generalization pattern but also the size of the actual aftereffects even when the training was simultaneously performed at multiple movement configurations. In contrast, due to the nonlinear dependence of the force direction on the movement

direction, the additive model could not adapt to this force field at all (Fig. 3.5*C*), which sharply contrasts from the patterns of the aftereffects exhibited by the participants.

Experiments 4 and 5: Construction of arbitrary force output by the internal model

Experiments 4 and 5 were designed to investigate whether the participants could actually adapt their arm movements to a much more complicated force field that depended on the movement directions of both arms in a nonlinear fashion. The multiplicative model, whose predictions were already demonstrated to be very accurate, should enable the participants to learn such complicated force fields. As expected, the observed pattern of the aftereffects measured after a sufficient amount of training was similar to that with imposed force fields (Fig. 3.6*A, B*). These patterns were similar to those predicted by the multiplicative encoding model whose parameters were identified in Exp. 1 (Fig. 3.6*C, D*). The same linear regression analysis as the one used in Experiment 3 showed that the R^2 values between the predicted and actual aftereffects were significant ($P < 0.001$) for Exp. 4 (0.72) and Exp. 5 (0.76). In addition, the intercept and slope of the regression line of Exp. 4 and 5 were close to 0 and 1 (0.02 ± 0.05 and 1.08 ± 0.08 for Exp. 4; 0.17 ± 0.06 and 1.45 ± 0.09 for Exp. 5; mean ± SD). The slope was significantly greater than 1 in Exp. 5 ($P < 0.05$), while it was not significantly different from 1 in Exp. 4 ($P > 0.05$). Thus, although the actual aftereffects tended to be greater than the predicted aftereffects in Exp. 5, the multiplicative model was able to predict the size of the aftereffects without adjusting the parameters. In contrast, the additive model could not learn

the force fields due to the nonlinear dependence on the movement directions (Fig. 3.6*E, F*). These results indicate great flexibility in constructing internal models through the linear combination of primitives that multiplicatively encode the movement directions of both arms.

3.5 Discussion

Performing flexible bimanual movement requires the internal model for each arm to predictively compensate for mechanical interactions resulting from the movement of both arms. Thus, the internal model must integrate the kinematics information from the opposite arm in addition to the relevant arm. By examining the adaptation of reaching movements to novel force fields, we demonstrated that an internal model for each arm multiplicatively encodes the movement directions of both arms and that such multiplicative encoding provides us with a flexible ability to compensate for the mechanical interaction between arms.

Encoding of opposite-arm kinematics in the primitives

As demonstrated by previous studies using a bimanual task in which the position of one arm is maintained during a disturbance resulting from the movement of the opposite arm (Viallet et al., 1992; Bays and Wolpert, 2006; Johansson et al., 2006; Jackson and Miall, 2008), the brain can predictively compensate for mechanical disturbance by utilizing information about the opposite arm's movement. Recent studies suggest that the brain displays such an ability even during reaching

movements. Two distinct internal models for an arm movement can be constructed depending on whether the other arm is moving or stationary (Nozaki et al., 2006), and whether the other arm is moving in the same or opposite (or orthogonal) direction (Howard et al., 2010). Although it is highly difficult to evaluate the details of the encoding scheme from only these results, the data suggest the possibility that the primitives of the internal models do encode the kinematics of the opposite arm.

Previous neurophysiological findings on the role of neurons in motor areas for motor learning also imply that the encoding of opposite-arm kinematics is very likely. Many neurons in the contralateral primary motor cortex (MI) are load sensitive (Evarts, 1968; Kalaska et al., 1989), and this load sensitivity emerges during motor learning (Gandolfo et al., 2000; Li et al., 2001; Arce et al., 2010). The neurons of the supplementary motor area (SMA) (Padoa-Schioppa et al., 2002; Padoa-Schioppa et al., 2004) and the premotor area (Xiao et al., 2006) of the contralateral hemisphere are also involved in the adaptation to novel loads. Thus, the adaptation to a novel force field can be viewed as the development of a load representation in a population of neurons in these areas.

Interestingly, movement of the ipsilateral arm also modifies the activity of neurons in these motor areas (Donchin et al., 1998; Cisek et al., 2003; Ganguly et al., 2009). Therefore, when the left arm is adapted to a force field while the right arm is being moved in a particular direction, the representation of the force field is constructed specifically for the right-arm movement direction. As

such, when the movement direction of the right arm changes from this original direction, the neuronal influence of the right arm also changes, which should result in the degradation of left-arm motor learning. Furthermore, considering that the influence on the MI neuron response smoothly changes with ipsilateral arm movement direction during bimanual movement (Rokni et al., 2003), the degree of the interfering effects is also likely to change smoothly with movement direction.

Consistent with these speculations, we found that the influence of the opposite-arm movement direction on motor learning (i.e., aftereffects) smoothly changed with direction (Fig. 3.2*F*). This indicates that the primitive encodes neuronal information that changes smoothly with the movement of the opposite arm. It also provides strong evidence against the view that the formation of distinct motor memories according to the kinematics of the opposite arm (Nozaki et al., 2006; Howard et al., 2010) can be explained by regarding the kinematics as cognitive cues (Osu et al., 2004; Cothros et al., 2009); such a scheme would result in abrupt, not smooth, changes in the aftereffect.

Gain-field encoding in the primitives

Our next hypothesis was that the primitives integrate the movement directions of both arms multiplicatively rather than additively. Multiplicative neuronal integration, known as "gain fields", was first reported for neurons in posterior parietal cortex (LIP and 7a) (Andersen and Mountcastle, 1983; Andersen et al., 1985) and later found in many other areas in the brain, including subcortical

structures (Lal and Friedlander, 1990; Van Opstal et al., 1995; Boussaoud et al., 1998; Wang et al., 2010). It has been theorized that such gain-field encoding is beneficial for sensorimotor transformation from multiple neuronal inputs (Pouget and Sejnowski, 1997; Salinas and Sejnowski, 2001). More specifically, neurons with gain-field encoding work as a set of basis functions enabling downstream neurons to construct arbitrary outputs by flexibly and linearly combining them (Pouget and Sejnowski, 1997).

Similar to the above problem of creating a sensorimotor transformation mapping, the construction of internal models for arm movement can be regarded as a process of creating an arbitrary map from desired sensory states to a motor command for the relevant arm by flexibly combining primitives. Thus, if the gain-field encoding is equipped with the primitives, this property would give the brain great flexibility in constructing an arbitrary force output from the desired state of both arms to a motor command for each arm.

We tested these multiplicative and additive encoding schemes in the primitives by investigating the generalization function of motor learning (Hwang et al., 2003; Wainscott et al., 2005). Multiplicative or additive encoding predicts, respectively, multiplicative or additive generalization functions [Eqs. (3-8) and (3-9)]. Our results clearly indicate that multiplicative encoding is more likely (Fig. 3.3 and 3.4), which is consistent with our speculation based on previous theoretical work.

The strength of multiplicative encoding was exemplified by Experiments 4 and 5, in which participants adapted their left-arm movements to force fields that nonlinearly depended on the movement directions of both arms (Fig. 3.6). We used 2 different force fields with magnitudes that depended on the directional difference between the arms in either an extrinsic or intrinsic workspace (Fig. 3.1*E, F*). Due to the nonlinear dependence of the force fields on the movement directions of both arms, the additive encoding model cannot adapt to them (Fig. 3.6*E, F*), indicating that the motor learning system of bimanual movement is unlikely to place special emphasis on bimanual movement patterns, such as mirror-symmetric, parallel movements. Rather, any meaningful association between the force field and the movement patterns of both arms (Ahmed et al., 2008) may arise as a consequence of the greater flexibility in motor learning offered by multiplicative encoding of primitives.

Possible scheme of bimanual movement control

On the basis of the present results, we can speculate about a possible scheme of bimanual movement control that compensates for the mechanical interaction between both arms (Fig. 3.7). This scheme assumes that the information regarding the desired movement of the opposite arm, the efference copy from the opposite arm's movement controller, or both multiplicatively influences the internal model of each arm. The assumption that the contribution of sensory input is negligible can be justified by the results of a recent study demonstrating that distinct internal models cannot be

established when the opposite arm is passively moved (Howard et al., 2010). We also assume that the contribution of the efference copy is relatively weak, because the trajectory of the right arm was not affected by the adaptation of the left arm (Fig. 3.2*B*). The adaptation to the force field should change the efference copy, which should influence the controller of the opposite arm.

It is well known that bimanual neuronal interactions exist when bimanual actions are performed (Swinnen, 2002; Rokni et al., 2003; Swinnen and Wenderoth, 2004; Carson, 2005). However, the functional role of such neuronal interactions remains unclear. In fact, such interactions are often considered to be a source of bimanual interference that needs to be overcome (Swinnen, 2002). The results of the current study provide a novel interpretation of how these neuronal interactions may play a crucial role in the flexible control of bimanual movements (Fig. 3.7). Without such multiplicative interfering effects, the neural control process for the movement of an arm is unable to take movement of the other arm into account to compensate for the mechanical interaction between both arms' movements. The present study provides, to our knowledge, the first behavioral example that gain-field encoding is essential for flexible bimanual movement control and provides a possible clue to how the brain orchestrates the movements of multiple body parts into a single unified action.

Figures and Tables

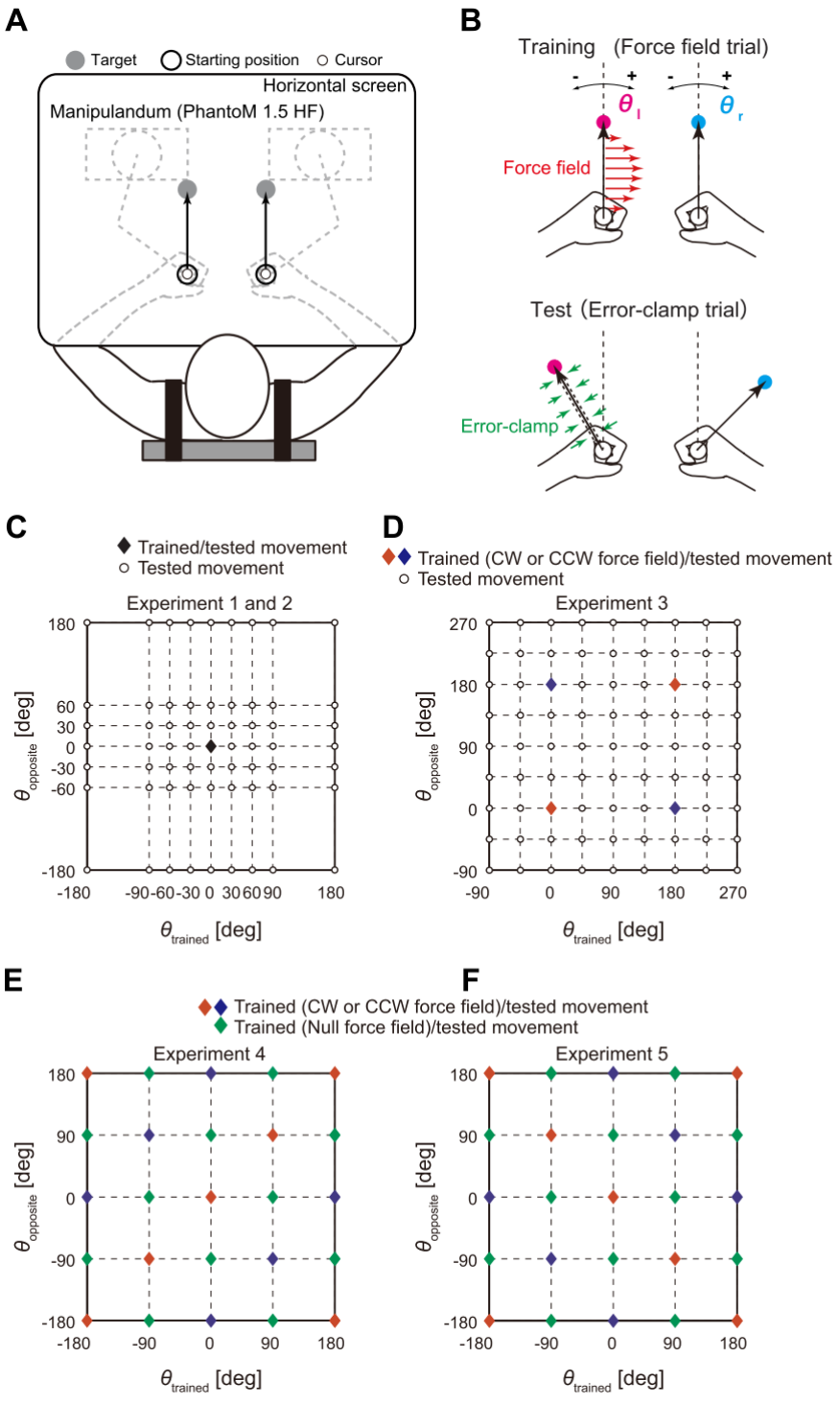

Figure 3.1. Experimental setup.

A, The participants made simultaneous bimanual reaching movements from the starting point toward a peripheral target for each arm presented on a horizontal screen. **B,** A force field was applied to the participants' trained arm for the training (top panel). Error-clamped trials were alternated with standard trials in order to test the degree of motor adaptation (bottom panel). The movement direction toward a forward target was defined as 0º, and the movements in clockwise (CW) and counterclockwise (CCW) directions were positive and negative, respectively. **C–F,** Movement configurations for the training and testing trials. The diamonds indicate the movement configurations used for the training, while the open circles indicate the movement configurations for which the training effect was tested. For example, in Experiments 1 and 2 (**C**), participants learned the force field for the trained arm while moving both arms forward, as indicated by the diamond [$(\theta_{\text{trained}}, \theta_{\text{opposite}}) = (0, 0)$]. This training effect was then tested at the other movement configurations represented by open circles [e.g., $(\theta_{\text{trained}}, \theta_{\text{opposite}}) = (30, 60)$]. In panels **D–F**, the color of the diamonds indicate the kind of force field: blue and red indicate CW and CCW force fields, respectively (the direction of force field was reversed for half of participants), and green diamond indicates a null force field. It should be noted that several tested configurations are plotted twice [e.g., (180, 180) and (-180, -180) in (**C**), and (-90, -90) and (270, 270) in (**D**)]. It should also be noted that unimanual movements were also tested in Experiments 1 and 2, but these movements are not displayed in **B**.

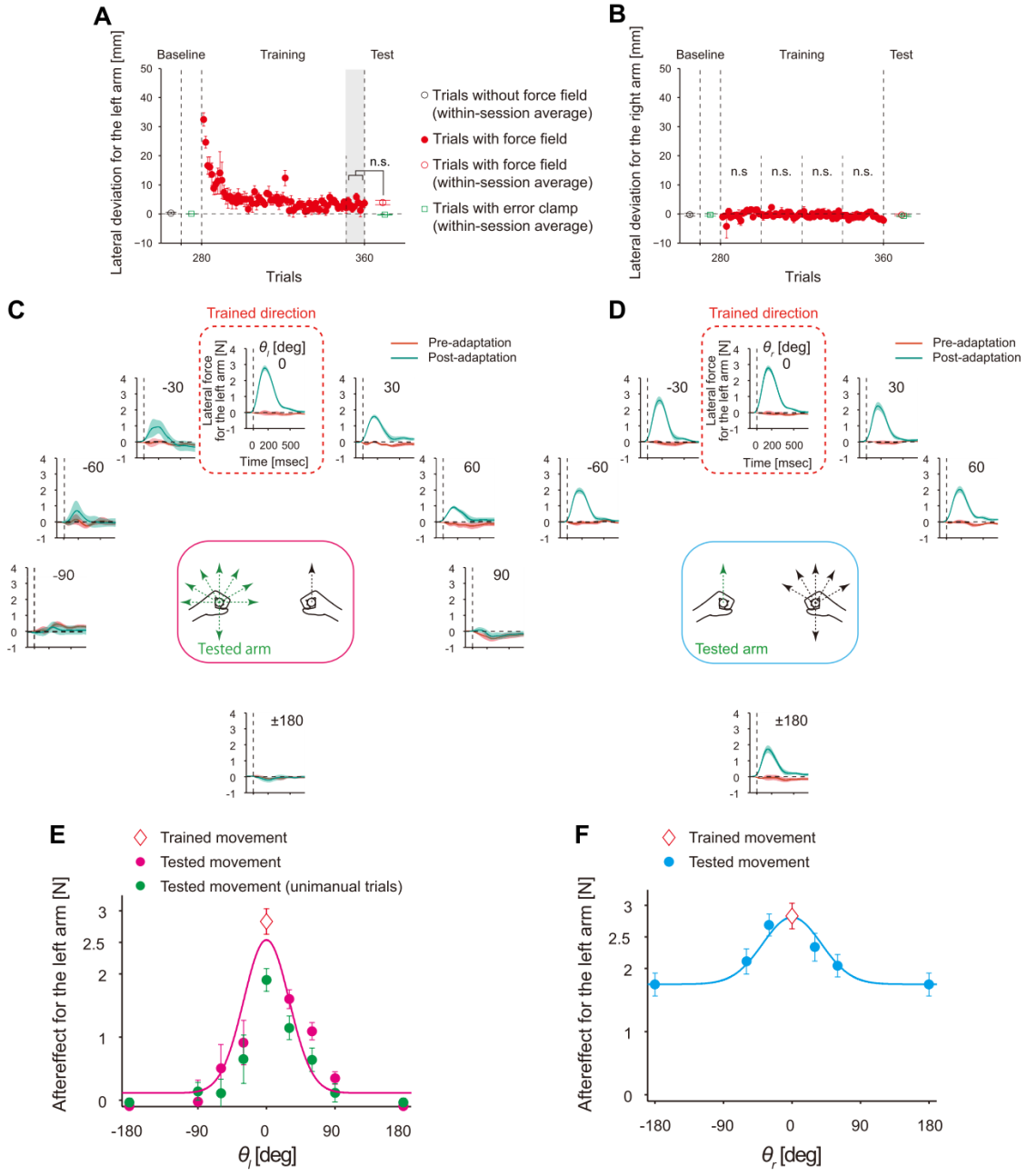
A
Baseline
Training
Test
Lateral deviation for the left arm [mm]
Trials
n.s.
Trials without force field (within-session average)
Trials with force field
Trials with force field (within-session average)
Trials with error clamp (within-session average)
B
Lateral deviation for the right arm [mm]
n.s
C
Trained direction
Pre-adaptation
Post-adaptation
Lateral force for the left arm [N]
Time [msec]
Tested arm
D
E
Trained movement
Tested movement
Tested movement (unimanual trials)
Aftereffect for the left arm [N]
F

Figure 3.2. Generalization pattern of motor learning of the left arm with the movement direction of each arm (Experiment 1).

A, **B**, Learning curves for the trained left arm (**A**) and untrained right arm (**B**). The data from all participants were averaged (error bars indicate SE). Filled red circles indicate trial-by-trial values of lateral hand deviation at the peak movement speed. Open red circles indicate within-session averaged values. Open green squares indicate within-session averaged values of lateral hand deviation during the error-clamp trials. Averaged lateral deviation of the left hand across the last 10 trials during the training session (grey shaded area) and within-session averaged values during the test session (open red circle in the test session) were not significantly different ($P > 0.05$ by *t*-test, **A**). It should be noted that no significant lateral deviation was observed for the right arm throughout the experiments ($P > 0.05$ by *t*-test with Bonferroni correction, **B**). **C**, **D**, Each peripheral plot displays the time-dependent profile of lateral force exerted by the trained left arm during the error-clamp trials before (pre-adaptation; red) and after (post-adaptation; green) the training session. The data were averaged over all participants and shaded areas indicate the SE. The location of each plot corresponds to the movement direction of the left (**C**) and right (**D**) arms, as illustrated by the center panel. **E**, **F**, Generalization patterns when the movement direction of the left (**E**) and right (**F**) arms was changed while the movement direction of the other arm was fixed (mean ± SE). Each point indicates the aftereffect of the trained left arm. Open diamond at the center indicates the data for the trained movement. The solid line is a Gaussian function fitted to the data.

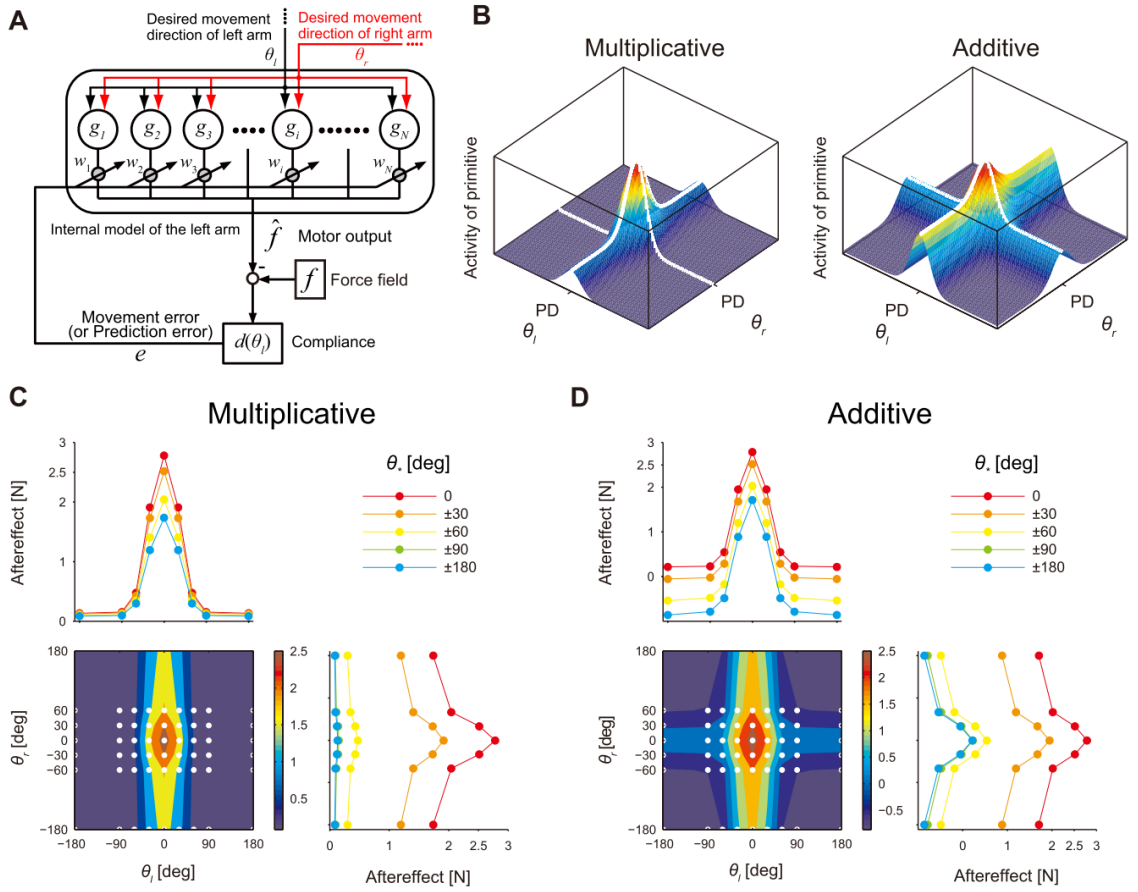

Figure 3.3. State space model for motor learning.

A, We assumed that the internal model for the left arm was composed of N primitives ($\boldsymbol{g} = (g_1, g_2, \ldots, g_N)$) for motor learning that receive the signals of desired movement directions of both arms (θ_r, θ_l). The contribution of each primitive ($\boldsymbol{w} = (w_1, w_2, \ldots, w_N)$) to net output ($\hat{f}$) was updated trial-by-trial according to the movement error (e). **B**, The response of a primitive with multiplicative (left) or additive (right) encoding predicted from the data shown in Fig. 3.2*D, E*. **C**, **D**, Simulated generalization patterns for multiplicative encoding (**C**) and additive encoding (**D**). Bottom left, contour plot of the generalization pattern. The color bar indicates the magnitude of the model output (i.e., aftereffect). White dots indicate the movement configurations at which the aftereffects were measured. Top left, generalization curve (aftereffect vs. θ_l). Bottom right, generalization curve (aftereffect vs. θ_r).

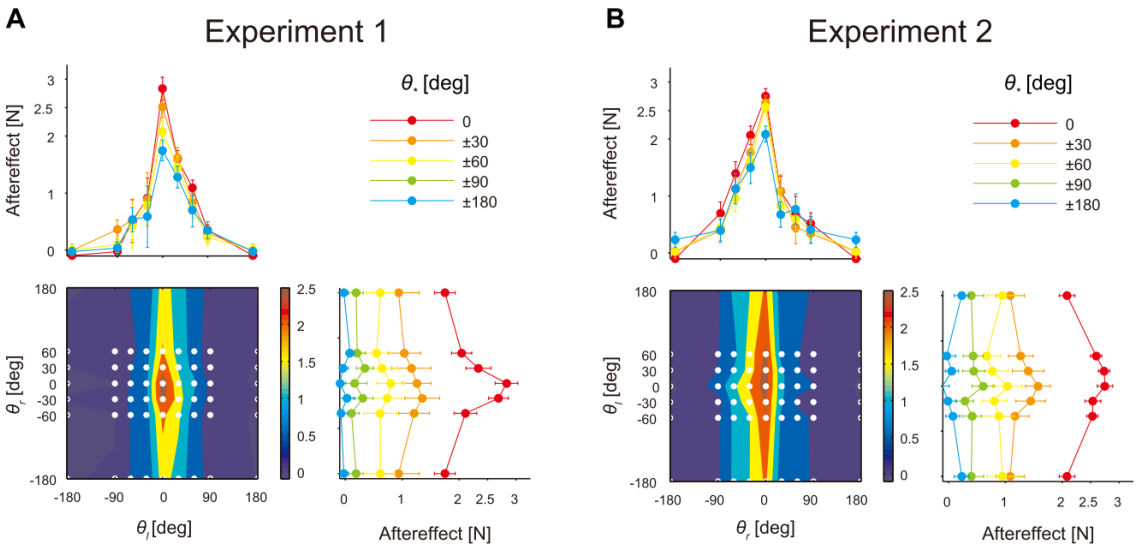

Figure 3.4. Gain modulation of the generalization pattern.

The whole structure of the generalization pattern for the trained left (**A**) and right (**B**) arms when reaching each arm in different directions after the training at $\theta_r = \theta_l = 0$. Bottom left, contour plot of the generalization pattern averaged across all participants. The color bar indicates the magnitude of the lateral force at the peak movement velocity. White dots indicate the movement configurations at which the aftereffects were measured. Top left, generalization curve (aftereffect vs. the movement direction of the trained arm). Bottom right, generalization curve (aftereffect vs. the movement direction of the opposite arm). Each point represents the aftereffect averaged across all participants (error bar indicates SE).

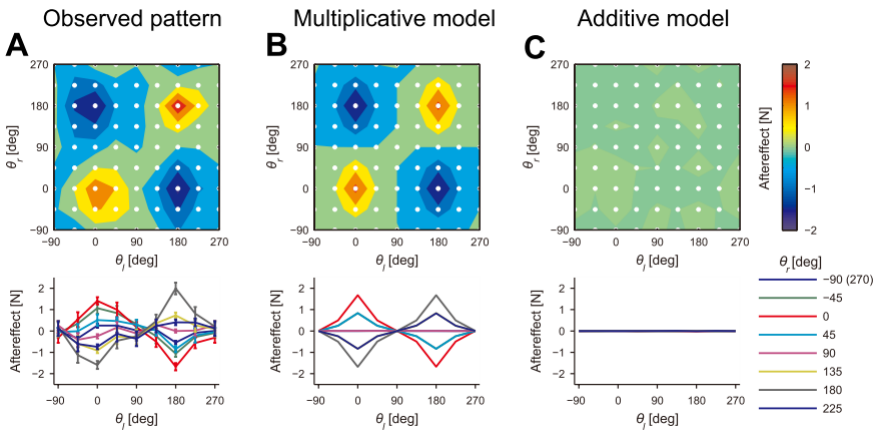

Figure 3.5. Generalization pattern when training was performed at multiple movement configurations.

A, Contour plot of the aftereffects in Experiment 3 (upper panel). The training was performed at 4 movement configurations [(θ_l, θ_r) = (0, 0), (0, 180), (180, 0), (180, 180)], and the aftereffects were measured at 64 movement configurations (8 movement directions for each arm) represented by the white dots. The lower panel indicates the relationship between the aftereffects and movement direction of the trained left arm for each movement direction of the untrained right arm (mean ± SE). **B**, **C**, The generalization pattern predicted by the multiplicative (**B**) and additive models (**C**).

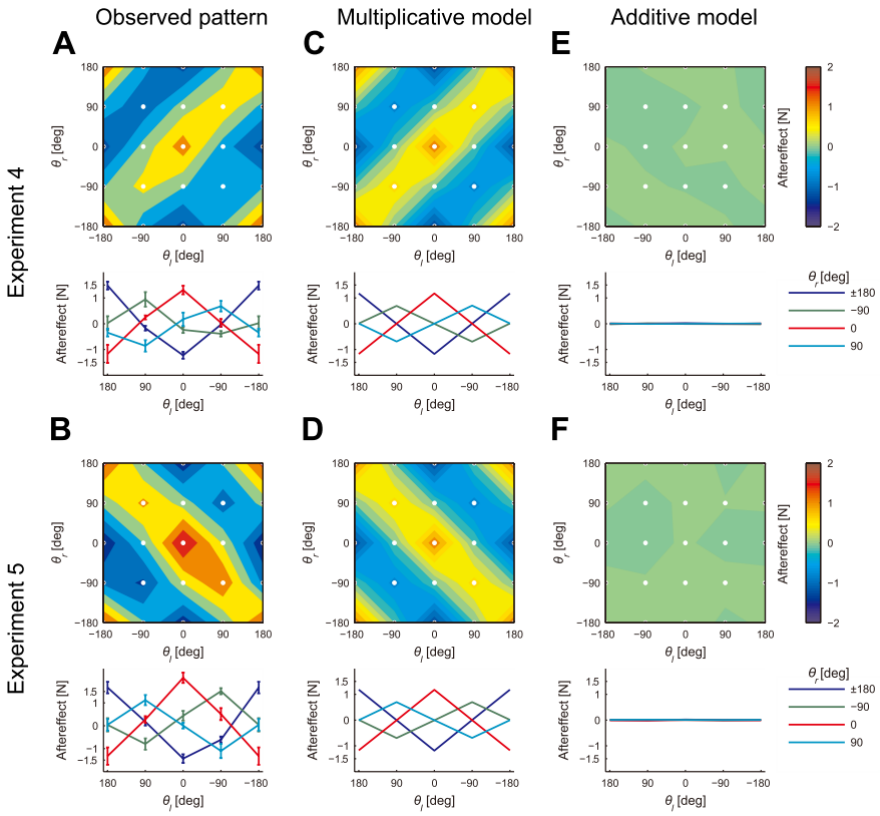

Figure 3.6. Simultaneous adaptation to complicated force fields. A, **B**, The upper panel shows the contour plot of the aftereffects for the trained left arm for Experiments 4 (**A**) and 5 (**B**). The white dots represent the training and tested movement configurations (4 movement directions for each arm). The lower panel shows the relationship between the aftereffects and movement direction of the trained left arm for each movement direction of the untrained right arm (mean ± SE). **C–F**, The aftereffects predicted by the multiplicative (**C, D**) and additive models (**E, F**).

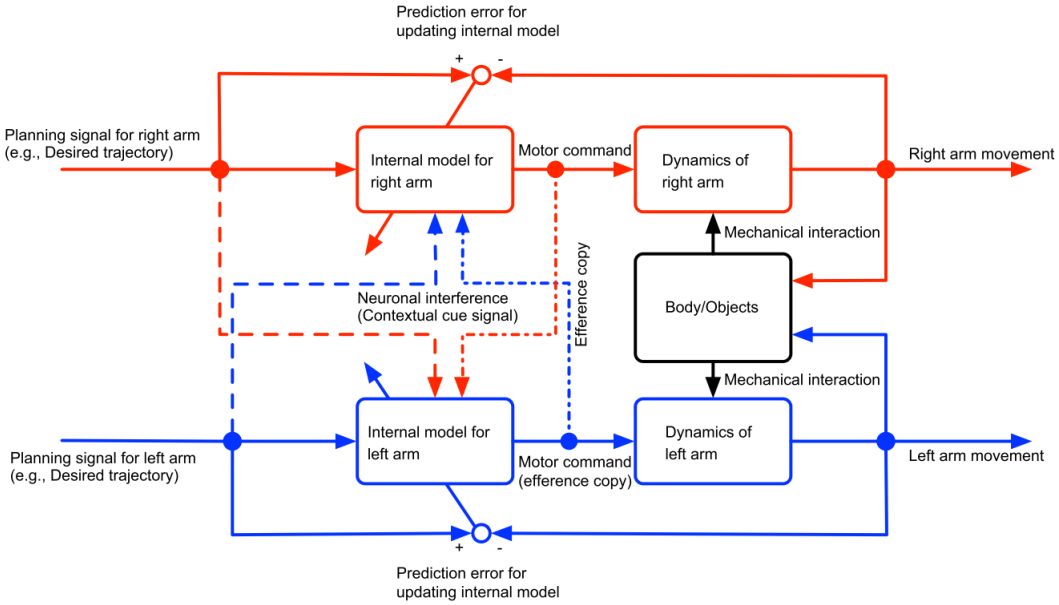

Figure 3.7. A possible feed-forward control scheme for the flexible bimanual movement deduced from our experimental results.

In bimanual movement, the internal model for each arm must compensate for the mechanical interactions resulting from movements of the other arm. Neuronal signals reflecting planned movements (broken lines) and/or efference copy of the other arm (dashed-dotted lines) may be multiplicatively integrated within the internal model of each arm. This multiplicative integration in the primitives contributes to construct a flexible output from each controller depending on the kinematics of both arms.

Table 3.1. Experimental conditions

Experiment	Trained arm	Movement configuration		Trial number		
		Training	Baseline/Test	Baseline	Training	Test
Exp 1 (N = 8)	Left	1	48	280	80	463
Exp 2 (N = 8)	Right					
Exp 3 (N = 10)	Left	4	64	192	160	399
Exp 4 (N = 5)	Left	16	16	144	960	192
Exp 5 (N = 5)	Left					

Table 3.2. Parameter estimates of generalization functions and primitives

	c	d	σ [°]	R^2
$\Phi(0, \Delta\theta_l)$	0.955	0.045	29.9	0.849
$\Phi(\Delta\theta_r, 0)$	0.377	0.623	38.5	0.940

Multiplicative	a_r	b_r	σ_r [°]	a_l	b_l	σ_l [°]
	1.00	0.318	27.2	1.00	0.0158	21.1

Additive	a_r	σ_r [°]	a_l	σ_l [°]	b
	0.553	27.2	1.00	21.1	-0.252

Common	N	α	K	$d(\theta_l)$
	100	0.996	0.00724	10 ($\theta_l = 0, 180$) 5 ($\theta_l = 90, 270$)

Chapter 4

Uncovered Hidden Functional Advantage of Non-dominant Arm For Flexible Bimanual Action

4.1 Abstract

The presumed inferiority of the non-dominant arm is so profound that the word “left” is often associated with negative concepts such as sickness, poverty, and evil in many cultures (Wilson; Beidelman, 1961; Needham, 1967). While it is often assumed that the dominant and non-dominant arms possess different inherent capabilities, recent studies have proposed distinct and specialized control strategies for both arms (Serrien et al., 2006; Sainburg, 2010). However, the functional role and mechanisms of this laterality are not well understood. Here, we demonstrate that the non-dominant arm has a superior ability that is uncovered only during the execution of bimanual movements. Participants performed bimanual reaching movements while the non-dominant hand was subjected to a force field. When the movement direction of the opposite arm differed from the trained direction, we found that the adaptation of the non-dominant arm was more poorly generalized. Applying our proposed theory presented in the previous chapter (Yokoi et al., 2011) to the generalization data revealed that the poorer generalization originated from a difference in parameters characterizing the motor memory; the motor memory of the non-dominant arm was more

strongly influenced by the kinematics of the opposite arm. We built a computational model that implemented this lateralized memory organization strategy. Remarkably, this model predicted that the non-dominant arm would demonstrate greater adaptability to the force fields associated with the opposite arm's movement, consistent with our experimental results. We conclude that the secondary supporting role often played by non-dominant arm in bimanual actions reflects its specialization rather than its inferiority.

4.2 Introduction

The motor learning system enables humans to perform limb movements and manipulate tools, even in the face of changing environmental constraints. This ability has been extensively investigated using an experimental paradigm in which a novel force field is imposed during a reaching movement (Shadmehr and Mussa-Ivaldi, 1994; Thoroughman and Shadmehr, 2000; Nozaki et al., 2006; Howard et al., 2012). Using this paradigm, previous studies have suggested that adaptation to a force field, f, is accomplished by the brain's ability to construct an internal model. This is accomplished through the flexible combination of the motor primitives, as $\hat{f} = \boldsymbol{w}^t \boldsymbol{g}$, where $\boldsymbol{g} = (g_1, g_2, .., g_N)^t$ and $\boldsymbol{w} = (w_1, w_2, .., w_N)^t$ are vectors comprised of motor primitives and weighting parameters, respectively (Thoroughman and Shadmehr, 2000; Donchin et al., 2003; Gonzalez Castro et al., 2011) (t indicates transpose). In Chapter 3, it was demonstrated that $\boldsymbol{g}$ encodes not only the

kinematics of the relevant limb, but also those of the opposite limb (Yokoi et al., 2011). In other words, $\boldsymbol{g}$ is function of both arms' kinematics.

From this perspective, the laterality in motor learning between dominant and non-dominant arms, if any, should be reflected as a difference in how $\boldsymbol{g}$ encodes the kinematics of both arms. In particular, flexible bimanual action depends on how $\boldsymbol{g}$ is altered by the kinematics of the opposite arm. Thus, we first investigated whether there was any difference between arms in the dependence of $\boldsymbol{g}$ with the movement direction, θ, of the opposite arm (i.e., the shape of $\boldsymbol{g}(\theta)$). To this end, we examined the generalization function, $\Phi(\Delta\theta)$. This function describes how the adaptation of 1 arm to a force field is generalized when the movement direction of the opposite arm changed by $\Delta\theta$.

4.3 Materials and Methods

Participants. A total of 45 healthy right-handers and 12 left-handers participated in this study. They participated in the current study after providing written informed consent. All experimental procedures were approved by the ethics committee of the Graduate School of Education, The University of Tokyo. Basic information [age, sex, and Laterality Quotient (L.Q.)] of participants for each experiment are summarized in the following table.

General task settings. The participants were instructed to make center-out reaching movements (amplitude: 10 cm, duration: 400 ms) both bimanually or unimanually holding the handles of 2 robotic manipulanda (Phantom 1.5 HF; SensAble Technologies, Woburn, MA, USA; Fig. 4.1*A*). The position of each handle was fed back as a white cursor (diameter, 6 mm) on a horizontal screen placed over the participants' arms (thus, they could not see their arms directly). The movements of the handles were constrained to a virtual horizontal plane by a simulated spring (1.0 kN/m) and dumper [0.1 N/(m/s)]. In order to reduce unwanted movement components, participants wore a wrist brace on each hand and the trunk was strapped to the chair. To reduce fatigue and allow maintenance of a constant arm posture, the upper arms were supported by slings.

Task flow. Initially, participants were instructed to move each cursor into its starting position (diameter = 10 mm; the distance between the starting positions for both arms was 16 cm). After a 2-s holding time, a gray target (diameter = 10 mm) appeared for each hand peripherally (10 cm) from each starting position. In the unimanual trial, only 1 target appeared and participants were instructed not to move the handle for the non-target side. After a further random holding time (1-2 s), the "go" cue was provided as a color change of the target. A warning message was presented on the screen if the movement speed of either handle was above ("Fast") or below ("Slow") a target range (399.5 ~ 540.5 mm/s). At the end of each trial, the handle of each manipulandum automatically returned to its starting position.

Force field. In each experiment, velocity-dependent force fields were generated to affect the handle's movement (Fig. 4.1*B*). The force is represented as $\boldsymbol{f} = \boldsymbol{B}\boldsymbol{v}$, where $\boldsymbol{f} = (f_x, f_y)^t$ [N] is the force to the handle, $\boldsymbol{v} = (v_x, v_y)^t$ [ms^{-1}] is the velocity of the handle, and $\boldsymbol{B}$ [N/ms^{-1}] is the viscosity matrix. For clockwise (CW) force field, $\boldsymbol{B} = [0 - 10; 10\ 0]$, and for counter-clockwise (CCW) force field, $\boldsymbol{B} = [010; -10\ 0]$.

Error clamp. To quantify motor adaptation, we employed the "error clamp" method (Scheidt et al., 2000; Smith et al., 2006; Sing et al., 2009). During error-clamped trials, the trajectory of the handle was constrained to a straight line toward the target by a virtual "channel" (Fig. 4.1*B*), in which any motion perpendicular to the target direction was constrained by a 1-dimensional spring (2.5 kN/m) and damper (25 N/ms^{-1}). This method enabled us to measure directly the lateral force exerted against the "channel". Post-experimental interview confirmed that only 1 out of 61 participants was aware of the presence of the channel during experiment. The data from this participant was excluded from the analysis.

Experiment 1. Experiment 1 was designed to examine laterality in the generalization of motor learning. That is, we investigated how the motor learning acquired while moving both arms forward is transferred when the movement direction of the opposite arm was changed. Participants (n = 24) were divided into 2 groups according to the arm used for training [group 1 (right arm, n =12); group

2 (left arm, n = 12)]. The experiment consisted of 135 trials for the baseline session, 100 trials for the training session, and 90 trials for the generalization session.

Baseline session. The participants began by performing bimanual movements under a null force field condition. The target for the trained arm was always presented at the forward position (i.e. 0º) and that for the untrained opposite arm was presented pseudo-randomly at 1 of 8 different positions (0º, 45º, …, 315º; Fig. 2*A*). Before the baseline session, participants performed 90 trials for practice. The error-clamped trials were also randomly interleaved once in 3 trials to obtain the lateral force against the channel for the baseline condition.

Training session. A CW (or CCW for a half of subjects) force field was imposed to one of the arms while the opposite arm was not subjected to the force field. Participants learned to move both cursors forward toward the targets simultaneously [i.e., the targets for both arms were always presented at 0º (Fig. 2*A*)]. To evaluate how the motor learning developed with the training, error-clamped trials were randomly interleaved once in 5 trials to quantify the lateral force against the channel.

Generalization session. The participants continued the training while moving both arms forward. Error-clamped trials were interleaved in every other trial to quantify how the lateral force against the wall was influenced by the movement direction of the opposite arm. Thus, in the

error-clamped trials, the target for the untrained arm was presented pseudo-randomly at 1 of 8 positions (0º, 45º,.., 315º; Fig. 4.2*A*).

In order to make a precise evaluation of the generalization of learning, we discarded the data from subjects who did not attain at least 80% adaptation to the imposed force field (one-sample *t*-test on last 10 channel trials). As a result, 8 subjects were excluded from analysis and 16 out of 24 subjects remained for further analysis (8 participants for each group). For group 1, 5 participants learned CW force field. In group 2, 4 participants learned CW field.

Experiments 2 and 3. These experiments were designed so that the same forward reaches of the left/right arm were exposed to conflicting (both CW and CCW) force fields associated with different movement directions of contralateral arm [i.e., (0º: CW), (90º: CCW), (180º: CW), (270º: CCW)] (Fig. 4.4*A*). The order of the 4 movement configurations was randomized. It should be noted that the movement direction for the trained arm was fixed to the forward direction. The experiment consisted of 340 trials: 60 trials for the baseline session, and 280 trials for the training session. The error clamp trials were randomly interleaved in 1 of 3 trials for the baseline session, and 1 of 7 trials for the training session. Thus, each movement was performed for 10 trials in the baseline session, and 60 trials for the training session. Twenty participants were divided into 2 groups (Exp 2; n = 10 each). For group 1, training was performed with the left arm, while subjects in group 2 learned the force

field with the right arm. The association between the force field direction and the movement direction was reversed for a half of subjects in each group [i.e., (0º: CCW), (90º: CW), (180º: CCW), (270º: CW)].

The same task described in experiment 2 was performed by left-handed participants (Exp 3; n = 12). Half of participants were assigned to the left arm learning group. The rest were assigned to the right arm learning group.

Data analysis. All data shown are baseline-subtracted values. The motion data for each manipulandum were recorded at a sampling rate of 500 Hz. The data for the handle velocity and force were low-pass filtered using a fourth-order Butterworth filter with a cutoff frequency of 8 Hz. For the index of adaptation, we calculated the learned viscosity coefficient, which was the lateral force, f, during the error-clamped trial measured at the time t_{pv} of peak movement velocity, v, divided by the velocity as, $\hat{B} = f(t_{pv})/v(t_{pv})$ [N/(m/s)]. The deviation of this value from that measured in baseline sessions was defined as "aftereffect". The performance of the trials in which the error-clamp method was not adopted (e.g., trials in the training session) was evaluated by the lateral deviation of each handle trajectory from a straight line between the starting position and target measured at the peak movement velocity. The data were then averaged across participants for

each experiment. The sign of the aftereffect from those who adapted to CCW force field were flipped before averaging.

Statistics. For Experiment 1, two-way ANOVA with factors of group (group 1 and group 2) and epoch (baseline, early, mid, and late) was performed on the aftereffect data. Epoch was defined as average values of 1-st to 5-th (baseline), 6-th and 7-th (early), 9-th and 10-th (mid), and 21-st to 25-th (late) channel data. For Experiments 2 and 3, two-sample *t*-tests were performed on the aftereffect data averaged across the last 5 channel trials. Effect size (Choen's *d*) was also calculated. For two-sample *t*-tests, if the variance of 2 groups were significantly different (by *F*-test), a Greenhouse–Geisser correction was applied to adjust for the appropriate degree of freedom. We applied either the Wilcoxon rank sum test or Fisher's exact test on the basic data (age, L.Q., and sex) of subjects whose data were used for subsequent analysis. The significance level was set at $P < 0.05$.

Parameter estimation and simulation.

State-space model. The force output of the internal model, $\hat{f}$, at the *i*-th trial is assumed to be represented by a linear combination of the activity of primitives [6, 9-11] as

$$\hat{f}^{(i)} = \left[\boldsymbol{w}^{(i)}\right]^t \boldsymbol{g}(\theta^{(i)}), \tag{4-1}$$

where θ is the movement direction of the *opposite* arm, and $\boldsymbol{g}(\theta) = [g_1(\theta), g_2(\theta), \cdots, g_N(\theta)]^t$ (Fig. 4.3*A*) and $\boldsymbol{w} = [w_1, w_2, \cdots, w_N]^t$ are column vectors whose

elements represent the output and weight of each primitive, respectively. Here, $\boldsymbol{g}$ should be a function of the movement directions not only of the opposite arm, but also of the trained arm. However, we considered only the dependence on the opposite arm since the movement direction of the trained arm was fixed in our experiment.

We assumed that the weighting parameter $\boldsymbol{w}$ is updated with the trials according to the movement error, e. This process can be represented as the state space model:

$$e^{(i)} = d(f^{(i)} - \hat{f}^{(i)}), \tag{4-2}$$

$$\boldsymbol{w}^{(i+1)} = \alpha \boldsymbol{w}^{(i)} + e^{(i)} K \boldsymbol{g}(\theta^{(i)}), \tag{4-3}$$

where f is the imposed force field, d is the compliance of the trained arm, and α and K are constants representing, respectively, the spontaneous loss of memory and the learning rate.

Estimation of parameters for the motor primitive. After sufficient training with the movement direction θ of the opposite arm, the force output should reach a plateau level. The generalization function $\Phi(\Delta\theta)$ is defined as the relative value of the force output when the movement direction of the opposite arm is changed by $\Delta\theta$. We previously demonstrated the generalization function can be represented [11] as:

$$\Phi(\Delta\theta) = \frac{\boldsymbol{g}(\theta)^t \boldsymbol{g}(\theta+\Delta\theta)}{\boldsymbol{g}(\theta)^t \boldsymbol{g}(\theta)}. \tag{4-4}$$

Further, we assume that each component of $\boldsymbol{g}(\theta)$ is represented by a Gaussian-like function [6, 9-11, 14, 15] as:

$$g_j(\theta) = a \exp\left[-\frac{(\theta-\varphi_j)^2}{2\sigma^2}\right] + b, \quad (4\text{-}5)$$

where a, b, σ, and φ_j are amplitude, offset, tuning width, and the preferred direction of the primitives (without loss of generality, we set $b = 1 - a$). When the preferred directions are assumed to be distributed uniformly, the generalization function can be simply represented as [11]:

$$\Phi(\Delta\theta) = c \exp\left\{-\frac{\Delta\theta^2}{4\sigma^2}\right\} + d, \quad (4\text{-}6)$$

where

$$c = \frac{a^2\sigma}{a^2\sigma + 2\sqrt{2}ab\sigma + 2\sqrt{2}b^2}, \quad (4\text{-}7)$$

$$d = \frac{2\sqrt{2}ab\sigma + 2\sqrt{2}b^2}{a^2\sigma + 2\sqrt{2}ab\sigma + 2\sqrt{2}b^2}. \quad (4\text{-}8)$$

We fit the generalization data (Fig. 4.2*C*, *D*) with Eq. (4-6), and then obtained a, b, and σ using Eqs. (4-7, 4-8). To increase the estimation accuracy, we pooled the data from the current experiment (Experiment 1) and the data from our published work (the data in Experiment 1 and 2 in Chapter 3 [11] were re-analyzed to the same form as used in the current study).

Calculation of parameters distributions. We estimated the distributions of parameter sets (a and σ) by bootstrapping (5000 re-samplings). First, Eq. (4-6) was fitted to the pooled data (here, this fitted function is referred as the estimated model), and the residual vector [size: {72 (the number of data points obtained in the current experiment) + 56 (the number of data points obtained in our previous experiment [11])} × 1] was obtained. Next, 5000 bootstrap residual vectors (size of each

vector: 128 × 1) were generated by randomly re-sampling from the original residual vector. Then, 5000 bootstrap data sets were generated by adding bootstrap residual vectors to the estimated model. By fitting Eq. (4-6) with the 5000 bootstrap data sets, we obtained 5000 bootstrap parameters. Finally, the density distributions of parameters were estimated by 2-dimentional kernel density estimation using Matlab *kde2d* function (Botev et al., 2010).

Simulation of motor learning. We wished to quantify the effect of the difference in the parameters for both arms on the adaptation to force field caused by the opposite arm's motion. To accomplish this, we simulated Experiment 2 with the state space model [Eqs. (4-1 - 4-3)] using the 5000 sets of bootstrapped parameters. For other parameters [α, d, and K in Eq. (4-3)], we used the same values for both arms because we did not observe a significant difference in initial error between groups (two-sample t-test, $P > 0.05$) or the amount of learning (two-way ANOVA, see *Statistical analysis*) in Experiment 1. Parameter values are summarized in the following table 4.2.

To mimic Experiment 2, in which 10 participants participated, we first randomly sampled 10 parameter sets from bootstrapped estimates of tuning parameters and then simulated Experiment 2. Simulated learning curves were then averaged across these 10 parameters sets. This process was iterated 1000 times to obtain 95% confidence intervals of simulated learning curves.

4.4 Results

Sixteen right-handed participants adapted to a velocity-dependent force field (FF) imposed on either the left or right arm (n = 8 for each) while they moved the handles of the manipulanda bimanually in the forward direction (Fig. 4.1*A*). The amount of motor learning was quantified by randomly interspersing probe trials. The force that the participants exerted against the virtual force channel (i.e., aftereffect) was directly measured (Gonzalez Castro et al., 2011) both during the training and generalization sessions (Fig. 4.1*B* and 4.2*A*, see Materials and Methods).

Previous studies have reported that the dominant arm exhibits a greater ability to adapt to novel dynamics during unimanual reach (Duff and Sainburg, 2007; Schabowsky et al., 2007). However, for the training session in the present study, the trial-dependent changes in the aftereffect (i.e., learning curves) were almost indistinguishable between the groups trained with right and left arms (two-way ANOVA, no significant main effect of group; $F(1, 14) = 1.5$, $P = 0.240$, Fig. 4.2*B*). Therefore, we observed no substantial difference between dominant and non-dominant arms in the ability to adapt limb movements to a novel dynamics during bimanual reach.

The generalization of motor learning was evaluated by changing the movement direction of the *untrained arm* (8 different target directions, Fig. 4.2*A*). As was observed in our previous study (Yokoi et al., 2011), the aftereffect for the *trained arm* decayed as the movement direction of the opposite, untrained arm deviated from the original trained direction (Fig. 4.2*C*). Notably, the shape

of the generalization function, $\Phi(\Delta\theta)$, had different amplitudes between both arms; the amplitude [i.e., $\{\Phi(0°) - \Phi(180°)\} \times 100$] was significantly greater for the left arm (43.7 ± 15.9 %) than for the right arm (28.6 ± 8.7 %) ($t(14) = 2.35$, $P = 0.03$).

These results indicate that when the movement direction of the opposite arm changes from the original training direction, the motor learning of 1 arm during bimanual movement is more fragile for the non-dominant left arm than for the dominant right arm. In other words, the interfering effect from the right arm to left arm was stronger than vice versa, showing the dominance of the right arm.

The lateralized generalization patterns indicate that how the primitives encode opposite arm motion differs between the right and left arms. Based on our previous paper, we estimated the function of primitives, $\boldsymbol{g}(\theta)$, from the generalization function $\Phi(\Delta\theta)$ using the theoretical relationship $\Phi(\Delta\theta) = \boldsymbol{g}(\theta)^{\boldsymbol{t}}\boldsymbol{g}(\theta + \Delta\theta)/\{\boldsymbol{g}(\theta)^{\boldsymbol{t}}\boldsymbol{g}(\theta)\}$. In particular, when we assume that each primitive is expressed as a Gaussian-like function, $g_j(\theta) = a \exp\left\{-\frac{(\theta-\phi_j)^2}{2\sigma^2}\right\} + b$ (Thoroughman and Shadmehr, 2000; Gonzalez Castro et al., 2011; Ingram et al., 2011; Yokoi et al., 2011; Brayanov et al., 2012), where $a + b = 1$ without loss of generality, and that the preferred direction ϕ_j is distributed uniformly, the generalization function can be also expressed by a Gaussian-like function: $\Phi(\Delta\theta) = c \exp\left\{-\frac{(\Delta\theta)^2}{4\sigma^2}\right\} + d$.

We began by fitting the data of the generalized pattern with the function $\Phi(\Delta\theta)$. Then, a and b were obtained from the c, d, and σ using the theoretical relationship between $\Phi(\Delta\theta)$ and $g_j(\theta)$. To investigate the possible distribution of the parameters a (tuning depth) and σ (tuning width) of the primitive, we repeated the estimation procedure for 5000 bootstrapping samples from the pooled data of the present experiment and that obtained in Experiment 1 and 2 of previous Chapter (Yokoi et al., 2011).

The distributions of estimated parameters for each arm were clearly dissociated (Fig. 4.3*B*). The probability of overlapping area between 2 density distributions (i.e., optimal Bayes error rate (Duda et al., 2001)) was smaller than 0.05. The values of a and σ were 0.73 ± 0.03 and 37.2° ± 12.1° for the left arm and 0.64 ± 0.03 and 45.0° ± 14.0° for the right arm (mean ± SD of the bootstrapping samples). Such greater tuning depth a and narrower tuning width σ for the left arm indicate that the primitives for the left arm are more sharply tuned with the opposite arm's movement direction. As was already argued in the generalization function, such sharper modulation with the opposite arm's movement direction suggested the dominant influence of the dominant right arm; the primitives of the non-dominant left arm were more strongly influenced by the dominant right arm.

The stronger influence from the opposite arm contributes to the steeper decay of $\Phi(\Delta\theta)$ with the change in the movement direction, $\Delta\theta$ (i.e., poorer generalization; Fig. 4.2*C*). However,

this does not necessarily have adverse effects. From the opposite viewpoint, poorer generalization leads to weaker interference in learning when moving the opposite arm in different directions. During bimanual action, mechanical interactions between the 2 arms can be mediated by the body and/or objects. Thus, the same motion of 1 arm could be exposed to various perturbations caused by the opposite arm's motion. Therefore, the successful control of bimanual action largely relies on the ability of neural controllers to predictively compensate for mechanical interactions arising from the motion of the opposite arm.

The poorer generalization (or equivalently, smaller interference) implies that a greater amount of motor memory is available when the opposite arm's motion changes. Thus, the sharper encoding of the opposite arm's motion could provide the non-dominant arm with a beneficial ability to adapt more flexibly to dynamics caused by the opposite arm's motion. Experiment 2 was designed to test this ability of the non-dominant arm. Twenty right-handed participants performed simultaneous bimanual reaching movements under the presence of FFs to 1 arm. Half of participants adapted to FFs applied to the right arm, while the others adapted to FFs applied to the left arm. The direction of the FF was switched between clockwise (CW) or counterclockwise (CCW) every time the movement direction of the opposite arm was changed by 90° [e.g., (0°: CW), (90°: CCW), (180°: CW), (270°: CCW), Fig. 4.4*A*]. The directions of the FFs were counterbalanced. Each of the 4 movement directions for the opposite arm was performed once within each cycle in a random order.

Many previous studies have shown that adaptation of limb movement to such conflicting force fields is extremely difficult (Gandolfo et al., 1996; Osu et al., 2004; Nozaki et al., 2006; Yokoi et al., 2011; Hirashima and Nozaki, 2012; Howard et al., 2012). The degree of motor learning was evaluated by interleaving probe trials, as was done in Experiment 1.

Before performing the experiment, we investigated how the amount of learning depended on the parameters a and σ of the primitives by simulation with a state-space model (Thoroughman and Shadmehr, 2000; Donchin et al., 2003; Lee and Schweighofer, 2009; Yokoi et al., 2011). The amount of motor learning was evaluated by averaging the compensatory force output of the model over 1 cycle (i.e., 4 movement directions). The simulated result indicates that deeper tuning amplitudes and narrower tuning widths are associated with increased adaptation (Fig. 4.4*B*). The simulation also predicts that the non-dominant left arm should demonstrate almost two-fold greater learning than the dominant right arm (Fig. 4.4*C, D*).

Figure 4.4*C* shows the experimental changes in the aftereffects averaged over the 4 movement directions. The aftereffects gradually increased with the training, but as the computational model predicted, the participants trained with the left arm exhibited significantly greater aftereffects than those trained with the right arm (one-tailed *t*-test, $t(16.33) = 3.01$, $P < 0.005$, Cohen's $d = 1.42 \pm 8.78$). Furthermore, these behavioral data were quite similar to the predicted values with respect to not only the amount of adaptation, but also the trial-dependent change of the learning curve (Fig.

4.4*C*). These results indicate that the observed laterality in learning ability between the right and left arms resulted from the laterality of the tuning parameters of the motor primitives.

We also had 12 left-handed participants perform the same task (Experiment 3). Half of participants trained with the dominant left arm, and another half with the non-dominant right arm. The superior left-handed motor learning observed in the right-handed participants disappeared in the left-handed participants, and the amount of adaptation did not differ significantly between groups ($P > 0.05$; Fig. 4.4*E, F*).

4.5 Discussion

It has been thoroughly reported that the dominant arm exhibits superior motor function in terms of movement accuracy, muscle strength, etc. (Woodworth, 1899; Annett, 1985; Elliott and Roy, 1996; Armstrong and Oldham, 1999; Duff and Sainburg, 2007). Popular beliefs about the absolute inferiority of the non-dominant arm have led numerous societies to associate the left hand with weakness, evil, or negativity (Wilson, 1891; Beidelman, 1961; Needham, 1967). However, recent several studies have focused on the lateralized function of each arm instead of emphasizing the superiority of the dominant arm. For example, Sainburg and colleagues have demonstrated that the dominant arm has a more specialized ability to control limb dynamics, while the non-dominant arm is more specialized for limb impedance control (Sainburg, 2010). However, evidence of superior

functional abilities of the non-dominant arm is not always apparent. In addition, the neuronal mechanisms behind the laterality remain poorly understood.

When performing bimanual actions, the movement of 1 limb may exert mechanical influences on the opposite limb. Therefore, it would be advantageous for a motor control system to generate appropriate motor commands considering these influences. We propose the following motor learning mechanism to accomplish this: the primitives of motor learning encode not only movement of the relevant arm, but also that of the opposite limb. This mechanism enables the controller of each arm to flexibly adapt to mechanical influences depending on the kinematics of the opposite arm. Importantly, this adaptability is determined by how the primitives of the motor learning system encode both arms' kinematics. Considering the possible supporting role of the non-dominant arm in bimanual action (Guiard, 1987; Johansson et al., 2006), we speculated that the lateralized ability of each arm, if any, could be more visible during bimanual movement. We further predicted that the laterality should be manifested as a difference in shape of the primitives function.

As expected, our experiment revealed a superior ability of the non-dominant arm that could only be observed while performing bimanual actions. The non-dominant arm has a greater capacity to adjust motor commands in dynamical environments resulting from opposite arm movement. This advantage is occluded when observing adaptation to a single FF, which only depends on the motion of the relevant arm during both bimanual (Experiment 1, Fig. 4.2*B*) (Tcheang

et al., 2007) and unimanual movements (Duff and Sainburg, 2007; Schabowsky et al., 2007; Tcheang et al., 2007). However, this effect emerges when faced with a complicated FF that depends on the motion of the *opposite* arm (Experiment 2, Fig. 4.4*C*, *D*), which is a characteristic of bimanual actions. Furthermore, we have also showed that this hidden advantage of non-dominant arm (Experiment 2) was well explained from the laterality of the primitives encoding the kinematics of the opposite arm (Fig. 4.3*B*).

Although the neural substrates for the primitive of motor learning are not fully elucidated, neurons in frontal motor areas, posterior parietal cortex, and cerebellum are thought to be involved (Li et al., 2001; Della-Maggiore et al., 2004; Padoa-Schioppa et al., 2004; Xiao et al., 2006; Mandelblat-Cerf et al., 2011; Donchin et al., 2012). For example, the neurons in primary motor cortex (MI) or premotor cortex (PM) that are tuned with the movement direction of the reaching hand (Georgopoulos et al., 1982; Cisek et al., 2003) change their tuning properties (e.g., preferred direction) after adaptation to a force field (Li et al., 2001; Xiao et al., 2006). This suggests that neurons in these motor areas are constituents of the primitives of motor learning. These neurons also receive the neuronal input from the contralateral hemisphere that depends on the kinematics of the opposite arm (Cisek et al., 2003; Rokni et al., 2003; Ganguly et al., 2009). In addition, neurons within the parietal reach region (PRR) show tuned activity for bilateral limb movement (Chang and

Snyder, 2012). Such interhemispheric neuronal influences on motor cortices have been also reported in humans using fMRI (Diedrichsen et al., 2012).

These previous findings led us to hypothesize that the motor memory formed with a particular movement pattern of bimanual movement could be deteriorated when the movement of the opposite arm changes, which is consistent with the results of the current and previous experiments (Yokoi et al., 2011). From this perspective, the laterality observed in the tuning pattern of the primitives (i.e., tuning depth and width) can be interpreted as the difference in the strength of the neuronal influence from the opposite arm, possibly through the corpus callosum (Franz et al., 2000). We suspect that the strength of this influence should be greater from dominant to non-dominant hemisphere than vice versa. It is well known that the sensory-motor areas in dominant hemisphere have greater influence over the non-dominant hemisphere than vice versa in both fMRI (Hayashi et al., 2008; Diedrichsen et al., 2012) and electrophysiological studies (Netz et al., 1995; Ziemann and Hallett, 2001; Duque et al., 2007). Such asymmetrical interhemispheric interaction is a possible neural substrate for the lateralized tuning in the primitives of motor learning.

One could argue that another possible factor for the lateralized primitive is a difference in attentional load. Reaching with the non-dominant arm to different directions may be more demanding than reaching with the dominant arm, which might contribute to a different motor generalization function shown in Fig. 4.2*C*. However, we consider this possibility to be unlikely,

because a large difference in attentional load would be expected to deteriorate motor learning. Consequently, we would expect to see the opposite of the results observed in Experiment 1 (Fig. 4.2*C*); the right arm should have exhibited greater decay than the left arm because of the greater attentional load associated with the motion of the left arm. In addition, a previous study has reported that simultaneous reaching of the second arm in different directions had no effect on the motor learning of the perturbed arm for both dominant and non-dominant arms (Tcheang et al., 2007). Taken together, the lateralized tuning property of motor primitive gives a more plausible explanation for the current results (Fig. 4.3*B* and Fig. 4.4*C, D*).

In conclusion, our results provide novel evidence that the functional advantage of the dominant arm does not extend to all aspects of motor planning (Annett, 1985; Elliott and Roy, 1996; Serrien et al., 2006). Further, the functional advantages of the non-dominant arm can be mechanistically explained by the concept of a motor primitive. We speculate that this functional asymmetry of the 2 arms during bimanual actions contributes to the sophisticated bimanual action by assigning the appropriate functional role for each arm (Guiard, 1987; Stout et al., 2008), but concrete evidence for this is still lacking. Furthermore, it remains unknown whether such laterality in the primitive is innate or emerges with development. We also do not understand how laterality is modified by extensive training, such as with musical instruments (Schlaug et al.; Fujii et al., 2010).

Future comparative studies using both behavioral and physiological approaches may provide some insight into these questions.

Figures and Tables

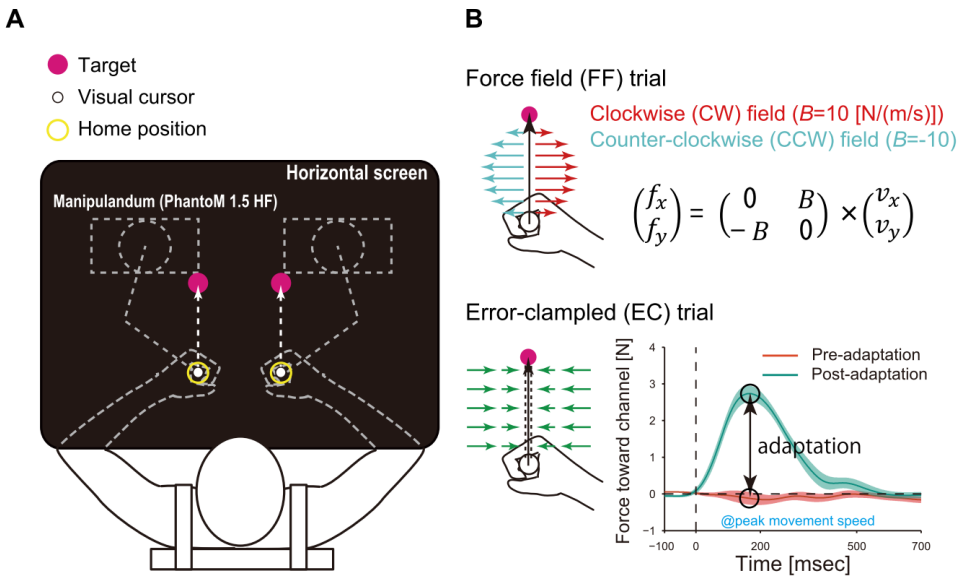

Figure 4.1. The basic description of experiment.

A, Participants were instructed to make center-out reaching movements holding the handles of 2 robotic manipulanda (Phantom 1.5 HF). The position of each handle was fed back as a white cursor on a horizontal screen over the participants' arms (thus, they could not see their arms directly). Movement of each handle was constrained to a virtual horizontal plane by a simulated spring. Participants wore a wrist brace on each hand, and the upper arms were supported by slings (not illustrated). The trunk was strapped to the chair. **B**, In each experiment, velocity-dependent force fields were generated by manipulanda. The force is represented as $\boldsymbol{f} = \boldsymbol{B}\boldsymbol{v}$, where $\boldsymbol{f} = (f_x, f_y)^t$ [N] is the force to the handle, $\boldsymbol{v} = (v_x, v_y)^t$ [ms^{-1}] is the velocity of the handle, and $\boldsymbol{B}$ [N/ms^{-1}] is the viscosity matrix. For clockwise (CW) force fields, $\boldsymbol{B} = [0 -10; 10\ 0]$, and for counter-clockwise (CCW) force fields, $\boldsymbol{B} = [0\ 10; -10\ 0]$. **C**, To quantify the motor adaptation we employed the "error clamp" method. During error-clamped trials, the trajectory of the handle was constrained to a straight line toward the target by a virtual "channel", in which any motion perpendicular to the target direction was constrained by a 1-dimensional spring. This method enabled us to measure directly the lateral force exerted toward the "channel". Aftereffect was defined as the difference between the pre and post training data measured at peak movement speed.

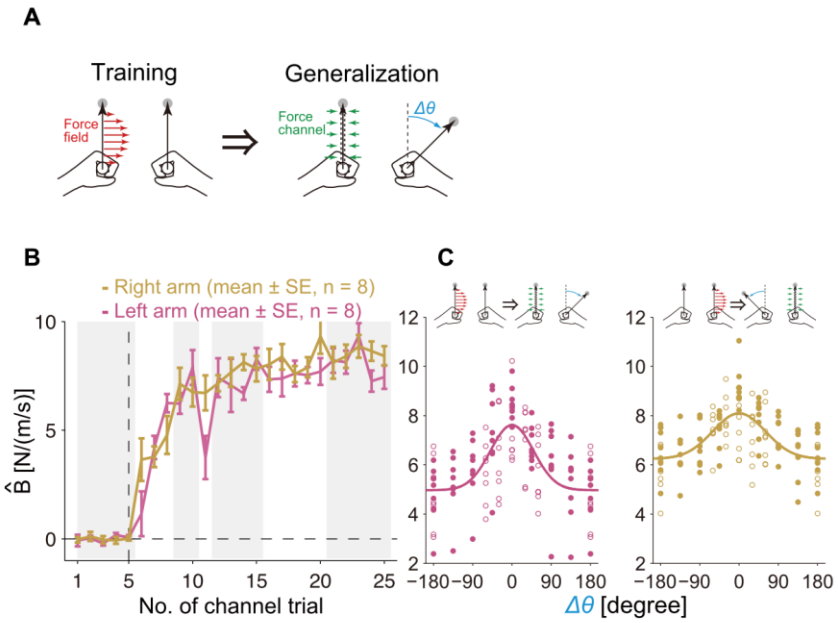

Figure 4.2. Experiment 1.

A, Subjects adapted to a force field (FF; either CW or CCW) applied to either the left or the right arm while making forward reaching movements with both arms. Then, the generalization was assessed by using the channel trial changing the movement direction of the unperturbed arm. Note that the illustrated case shows learning CW FF with the left arm. **B**, Trial-by-trial profile of aftereffect (lateral force at peak movement speed divided by the speed) measured at randomly introduced channel trials for baseline and training sessions averaged across subjects (mean ± SE). Purple: Data for the group 1 subjects (learning with the left arm). Gold: Data for the group 2 subjects (learning with the right arm). The data within the shaded area were averaged and used for subsequent statistical analysis. **C**, Generalization patterns for all subjects in both groups (left: group 1, right: group 2) plotted with our previous data (Experiment 1 and 2 in Chapter 3; (Yokoi et al., 2011)). Vertical axis and the color code are the same as in (**B**). These data were fitted with Gaussian functions (solid lines).

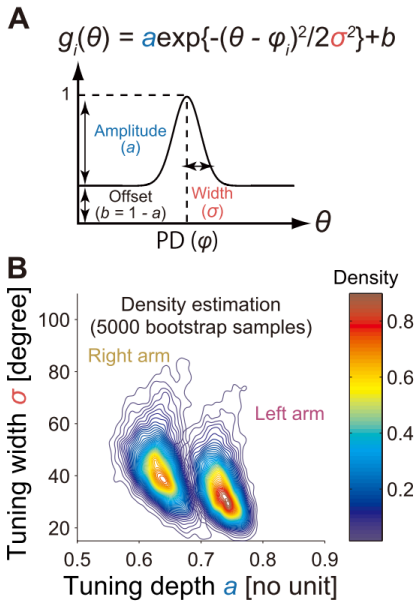

Figure 4.3. Estimated parameters for the motor primitive.

A, Activity of each primitive (g_i) was assumed to be a Gaussian-like function. Each primitive has its own preferred direction (PD) of *opposite arm* motion. Note that θ indicates the movement direction for the *opposite arm*. We assumed that the PD was uniformly distributed on [0°, 360°] space. Free parameters are the tuning width (σ), and the amplitude (a). **B**, Estimated density distributions of tuning parameters for the right and the left arms were clearly dissociated from each other. Two-dimensional Gaussian kernel was applied on 5000 bootstrapped estimates of parameters estimated from the generalization data. Color code indicates the density.

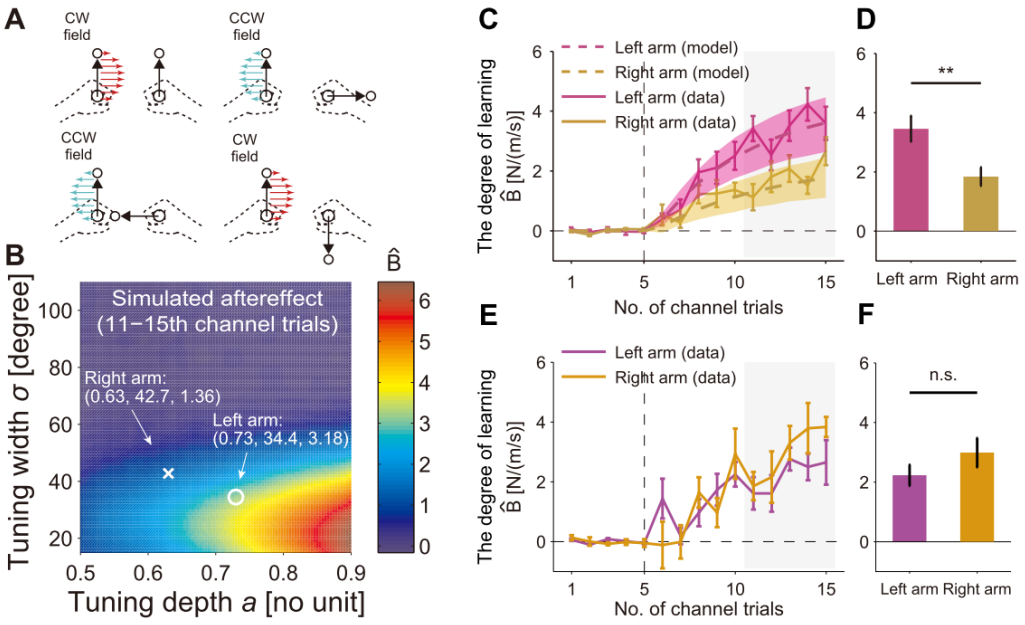

Figure 4.4. Experiment 2 (and 3).

A, The direction of force field (FF) to the perturbed arm was changed depending on the movement direction of the unperturbed arm (CW or CCW). The perturbed arm reached in the same direction throughout the experiment. The case of the left arm learning group (group 1) is illustrated. **B**, Simulation of Experiment 2 in various combinations of a and σ. Color code indicates the amount of the aftereffect averaged across the late phase of motor learning (11-15-th channel trials, **C**). **C**, Learning curve averaged across all movement directions of the *unperturbed arm* for both groups, displayed with simulated result. Color codes are the same as in Fig. 4.2. Thick lines: observed data (mean ± SE). Dotted lines: simulated data using the parameter set estimated from the behavioral data. Filled areas around dotted lines: 95% confidence interval for the simulated aftereffects. Shaded area indicates the data used for subsequent statistical testing (11-th to 15-th channel trial). **D**, The left arm showed significantly larger learning (**: $P < 0.005$) than the right arm. The data of the last 5 channel trials (specified by the shaded area in **C**) were averaged within each subject. **E** and **F,** The results for the left-handed participants. The display is the same as in (**C**) and (**D**).

Table 4.1. The basic information of participants whose data were used for analysis.

	Experiment 1 (N = 16)			Experiment 2 (N = 20)			Experiment 3 (N = 12)		
Trained arm	Age	Sex	L.Q.	Age	Sex	L.Q.	Age	Sex	L.Q.
Left	22.4 (2.6)	M 9 F 7	86.9 (10.8)	21.8 (1.0)	M 7 F 3	92.8 (8.3)	23.2 (2.5)	M 5 F 1	-66.4 (26.4)
Right	24.0 (3.7)	M 9 F 7	85.0 (21.1)	23.1 (1.4)	M 7 F 3	91.0 (10.8)	21.5 (1.4)	M 5 F 1	-70.9 (33.4)
	n.s.	n.s.	n.s.	n.s.	n.s.	n.s.	n.s.	n.s.	n.s.

Wilcoxon rank sum tests were performed on Age and L.Q. data [mean (SD)]. Fisher's exact test was performed on Sex data (M, Male; F, Female). α was set to 0.05.

Table 4.2. Common parameters for model simulation.

N	α	K	d	φ
100	0.996	0.00724	8	Uniform distribution [0°, 360°]

Chapter 5

General Discussion

In this thesis, I investigated the possible neural mechanism of the flexible control of bimanual movement. In the experiments presented in this thesis, I asked how the information of movement of both arms is jointly represented in the control process by using human psychophysics and computational modeling. In this chapter, I summarize the results of these experiments and discuss directions and implications for future studies.

5.1 Summary of findings

In the first study (Chapter 3), I designed a series of experiments to elucidate how the movements of both arms are represented together in motor primitives in the internal models for each arm. With a combined approach of behavioral and computational analyses, I revealed the following findings:

1. The pattern of generalization revealed that information about the kinematics of both arms is multiplicatively encoded in the internal model of each arm (Experiments 1 and 2). Multiplicative encoding of neural signals is known as “gain fields” (Andersen et al., 1985) and is considered as a computational foundation to construct arbitrary input-output mapping (Pouget and Sejnowski, 1997).

2. Indeed, the subjects easily adapted to complex dynamics that depend nonlinearly on the movements of two arms (Experiments 3–5). Furthermore, our computational model, the parameters of which were tuned by using the data of Experiment 1, was able to predict how well subjects adapt to these complex dynamics without additional tuning of parameters, suggesting that multiplicative encoding of the movement of both arms is a robust feature of the motor system.

In the second study (Chapter 4), I examined laterality in the encoding pattern of the movement of the opposite limb in the motor primitives. The two major findings of this second study are as follows:

1. As reflected in the generalization pattern, we demonstrated that the motor primitives of the nondominant arm encode the motion of the dominant arm more sharply than the opposite scenario (Experiment 1). That is, motor primitives of the nondominant arm had a smaller tuning width and greater amplitude of tuning function than those of the dominant arm.
2. The most striking finding of this study was that the difference in the tuning property of the motor primitives predicted a greater ability of the nondominant arm in compensating for mechanical perturbation from the other arm's motion in bimanual movement, and this prediction was experimentally supported. Right-handed subjects who experienced a force field that was imposed on the nondominant arm and depended on the motion of the opposite arm, showed ~200% greater adaptation than subjects who experienced a force field with the

dominant arm (Experiment 2). In contrast, both arms showed comparable adaptation to an ordinary force field that only depended on the motion of the relevant arm (Experiment 1), despite the fact that previous studies on unimanual reaching reported the superiority of the dominant arm in adapting to novel dynamics (Duff and Sainburg, 2007; Schabowsky et al., 2007).

These findings are summarized in Fig. 5.1. The results of the first study provided convincing evidence that the motor system integrates the motion of different body parts in a mathematically plausible manner for flexible movement control. Such integration may be a foundation for the problem of controlling individual arm movements in bimanual movements. In addition, the results showed concrete evidence of the functional role of neural interactions between hemispheres that were previously regarded as a source of interference (Swinnen, 2002; Swinnen and Wenderoth, 2004). The results of the second study clearly countered the conventional notion of the absolute superiority of the dominant arm. Considering that bimanual coordination requires that the neural controller for each arm anticipate the consequence of the motion of its counterpart, asymmetry in this ability would be a critical constraint when assigning different roles to each arm.

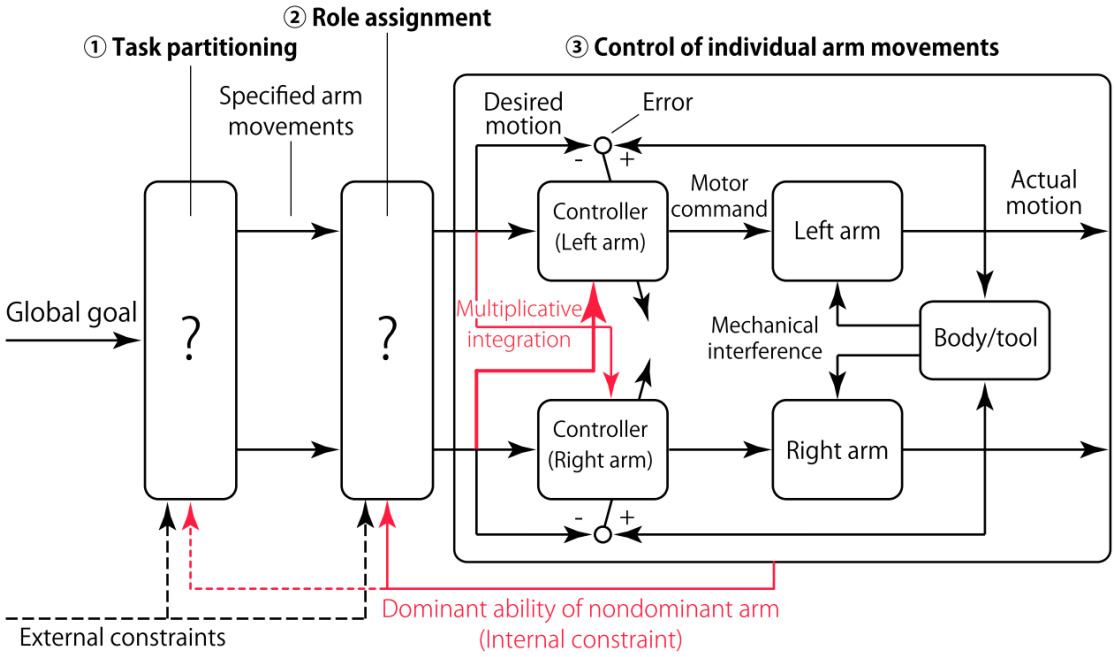

Figure 5.1. A hypothetical scheme of bimanual movement control proposed in the present thesis. Red arrows and text show the contribution of the present thesis.

5.2 Perspectives

5.2.1 Possible neural substrates

As noted in Chapter 2, compared to the neurophysiological approach, the behavioral approach that was taken in this thesis lacks the power to localize the responsible neural sites. For instance, there is accumulating neurophysiological evidence about motor primitives implemented in the relatively lower part of the CNS, e.g., spinal cord. However, it is noteworthy that like previous models, the present one captures some important aspects of the motor system; specifically, it was able to explain/predict important features of the behavioral data. In addition, while there have been extensive neurophysiological studies on various parts of the cerebral cortex during arm movement, we still lack the conclusive view of how motor primitives are implemented within the cerebral cortex. Thus, it would be fruitful for future behavioral and electrophysiological studies to advance previous and present findings.

According to the studies summarized in Chapter 2, it is conceivable that the process of sensorimotor transformation (i.e., the internal model) is implemented by two main types of motor primitives. One type includes the motor primitives implemented within the spinal cord (Giszter et al., 1993; Mussa-Ivaldi et al., 1994) and brainstem (Roh et al., 2011). Their activation causes contraction of certain groups of muscles, and the pattern is highly similar to the set of basic patterns decomposed from naturalistic behaviors (i.e., muscle synergy) (Tresch et al., 1999). In the following discussion, I

refer to these as *lower primitives*, for convenience.

It would be natural, then, to speculate that what constitutes the descending signals to activate these lower primitives would be the primitives implemented within cerebral cortices (Holdefer and Miller, 2002). For convenience, I term them *higher primitives*. The finding that muscle synergies are still preserved in stroke patients with different lesion sites supports the view that these rather fixed lower primitives are driven by descending signals from frontal motor cortices (Cheung et al., 2009b). Another weak line of support for this view is that the activation coefficients of muscle synergies extracted during arm reaching in humans (d'Avella et al., 2006; d'Avella et al., 2011) or postural tasks in cats (Ting and Macpherson, 2005) show clear directional tuning that is similar to the activity of neurons in cortical motor areas (e.g., the primary motor and premotor cortices) (Georgopoulos et al., 1982; Kalaska et al., 1989; Cisek et al., 2003). In addition, the activation coefficient of the muscle synergies of frogs changed under altered load conditions, while the extracted synergies were robust across loaded/unloaded conditions (Cheung et al., 2009a). Therefore, it is conceivable that the output of corticospinal neurons in these areas is comprised of the flexible combination of higher primitives located upstream of these areas.

To summarize, the mathematical expression of these process is represented as:

$$\boldsymbol{m} \approx \sum_{i=1}^{K} c_i \boldsymbol{\Phi}_i \tag{5-1}$$

$$c_i \approx \sum_{j=1}^{N} w_{ij} g_j(\boldsymbol{x}_d, \dot{\boldsymbol{x}}_d, \cdots), \tag{5-2}$$

where $\boldsymbol{m}$ is the vector of the muscle activation pattern, c_i is the activation coefficient (or descending signals to spinal cord) for the *i*-th lower primitive $\boldsymbol{\Phi}_i$, w_{ij} is the connection weight between the *i*-th corticospinal unit sending commands to the *i*-th lower primitive and the *j*-th higher primitive g_j, $\boldsymbol{x}_d$ and its derivatives are the vector of desired limb states and its derivatives, and K and N are the numbers of lower and higher primitives, respectively. I speculate that these higher primitives are what the present experiments and other studies have extracted from the generalization pattern of motor learning.

The main reason for this speculation is that the time scale for learning-induced plasticity is markedly different between the cerebral cortex and spinal cord. Behaviorally, adaptation to a novel force field during reaching tasks is nearly completed within a few hours of training (Lackner and Dizio, 1994; Shadmehr and Mussa-Ivaldi, 1994; Thoroughman and Shadmehr, 1999; Criscimagna-Hemminger et al., 2003; Donchin et al., 2003; Nozaki et al., 2006; Smith et al., 2006; Wagner and Smith, 2008; Yokoi et al., 2011). Neurophysiological evidence suggests that plastic change in the activation pattern of neurons in the frontal motor areas of monkeys performing these tasks also occurs during this time period (Gandolfo et al., 2000; Li et al., 2001; Padoa-Schioppa et al., 2002; Padoa-Schioppa et al., 2004; Xiao et al., 2006; Richardson et al., 2008; Arce et al., 2010). Moreover, a number of studies have shown that the activity pattern of neurons in these areas exhibits rapid change within hours following operant conditioning training of single-cell activity (Fetz, 1969),

patterns of cell and muscle activities (Fetz and Finocchio, 1971), brain–computer interface training (Moritz et al., 2008; Ganguly and Carmena, 2009, 2010; Ganguly et al., 2011), and adaptation to a new decoder (Jarosiewicz et al., 2008). These activation pattern changes are thought to be mediated by synaptic plasticity in these areas, e.g., synaptogenesis or synaptic potentiation (Buonomano and Merzenich, 1998; Adkins et al., 2006). A recent study demonstrated rapid formation of new dendritic spines (a site for receiving synaptic input) in the motor cortex contralateral to the trained forelimb of rats within an hour of reach-and-grasp training, which consisted of 30 reaches and also caused selective stabilization of these spines (Xu et al., 2009).

In contrast, although little is known about the contribution of the spinal cord to motor learning compared to cerebral cortex, growing evidence suggests that it takes more than 1 day to induce plastic changes within the spinal cord (Wolpaw and Tennissen, 2001; Guertin, 2008). For example, in the operant conditioning task to up- or downregulate the spinal stretch reflex or H-reflex, both of which are indices for spinal excitability, it requires a few days to weeks of training to induce stable behavioral changes in rats, primates, and humans (Wolpaw and O'Keefe, 1984; Wolpaw, 1987; Wolpaw and Lee, 1989; Chen et al., 2007; Thompson et al., 2009; Chen et al., 2011; Thompson et al., 2012) and to detect increases in synaptic terminals on spinal motor neurons in rats (Wang et al., 2009). For more naturalistic tasks, weeks of backward walking training induced a progressive decrease in the soleus H-reflex in the mid-swing phase (Ung et al., 2005; Meunier et al., 2007).

Therefore, although we still lack direct comparisons within the same learning paradigm, the timescale of training-related plasticity in the spinal cord seems to be much longer than that in the motor cortices. Assessing the timescale of plasticity following motor learning within both the cortex and spinal cord by using the same behavioral task during prolonged training periods will be the next major challenge in motor neuroscience.

Taken together, it is unlikely that the lower primitive changed within a few hours of a training session. Therefore, it is suggested that the adaptation-related change in motor output observed in previous reaching studies and ours is predominantly mediated by changes in descending signals from cortical motor areas, c_i in the Eqs. (5-1) and (5-2). Thus, generalization of the motor adaptation to a novel force field is more likely to reflect the activity of higher primitives.

The next topic is the responsible sites for synaptic plasticity. According to Eq. (5-2), adaptation to a novel force field changes w_{ij}, which represents the synaptic connection between output units within cortical motor areas[12] and higher primitives. Unfortunately, with the current knowledge, it would be difficult to determine exactly where plasticity occurs during adaptation because of the loop structure of the motor system, which includes frontal motor cortices, the

[12] The reason why I used the word "output unit" is as follows. In addition to corticospinal neurons, there are also inhibitory interneurons and lateral/recurrent connections among these types of neurons (Landry et al., 1980; Ghosh and Porter, 1988; Jackson et al., 2002). Thus, it is more appropriate to suppose that a certain group of neurons within the same area act as a functional unit to transmit signals from higher to lower primitives. For example, Jackson et al. (2002) found that some neurons in the monkey motor cortex that project to the same muscles tend to fire synchronously. The same discussion is applied to the organization of lower and higher primitives.

posterior parietal cortex, cerebellum, basal ganglia, and thalamus. This may be part of the reason why the activation patterns of higher primitives that were behaviorally estimated using generalization of learning, contain many reported characteristics of neurons in different brain regions (Georgopoulos et al., 1982; Georgopoulos et al., 1984; Andersen et al., 1985; Coltz et al., 1999) depending on the types of tasks, e.g., force field adaptation (Donchin et al., 2003) or visuomotor adaptation paradigms (Tanaka et al., 2009).

One possible approach to this problem is twofold: First, operationally define higher primitives and output units as regions that do or do not change their activation patterns following motor adaptation; then, identify them during an adaptation paradigm. Practically, it is nearly impossible to electrophysiologically record neural activities in these areas simultaneously in behaving animals. Potential approaches to this question are large-scale electrocorticogram recordings of behaving animals or human fMRI study.

An electrocorticography, also called intracranial electroencephalography, is a technique that measures postsynaptic potentials (local field potentials) from electrodes placed directly on the cortical surface; thus, it offers the same temporal resolution (~0.5 ms) and much higher spatial resolution (~1 cm) compared to electroencephalography. Recent works have demonstrated that this technique provides rich information to reconstruct arm movements, e.g., reaching, grasping, or individual finger movements, for both humans (Kubánek et al., 2009; Yanagisawa et al., 2011;

Pistohl et al., 2012; Yanagisawa et al., 2012) and chronic recording in monkeys (Chao et al., 2010; Shimoda et al., 2012). Combining this technique with simultaneous recordings from deep brain structures (Feingold et al., 2012) might allow us to monitor neural activities across global cortical and subcortical structures during short- and long-term motor adaptation.

It would also be possible to monitor activity changes in whole brain structures during relatively short-term motor adaptation by using fMRI. Recent human imaging studies have demonstrated successful extraction of directional-selective activation patterns in motor areas (Eisenberg et al., 2010, 2011), visual areas (Kamitani and Tong, 2005; Miyawaki et al., 2008), individual finger representation in both cortical sensorimotor areas and cerebellum (Wiestler et al., 2011; Diedrichsen et al., 2012), and the signature of motor adaptation (Diedrichsen et al., 2005; Donchin et al., 2012; Schlerf et al., 2012). In addition, a recent fMRI study by Diedrichsen et al. (2012) showed multiplicative representations of finger movements in both hands in the caudal premotor and anterior parietal cortices (Diedrichsen et al., 2012). Because the task in the study by Diedrichsen et al. (2012) was simple isometric finger pressing and did not include adaptation, extending the results of their work directly to our case of motor adaptation during arm movement might be too speculative. However, it is likely that we could also identify neural substrates for higher primitives that show multiplicative encoding of the motion of both arms in these areas.

5.2.2 Interhemispheric interaction and motor primitives

Another outstanding question is how arm motion information is transmitted to the internal model for the opposite arm. Although there are many interconnections between the right and left sides of the CNS, including cortical, subcortical, and spinal levels (Bloom and Hynd, 2005; Carson, 2005), the CC is considered as a primary contributor toward bimanual coordination (Soteropoulos et al., 2011; Diedrichsen, 2012). For example, callosotomy patients, in whom the CC was surgically transected to treat severe epilepsy, exhibit reduced intermanual coupling and are unable to acquire new bimanual skills (Franz et al., 2000; Kennerley et al., 2002)

For sensorimotor areas, it is widely accepted that the primary function of transcallosal interaction is inhibition (Asanuma and Okuda, 1962; Perez and Cohen, 2009; Soteropoulos and Perez, 2011), even though a relatively weak excitatory pathway also exists (Ugawa et al., 1993; Hanajima et al., 2001). Such an inhibitory interhemispheric interaction, known as interhemispheric inhibition (IHI), is considered important for bimanual coordination. It has been intensively studied using noninvasive transcranial magnetic stimulation in humans and direct recording in animals. For instance, a short conditioning transcranial magnetic stimulation pulse over either M1 reduces the subsequent motor evoked potential induced by a test pulse over the same area on the opposite hemisphere after certain interstimulus intervals ranging from around 10 to 40 ms (Ferbert et al.,

1992; Di Lazzaro et al., 1999; Chen, 2004)[13]. As expected, these inhibitory effects are known to be reduced or abolished in patients with agenesis of the CC (Meyer et al., 1995).

In addition to IHI between homologous areas, e.g., the left and right M1, it also occurs across several motor-related areas, e.g., between M1 and dorsal/ventral premotor areas, somatosensory areas, and the dorsolateral prefrontal cortex within the contralateral hemisphere (Mochizuki et al., 2004a; Mochizuki et al., 2004b; Ni et al., 2009). In addition, the magnitude of IHI is dependent on both muscle grouping (e.g., IHI during wrist flexion of the conditioned side has less effect on wrist extension of tested side) and the kinematic information of the movement (Duque et al., 2005). Importantly, evidence suggests that there is interaction between transcallosal inhibition and both intracortical inhibition and facilitation within the contralateral hemisphere (Chen, 2004; Avanzino et al., 2007; Lee et al., 2007; Udupa et al., 2010).

IHI is thought to be mediated through a combination of transcallosal input from excitatory glutamatergic pyramidal neurons, which release glutamate as neurotransmitter, and the gamma-aminobutyric acid (GABA)ergic local inhibitory interneurons within the contralateral hemisphere, which release GABA as neurotransmitter (Chen, 2004; Avanzino et al., 2007; Lee et al., 2007). Both pharmacological modulation with a $GABA_B$ receptor agonist (baclofen) and direct recording of cells in the rat somatosensory cortex support this view (Irlbacher et al., 2007; Palmer et

[13] IHI with shorter ISI (~10 ms) is called short-interval IHI (SIHI), and IHI with longer ISI (~40 ms) is called long-interval IHI (LIHI).

al., 2012). Notably, these GABAergic inhibitory interneurons are ubiquitous throughout the cortex, and the lateral or recurrent connection mediated by these interneurons determines the shape of neural response functions (Yajima and Hayashi, 1990; Crook et al., 1991; Crook and Eysel, 1992; Crook et al., 1998; Oswald et al., 2006).

Importantly, IHI is known to be affected by hand dominance; the dominant hemisphere more strongly inhibits the nondominant counterpart than vice versa (Netz et al., 1995; Ziemann and Hallett, 2001; Duque et al., 2007). Such asymmetrical inhibition has also been reported in a human fMRI study that employed bimanual finger tapping tasks (Hayashi et al., 2008) and in a human scalp electroencephalogram study that utilized bilateral isometric force production tasks (Oda and Moritani, 1995).

In summary, I think that the interaction between intracortical processing and interhemispheric inhibition at M1 or higher areas (e.g., premotor or possibly posterior parietal cortex) might be a neural substrate of multiplicative modulation of the activity of the motor primitives, which I have shown in this thesis (Chapter 3). Greater GABA-mediated inhibition from dominant to nondominant hemispheres is consistent with the laterality in the tuning pattern of the primitives (Chapter 4). Considering the ability of a balanced background excitatory and inhibitory synaptic input to create gain modulation of neuronal activity (Chance et al., 2002; Ingham and McAlpine, 2005; Beck et al., 2011; Louie et al., 2011), this would be one possible scenario.

Combining the application of our paradigm to the IHI study and using a pharmacological approach to block/enhance GABA activity would provide some evidence for this conjecture. Other than pharmacological modulation, one easy-to-apply method is transcranial direct current stimulation, which can noninvasively downregulate cortical GABA activity with relatively higher regional selectivity compared to the pharmacological approach (Nitsche et al., 2005; Stagg et al., 2009; Stagg et al., 2011a; Stagg et al., 2011b).

5.2.3 Extension to the feedback control process

Although the present thesis focused primarily on the adaptation and, hence, the representation of a feed-forward control process (e.g., inverse model) during bimanual movement, the result can be leveraged for future research to investigate the mechanism of how the feedback control process (e.g., forward model) flexibly integrates the information of the motion of both arms.

In general, there are two types of approaches to investigate the organization of a feedback control process. The first approach is to investigate the feedback response itself and involves both the effect of the feedback controller and the forward model (Fig. 2.1). As reviewed in Chapter 2, it is already evident that the feedback control process for one limb is capable of using the sensory input for the other limb (Ohki and Johansson, 1999; Ohki et al., 2002; Diedrichsen, 2007; Mutha and Sainburg, 2009; Dimitriou et al., 2012). The next questions would be how such a process is organized (e.g., possibly through population coding) and how the feedback control process adapts to

a novel environment. Indeed, for the single-arm reaching paradigm, several recent studies have demonstrated an alteration in the feedback response following adaptation of the feed-forward control process (Wagner and Smith, 2008; Ahmadi-Pajouh et al., 2012; Franklin et al., 2012). In addition, other reports have suggested that the feedback response to unexpected perturbation is also well described by a small set of muscle activation patterns (e.g., muscle synergies) shared with the feed-forward control of voluntary motion (Ting and Macpherson, 2005; d'Avella et al., 2011). Nevertheless, how the feedback control process integrates sensory inputs and motor commands from both limbs and how learning-induced changes are generalized across various movement parameters remain open questions.

The second approach to investigate the feedback control process is to analyze the forward model, which is one of the crucial components of the feedback control loop (Shadmehr and Krakauer, 2008), by quantifying its output. There have been two approaches to quantify the output of the forward model. Considering that the forward model transforms motor commands (i.e., cause) into the predicted sensory states (i.e., result), the most primitive approach would be to ask subjects to visually localize the position of their hand after termination of the movement without visual feedback (e.g., Wolpert et al., 1995). Several recent studies have addressed the adaptation of the forward model and its generalization to untrained movements using the above approach (Izawa et al., 2012a; Izawa et al., 2012b).

Another approach makes use of the fact that output of the forward model is considered to be used for cancelling out sensory feedback that results from our own movement (called re-afferent signal) from the total sensory input (Bays and Wolpert, 2007). This mechanism is thought to be a reason why we cannot tickle ourselves (Blakemore et al., 2000) and why the game of tit-for-tat often escalates endlessly (Shergill et al., 2003). In the context of bimanual coordination, previous studies have demonstrated that the subjective measure of ticklishness when subjects tickle their left arm using a robotic device controlled by their right arm, showed directional tuning. The amount of attenuation gradually decreased as the movement direction of the robotic device (consequence) deviated from that of the right hand (action) (Blakemore et al., 1998; Blakemore et al., 1999). Interestingly, the amount of attenuation was also modulated as a function of a delay between action and its consequence (Bays et al., 2005). These results may reflect how the motion of the right hand is represented in the forward model and suggest that the forward model for the left hand receives the motor command from the right hand. This is consistent with the view presented in this thesis.

Taken together, it is highly likely that the feedback control process, including the forward model and feedback controller, is implemented through the motor primitives. Thus, the experimental paradigm presented in this thesis seems to be readily applicable to investigate how the feedback control process is organized. It is possible to design an experiment to study how the feedback control process or forward model for an arm integrates the motion of the opposite arm by analyzing how an

adapted change in this process generalizes to the concurrent motion of the other arm with various movement parameters (e.g., direction).

5.2.4 Encoding time lag between the motion of both arms in the primitives

Both arms are coordinated spatially and temporally during bimanual action. This thesis revealed how the internal model for one arm integrates spatial information (i.e., kinematics) of two arms *when they are moving simultaneously.* Toward a more general understanding of flexible bimanual coordination, future studies can extend our paradigm by introducing an additional dimension (i.e., lag between each arm's motion) to the generalization function. Although there have been only a few studies on this topic, several have addressed this issue in part. As was previously described, bimanual sensory attenuation is also tuned to the lag between the motion of one arm and the consequence to the other arm (Bays et al., 2005). It has also been shown that subjects could learn to predictively compensate for the force perturbation to their left arm caused by the motion of the right arm, even when there was a time delay (Jackson and Miall, 2008). A recent study on single-arm reaching movement demonstrated that a recent movement can affect motor adaptation to a novel force field during the subsequent movement if the time lag between the two movements is less than 600 ms (Howard et al., 2012). Therefore, considering the results of this line of studies, it is likely that both inverse and forward models (and primitives) for arm movements encode motion information for both arms, as well as the time lag between them. These signals may also be multiplicatively integrated in the

internal model.

5.2.5 Postural control: Control of multiple body parts

One possible direction in which to extend our results is posture control, which is a good example for whole-body coordination. The CNS continuously maintains postural stability during any voluntary motor action both reactively (i.e., response to external perturbations) and proactively (i.e., predictive compensation of the effect of one's own motion). This latter kind of predictive (feed-forward) postural control accompanied with voluntary actions is called "anticipatory postural adjustment (APA)" (Massion, 1984; Bouisset and Zattara, 1987). The easiest example can be observed when we raise our arm forward in front of our body. To prepare for the shift in the center of mass that accompanies the arm motion, consistent activation of postural muscles around the ankle, knee, and hip joints precedes arm movement onset by around 50 ms. In addition, the amplitude of muscle activation is modulated by movement parameters, such as voluntary movement speed (Crenna and Frigo, 1991). Other than movement speed, APAs are modulated by the direction of motion, current position of the center of pressure, and even by instructions given to subjects (for a review, see Bouisset and Do, 2008). Therefore, APAs are controlled by taking the motor command for the relevant movement, current state of body, and task goal into account.

Importantly, bimanual coordination, which I dealt with in this thesis, shares several critical features with APAs. First, the feedforward motor output for the particular effector (i.e., postural

muscles) depends on the motion state of other body parts (i.e., voluntarily controlled body parts). Second, as described above, it is modulated by movement (e.g., motion speed and direction). Third, these predictive controls are adaptive and learned by experience (Haas et al., 1989; van der Fits et al., 1998; Schmitz et al., 2002; Diedrichsen et al., 2003). Therefore, our findings on bimanual coordination might be extended to research on how APAs are organized. For instance, the experimental paradigm presented in this thesis would help to investigate how the postural controller integrates the motion signals of various body parts by experimentally introducing a novel action-posture association, for example, associating the lateral motion of a platform with the forward raise of arms and thoroughly examining the pattern of generalization.

5.2.6 Extension to natural movement: Manipulating single objects

The studies presented in this thesis dealt with bimanual movement in which two separate visual cursors and goals were assigned to two arms. Whether the controlled object is single or separated (and hence whether there is a single goal or separate goals) seems to have little effect on the lowest level of the problem (i.e., control of individual arm motion) under the assumption of the three different problems for bimanual coordination, which were defined in the first chapter. However, several points should be noted in order to extend the present results to more general bimanual coordination. For example, how a single goal is broken down into two concrete arm movements is largely unknown.

Another important issue is how the information of movement error or task performance in a global sense is assigned to each individual arm movement. As reviewed in Chapter 2, an error observed when participants were controlling a single cursor is corrected by the arm receiving perturbation and by the other arm not receiving perturbation (Diedrichsen, 2007) (Fig. 2.11). Such assignment of single error information to both arm movements in the context of controlling a single object also occurs in trial-by-trial adaptation of the internal model, even when subjects explicitly understand the source of the error (Kasuga and Nozaki, 2011). On the other hand, when participants controlled two separate cursors, such "cross-talk" of error was not observed for feedback correction or trial-by-trial adaptation in previous studies (Diedrichsen, 2007; Kasuga and Nozaki, 2011) or in the present thesis (Fig. 3.2*B*). Thus, although the present results were not influenced by such an effect, this problem should be considered when dealing with more general bimanual coordination. A recent study suggested that the process of such credit assignment in redundant motion follows a Bayesian framework; thus, the more "uncertain" arm tends to correct and adapt more (White and Diedrichsen, 2010).

5.2.7 Laterality and bimanual skills: General perspectives

Lateralization of the nervous system and behavioral asymmetry are common phenomena in both vertebrates, such as fish (Miklosi and Andrew, 1999), birds (Hunt et al., 2001; Brown and Magat, 2011), and primates (Hopkins, 1996; Hopkins and Russell, 2004), and invertebrates, including

nematodes (Hobert et al., 2002), insects (Letzkus et al., 2006; Rogers and Vallortigara, 2008), and even octopi (Byrne et al., 2006b, a). While a tight link across genetic, structural, and functional levels of asymmetry has been revealed in some systems (Hobert et al., 2002; Kawakami et al., 2003; Aizawa et al., 2005; Wu et al., 2005; Bianco et al., 2008; Nakano et al., 2011; Shinohara et al., 2012), such a thorough systems-level approach would be difficult to apply in more complex animals, such as primates or humans. This is one of the reasons why most human investigations have been biased toward too macroscopic or microscopic studies (Toga and Thompson, 2003; Swinnen and Wenderoth, 2004; Sun and Walsh, 2006; Goble and Brown, 2008) and why we still lack a unified viewpoint to consolidate them. In addition, unfortunately, the computational neuroscience community has not paid much attention to this topic. My second study presented in Chapter 4 provided concrete evidence of lateralized motor ability during bimanual movement and the mechanistic description of such ability upon different levels of hierarchy. Notably, the present approach of analyzing the generalization pattern is applicable to systems other than the motor system; for example, it could be used to assess laterality in how stimuli are represented during a visual perceptual learning task (Poggio and Bizzi, 2004; Fahle, 2005; Solgi et al., 2013) or an associative learning task in animals (Ghirlanda and Enquist, 2007). However, it is important to note that the present results cannot answer the questions of the origin of lateralized tuning of motor

primitives or the origin of lateralization itself. To answer such nature-or-nurture questions would require cross-sectional and/or longitudinal studies on the developmental process of motor primitives.

As described in Chapter 2, the superior ability of the nondominant arm should facilitate the process of role-assignment during bimanual actions by providing strong information for the decision process. This is consistent with the notion that lateralization may enable efficient information processing and biological fitness (Vallortigara, 2006; Magat and Brown, 2009). Thus, it might be the case that strong laterality in motor primitives might promote the ability of sophisticated bimanual skills, e.g., tool use and/or tool making, in our species, because individuals with a consistent role-assignment would improve such skills faster than those with an inconsistent role-assignment. Analysis of prehistoric stone artifacts suggests that our ancestors held the stone core in the left hand and struck off flakes with the right hand; thus, handedness may have existed even then (for review, see Bradshaw and Rogers, 1996). I speculate that strong lateralization in humans might have allowed such skilled bimanual actions and played an important role in facilitating the future development of higher cognitive processes, e.g., belief of cause and effect (Wolpert, 2003) or strategic motor planning (Frey, 2008; Stout, 2011; Stout and Chaminade, 2012), which are necessary for more sophisticated tool use and tool-making. Further comparative studies in different species would provide some insight into this question.

5.2.8 Bimanual movement control and pathology

It is of note that abnormal morphology of CC is seen in patients with several psychiatric or developmental disorders, such as schizophrenia, bipolar disorder, borderline personality disorder, autism, attention-deficit and hyperactivity disorder (ADHD), etc. (van der Knaap and van der Ham, 2011). It is widely acknowledged that the size or integrity of the CC correlates with the performance or learning of bimanual coordination task. For example, Johansen-Berg et al. (2007) reported that, in normal subjects, there was high correlation between the integrity of white matter in the anterior part of CC mediating supplementary motor and cingulate motor areas and performance on a bimanual tapping task (Johansen-Berg et al., 2007). Similarly, a recent work by Sisti et al. (2012) reported that the integrity of anterior CC microstructure can predict the amount of learning of a novel bimanual visuomotor coordination task (Sisti et al., 2012). Notably, the common feature of CC in the above types of patients is smaller size of the anterior body of CC (van der Knaap and van der Ham, 2011). Therefore, performance and/or learning of bimanual tasks might be affected in these pathologies. For example, it has been suggested that abnormal serotonin (5-HT) type 2A receptor (5-HT_{2A}) expression in the neo cortex is a key factor of schizophrenia (Williams et al., 1996). A recent finding in mouse medial prefrontal cortex demonstrated that some of the callosal projection neurons in these areas show 5-HT_{2A}-dependent excitation, suggesting that there is an imbalance between excitatory and inhibitory input through CC in patients with schizophrenia (Avesar and Gulledge, 2012). As

previously mentioned, the balance between background excitatory and inhibitory synaptic inputs may be related to gain modulation (Chance et al., 2002), and performance of bimanual actions that require multiplicative integration (i.e., gain modulation) of movement of both arms, such as object manipulation, could be a behavioral marker for this pathology, possibly in the very early stages.

5.2.9 Structural and functional changes in the brain after prolonged training

From the viewpoint of physical education, elucidating the relationship between motor primitives and experience-induced changes in brain structures following prolonged training is an attractive issue (Zatorre et al., 2012). Musicians are ideal subjects in whom to investigate such a relationship because highly sophisticated bimanual coordination is required for professional musical performances. For instance, Schlaug et al. (1995) reported that highly skilled musicians who had started musical training before the age of 7 had larger CCs compared to control subjects and other musicians who had started training later (Schlaug et al., 1995). This is consistent with the fact that CC myelination finishes around the age of 10 (Rakic and Yakovlev, 1968), which is the age around which children start to show skilled bimanual control (Jeeves et al., 1988). Interestingly, the magnitude of IHI is known to decrease in these groups of subjects (Ridding et al., 2000). Possibly, the overall balance between excitation and inhibition of transcallosal input might be improved and/or interhemispheric interaction asymmetry might decrease. A recent study by Fujii et al. (2010) reported that professional drummers with around 20 years of experience showed clearly reduced

laterality in tapping performance compared to control subjects who had never played the drum (Fujii et al., 2010). Thus, it is likely that the motor primitives in these musicians might encode the movement of the opposite arm with equal sharpness and high efficiency.

Another important issue is acquisition of motor primitives following prolonged training or during the developmental process. One example is the lower primitives involved in locomotion, which is another example of inter-limb coordination. Recently, Dominici et al. (2011) compared the muscle synergies extracted during the stepping reflex of neonates and those extracted during walking of toddlers, preschoolers, and adults and found that some basic patterns in neonate stepping are preserved and incrementally augmented through development (Dominici et al., 2011). They have also reported that similar basic patterns are found in rats, cats, monkeys, and birds, suggesting that such patterns were acquired on a phylogenetic time scale. Another example might be related to higher primitives that are involved in dexterous finger coordination, such as violin playing. Gentner et al. (2010) reported that the TMS-evoked hand kinematics of skilled violinists contained some basic patterns that were specialized for creating violin playing motions through their flexible combination (Gentner et al., 2010). Their findings suggest that prolonged musical training forms some specialized primitives that normal people do not have within the functional network involving M1 and the spinal cord (Gentner et al., 2010). These examples clearly demonstrate the experience-dependent organization of the motor primitives. However, we still know very little about

how such processes proceed. Elucidating how existing primitives are modified and how new ones are formed depending on experience are open for future study.

5.4 Conclusion

The question of how we learn and control our body movements is relevant to every person, especially those who are involved in physical education, sports, and rehabilitation. Previous studies have progressively accumulated evidence of how the CNS controls our movements. In general, this progress has proceeded from simple to complex, e.g., regulation of a single muscle contraction toward the control of voluntary limb movements. It is currently possible to control a robotic arm by reading out the neural signals of behaving animals, including humans; however, we have not reached the level of simultaneously coordinating two robotic arms, let alone entire body parts.

With the goal of elucidating the neural mechanism of flexible bimanual movement, I investigated how the motor system flexibly integrates information about simultaneous movement of both arms when performing bimanual movements. Because no previous study has directly addressed this point, the work presented in this thesis achieved a large conceptual advance. These results provide a possible clue to understand how our nervous system orchestrates the movement of multiple body parts into unified actions.

Appendix

Appendix 1

Theoretical relationship between the generalization function and the primitives

A.1.1 State-space model and trial-dependent adaptation to a constant force field

We assumed that the output force is constructed by a linear summation of the output of primitives as:

$$\hat{f}^{(i)} = \left[\boldsymbol{w}^{(i)}\right]^t \boldsymbol{g}(\theta_r^{(i)}, \theta_l^{(i)}) \quad \text{(A1)}$$

where i is the trial number, and $\boldsymbol{g}(\theta_r, \theta_l) = [g_1(\theta_r, \theta_l), g_2(\theta_r, \theta_l), \cdots, g_N(\theta_r, \theta_l)]^t$ and $\boldsymbol{w} = [w_1, w_2, \cdots, w_N]^t$ are column vectors whose elements represent the output and weight of each primitive, respectively.

A state space model of the motor adaptation to the force field f can be represented as:

$$e^{(i)} = d(\theta_l^{(i)})(f^{(i)} - \hat{f}^{(i)}) \quad \text{(A2)}$$

$$\boldsymbol{w}^{(i+1)} = \alpha \boldsymbol{w}^{(i)} + e^{(i)} K \boldsymbol{g}(\theta_r^{(i)}, \theta_l^{(i)}) \quad \text{(A3)}$$

where e is the movement error, $d(\theta_l)$ is the compliance that depends on the movement direction of

the trained arm (here, we assume that the left arm is trained), and α and K are constants representing, respectively, the spontaneous loss of memory and the update rate to the error.

From these equations, we can obtain the trial-dependent changes in the movement error when a constant force f is imposed for only a particular movement combination (θ_r, θ_l) as:

$$e^{(n)} = \frac{K[d(\theta_l)]^2 f \boldsymbol{g}^t \boldsymbol{g}}{1-\alpha+Kd(\theta_l)\boldsymbol{g}^t\boldsymbol{g}}[\alpha - Kd(\theta_l)\boldsymbol{g}^t\boldsymbol{g}]^{(n-1)} + \frac{(1-\alpha)d(\theta_l)f}{1-\alpha+Kd(\theta_l)\boldsymbol{g}^t\boldsymbol{g}} \qquad \text{(A4)}$$

where $\boldsymbol{g}$ is the abbreviation of $\boldsymbol{g}(\theta_r, \theta_l)$.

From Eqs. (A1)-(A3), the weight vector after sufficient training of a constant force field f is obtained as:

$$\boldsymbol{w}^t = \frac{Kd(\theta_l) f \boldsymbol{g}(\theta_r,\theta_l)^t}{1-\alpha+Kd(\theta_l)\boldsymbol{g}(\theta_r,\theta_l)^t\boldsymbol{g}(\theta_r,\theta_l)}. \qquad \text{(A5)}$$

Therefore, the output force can be represented as:

$$\hat{f}(\theta_r, \theta_l) = \frac{Kd(\theta_l)\boldsymbol{g}(\theta_r,\theta_l)^t\boldsymbol{g}(\theta_r,\theta_l)}{1-\alpha+Kd(\theta_l)\boldsymbol{g}(\theta_r,\theta_l)^t\boldsymbol{g}(\theta_r,\theta_l)} f. \qquad \text{(A6)}$$

When movement directions of both arms are changed by $\Delta\theta_r$ and $\Delta\theta_l$, the force output (i.e., aftereffect) is represented as:

$$\hat{f}(\theta_r + \Delta\theta_r, \theta_l + \Delta\theta_l) = \boldsymbol{w}^t \boldsymbol{g}(\theta_r + \Delta\theta_r, \theta_l + \Delta\theta_l)$$

$$= \frac{Kd(\theta_l)\boldsymbol{g}(\theta_r,\theta_l)^t\boldsymbol{g}(\theta_r+\Delta\theta_r,\theta_l+\Delta\theta_l)}{1-\alpha+Kd(\theta_l)\boldsymbol{g}(\theta_r,\theta_l)^t\boldsymbol{g}(\theta_r,\theta_l)} f. \qquad \text{(A7)}$$

Thus, the function of how the training effect is transferred from (θ_r, θ_l) to $(\theta_r + \Delta\theta_r, \theta_l + \Delta\theta_l)$ is represented by:

$$\Phi(\Delta\theta_r, \Delta\theta_l) = \frac{\hat{f}(\theta_r+\Delta\theta_r, \theta_l+\Delta\theta_l)}{\hat{f}(\theta_r, \theta_l)} = \frac{\boldsymbol{g}(\theta_r, \theta_l)^t \boldsymbol{g}(\theta_r+\Delta\theta_r, \theta_l+\Delta\theta_l)}{\boldsymbol{g}(\theta_r, \theta_l)^t \boldsymbol{g}(\theta_r, \theta_l)}. \quad \text{(A8)}$$

A.1.2 Decomposition of the generalization function: Multiplicative encoding

If the primitives encode the movement directions of both hands multiplicatively as: $g_j(\theta_r, \theta_l) = r_j(\theta_r) l_j(\theta_l)$, then

$$\sum_{j=1}^{N} g_j(\theta_r, \theta_l) g_j(\theta_r + \Delta\theta_r, \theta_l + \Delta\theta_l) = \sum_{j=1}^{N} r_j(\theta_r)\, l_j(\theta_l) r_j(\theta_r + \Delta\theta_r) l_j(\theta_r + \Delta\theta_l)$$

$$= \sum_{j=1}^{N} r_j(\theta_r)\, r_j(\theta_r + \Delta\theta_r) l_j(\theta_l) l_j(\theta_l + \Delta\theta_l). \quad \text{(A9)}$$

When N is sufficiently large (N is assumed to be a square number), and $l_j(\theta_l)$ and $r_j(\theta_r)$ have translational symmetry with respect to j and are distributed uniformly on the (θ_r, θ_l) plane, then

$$\sum_{j=1}^{N} g_j(\theta_r, \theta_l) g_j(\theta_r + \Delta\theta_r, \theta_l + \Delta\theta_l)$$

$$\approx \frac{1}{N} \sum_{j=1}^{\sqrt{N}} r_j(\theta_r)\, r_j(\theta_r + \Delta\theta_r) \sum_{j=1}^{\sqrt{N}} l_j(\theta_l) l_j(\theta_l + \Delta\theta_l). \quad \text{(A10)}$$

Thus, the transfer function is:

$$\Phi(\Delta\theta_r, \Delta\theta_l) = \frac{\sum_{j=1}^{N} g_j(\theta_r, \theta_l) g_j(\theta_r + \Delta\theta_r, \theta_l + \Delta\theta_l)}{\sum_{i=1}^{N} g_j(\theta_r, \theta_l) g_j(\theta_r, \theta_l)}$$

$$= \frac{\sum_{j=1}^{\sqrt{N}} r_j(\theta_r)\, r_j(\theta_r + \Delta\theta_r) \sum_{j=1}^{\sqrt{N}} l_j(\theta_l) l_j(\theta_l + \Delta\theta_l)}{\sum_{j=1}^{\sqrt{N}} r_j(\theta_r)\, r_j(\theta_r) \sum_{j=1}^{\sqrt{N}} l_j(\theta_l) l_j(\theta_l)}$$

$$= \Phi(\Delta\theta_r, 0)\Phi(0, \Delta\theta_l). \quad \text{(A11)}$$

A.1.3 Decomposition of the generalization function: Additive encoding

If the primitives encode the movement directions of both hands additively as: $g_j(\theta_r, \theta_l) = r_j(\theta_r) + l_j(\theta_l)$, then

$$\sum_{j=1}^{N} g_j(\theta_r, \theta_l) g_j(\theta_r + \Delta\theta_r, \theta_l + \Delta\theta_l)$$

$$= \sum_{j=1}^{N} [r_j(\theta_r) + l_j(\theta_l)][r_j(\theta_r + \Delta\theta_r) + l_j(\theta_l + \Delta\theta_l)]$$

$$= \sum_{j=1}^{N} [r_j(\theta_r) + l_j(\theta_l)]\{[r_j(\theta_r + \Delta\theta_r) + l_j(\theta_l)]$$

$$+ [r_j(\theta_r) + l_j(\theta_l + \Delta\theta_l)] - [r_j(\theta_r) + l_j(\theta_l)]\}. \quad \text{(A12)}$$

Thus, the transfer function is:

$$\Phi(\Delta\theta_r, \Delta\theta_l) = \Phi(\Delta\theta_r, 0) + \Phi(0, \Delta\theta_l) - 1. \quad \text{(A13)}$$

It should be noted that a previous work (Wainscott et al., 2005) has obtained theoretically similar relationships (Eqs.(A11) and (A13)) in the generalization function calculated from the trial-by-trial changes in the aftereffects.

A.1.4 Special case: Gaussian encoding

Here, we assume that the encoding function can be represented by a Gaussian function. In the case of multiplicative and additive encoding, the primitive can be represented, respectively, as:

$$g_j(\theta_r, \theta_l) = \left\{a_r \exp\left[\frac{-(\varphi_{r_j}-\theta_r)^2}{2\sigma_r^2}\right] + b_r\right\}\left\{a_l \exp\left[\frac{-(\varphi_{l_j}-\theta_l)^2}{2\sigma_l^2}\right] + b_l\right\} \qquad \text{(A14)}$$

and

$$g_j(\theta_r, \theta_l) = a_r \exp\left[\frac{-(\varphi_{r_j}-\theta_r)^2}{2\sigma_r^2}\right] + a_l \exp\left[\frac{-(\varphi_{l_j}-\theta_l)^2}{2\sigma_l^2}\right] + b \qquad \text{(A15)}$$

where a and b are constants, and φ indicates the preferred direction.

Multiplicative case: The numerator of Eq. (A8) can be represented as:

$$\sum_{j=1}^{N} g_j(\theta_r, \theta_l) g_j(\theta_r + \Delta\theta_r, \theta_l + \Delta\theta_l)$$

$$= \sum_{j=1}^{N} \left\{a_r \exp\left[\frac{-(\varphi_{r_j}-\theta_r)^2}{2\sigma_r^2}\right] + b_r\right\}\left\{a_l \exp\left[\frac{-(\varphi_{l_j}-\theta_l)^2}{2\sigma_l^2}\right] + b_l\right\}$$

$$\left\{a_r \exp\left[\frac{-(\varphi_{r_j}-\theta_r-\Delta\theta_r)^2}{2\sigma_r^2}\right] + b_r\right\}\left\{a_l \exp\left[\frac{-(\varphi_{l_j}-\theta_l-\Delta\theta_l)^2}{2\sigma_l^2}\right] + b_l\right\}. \qquad \text{(A16)}$$

If N is sufficiently large and the preferred directions are uniformly distributed,

$$\approx \sum_{j=1}^{\sqrt{N}} \left\{a_r \exp\left[\frac{-(\varphi_{r_j}-\theta_r)^2}{2\sigma_r^2}\right] + b_r\right\}\left\{a_r \exp\left[\frac{-(\varphi_{r_j}-\theta_r-\Delta\theta_r)^2}{2\sigma_r^2}\right] + b_r\right\}$$

$$\times \sum_{j=1}^{\sqrt{N}} \left\{a_l \exp\left[\frac{-(\varphi_{l_j}-\theta_l)^2}{2\sigma_l^2}\right] + b_l\right\}\left\{a_l \exp\left[\frac{-(\varphi_{l_j}-\theta_l-\Delta\theta_l)^2}{2\sigma_l^2}\right] + b_l\right\}, \qquad \text{(A17)}$$

then each summation in Eq. (A17) can be expanded as:

$$\sum_{j=1}^{\sqrt{N}} \left\{ a \exp\left[\frac{-(\varphi_j-\theta)^2}{2\sigma^2}\right] + b \right\} \left\{ a \exp\left[\frac{-(\varphi_j-\theta-\Delta\theta)^2}{2\sigma^2}\right] + b \right\}$$

$$= a^2 \sum_{j=1}^{\sqrt{N}} \exp\left\{ -\frac{(\varphi_j-\theta)^2+(\varphi_j-\theta-\Delta\theta)^2}{2\sigma^2} \right\}$$

$$+ab \sum_{j=1}^{\sqrt{N}} \left[\exp\left\{\frac{-(\varphi_j-\theta)^2}{2\sigma^2}\right\} + \exp\left\{\frac{-(\varphi_j-\theta-\Delta\theta)^2}{2\sigma^2}\right\} \right] + \sqrt{N}b^2. \qquad \text{(A18)}$$

The first term of the right side of Eq. (A18) can be rewritten as:

$$\exp\left\{ -\frac{(\varphi_j-\theta)^2+(\varphi_j-\theta-\Delta\theta)^2}{2\sigma^2} \right\} = \exp\left\{ -\frac{\left(\varphi_j-\frac{2\theta+\Delta\theta}{2}\right)^2}{\sigma^2} \right\} \exp\left\{ -\frac{(\Delta\theta)^2}{4\sigma^2} \right\}. \qquad \text{(A19)}$$

If N is sufficiently large, the summation of Eq. (A19) can be approximated by the integral of the Gaussian function,

$$\sum_{j=1}^{\sqrt{N}} \exp\left\{ -\frac{\left(\varphi_j-\frac{2\theta+\Delta\theta}{2}\right)^2}{\sigma^2} \right\} = \frac{\sqrt{N}}{2\pi} \int \exp\left\{ -\frac{\left(\varphi-\frac{2\theta+\Delta\theta}{2}\right)^2}{\sigma^2} \right\} d\varphi = \frac{\sqrt{N}\sigma}{2\sqrt{\pi}}. \qquad \text{(A20)}$$

Similarly, the summations in the second term on the right-hand side of Eq. (A18) can be obtained from the following equation:

$$\sum_{j=1}^{\sqrt{N}} \exp\left\{\frac{-(\varphi_j-\theta)^2}{2\sigma^2}\right\} = \sum_{j=1}^{\sqrt{N}} \exp\left\{\frac{-(\varphi_j-\theta-\Delta\theta)^2}{2\sigma^2}\right\}$$

$$= \frac{\sqrt{N}}{2\pi} \int \exp\left\{ -\frac{(\varphi-\theta)^2}{2\sigma^2} \right\} d\varphi = \frac{\sqrt{N}\sigma}{\sqrt{2\pi}}. \qquad \text{(A21)}$$

Therefore,

$$\sum_{j=1}^{N} g_j(\theta_r, \theta_l) g_j(\theta_r + \Delta\theta_r, \theta_l + \Delta\theta_l)$$

$$= \left\{ {a_r}^2 \frac{\sigma_r}{2\sqrt{\pi}} \exp\left[-\frac{(\Delta\theta_r)^2}{4\sigma_r^2}\right] + 2a_r b_r \frac{\sigma_r}{\sqrt{2\pi}} + b_r^2 \right\} \left\{ {a_l}^2 \frac{\sigma_l}{2\sqrt{\pi}} \exp\left[-\frac{(\Delta\theta_l)^2}{4\sigma_l^2}\right] + 2a_l b_l \frac{\sigma_l}{\sqrt{2\pi}} + b_l^2 \right\},$$

(A22)

And, consequently,

$$\Phi(\Delta\theta_r, \Delta\theta_l) = \frac{\sum_{j=1}^{N} g_j(\theta_r,\theta_l) g_j(\theta_r+\Delta\theta_r,\theta_l+\Delta\theta_l)}{\sum_{j=1}^{N} g_j(\theta_r,\theta_l) g_j(\theta_r,\theta_l)}$$

$$= \frac{\left\{ {a_r}^2\sigma_r \exp\left[-\frac{(\Delta\theta_r)^2}{4\sigma_r^2}\right] + 2\sqrt{2}a_r b_r \sigma_r + 2\sqrt{\pi} b_r^2 \right\} \left\{ {a_l}^2 \sigma_l \exp\left[-\frac{(\Delta\theta_l)^2}{4\sigma_l^2}\right] + 2\sqrt{2}a_l b_l \sigma_l + 2\sqrt{\pi} b_l^2 \right\}}{\left\{ {a_r}^2\sigma_r + 2\sqrt{2}a_r b_r \sigma_r + 2\sqrt{\pi} b_r^2 \right\} \left\{ {a_l}^2 \sigma_l + 2\sqrt{2}a_l b_l \sigma_l + 2\sqrt{\pi} b_l^2 \right\}}.$$

(A23)

Additive model case: Similar to the case of the multiplicative encoding model under the assumption that N is sufficiently large and the preferred directions are uniformly distributed, additive encoding (Eq.(A15)) predicts $\Phi(\Delta\theta_r, \Delta\theta_l)$ as:

$$\Phi(\Delta\theta_r, \Delta\theta_l) = \frac{\sqrt{\pi}{a_r}^2\sigma_r \exp\left[-\frac{(\Delta\theta_r)^2}{4\sigma_r^2}\right] + \sqrt{\pi}{a_l}^2\sigma_l \exp\left[-\frac{(\Delta\theta_l)^2}{4\sigma_l^2}\right] + 2a_r a_l \sigma_r \sigma_l + 2\sqrt{2\pi}a_r b\sigma_r + 2\sqrt{2\pi}a_l b\sigma_l + 2\pi b^2}{\sqrt{\pi}{a_r}^2\sigma_r + \sqrt{\pi}{a_l}^2\sigma_l + 2a_r a_l \sigma_r \sigma_l + 2\sqrt{2\pi}a_r b\sigma_r + 2\sqrt{2\pi}a_l b\sigma_l + 2\pi b^2}.$$

(A24)

Appendix 2

Effect of the spatial location of visual cues on adaptation to force field

The experiments presented here were designed to reject the contribution of possible confounding effect of visual (spatial) information. If the spatial location of the target itself have some effect to modulate the control process, subjects could simultaneously adapt the same arm movement to different dynamics each of which is consistently associated with the spatial location of the visual cue.

A.2.1 Materials and Methods

Participants. Sixteen right-handed healthy volunteers (age, 20–26 years; 12 males, 4 females) participated in our study after providing written informed consent. All experimental procedures were approved by the ethics committee of the Graduate School of Education, The University of Tokyo.

General task setting. Participants were asked to simultaneously move the handles of 2 robotic manipulanda (Phantom 1.5 HF; SensAble Technologies, Woburn, MA, USA) from their starting positions toward targets presented on a horizontal screen (movement distance, 10 cm) with a peak velocity of 0.47 ± 0.045 $m \cdot s^{-1}$ (Fig. A.2.1A). The velocity was calculated using the minimum-jerk theory (Flash and Hogan, 1985) with a movement distance of 10 cm and duration of 0.4 s. Before

each trial, participants were required to move each cursor into its starting position (1-cm diameter). After a 2-s holding time, a gray target (1-cm diameter) appeared for each handle 10 cm from the starting position. After a further 1-s holding time, the target color changed to magenta, indicating that participants were permitted to begin the reaching movement. During the reaching movement, participants were instructed to fixate on the left target. A warning message was presented on the screen if the movement velocity of either handle was above ('Fast') or below ('Slow') the targeted range described above. Participants could not see their arms directly, and the position of each handle was indicated with a white cursor. Handle movements were constrained to a virtual horizontal plane generated by the manipulanda. Wrist braces were used to reduce unwanted wrist movements. Arm slings supported participants' upper arms to reduce fatigue and allow them to maintain a constant arm posture.

Experiment A1. Eight participants performed 80 trials without a force field (baseline session), 320 trials with a force field (learning session), and 160 trials without a force field (washout session). In each of the sessions, 8 different movement configurations of the right arm (ranging from 0º to 315º at 45° intervals; Fig. A.2.1B) were performed in randomized order. The movement direction of the left arm was always forward.

In the learning session, we applied force fields to the left arm that were dependent on the velocity of the right hand as follows: $\boldsymbol{f}^{L} = \mathbf{B}_1 \boldsymbol{v}^{R}$, where $\boldsymbol{f}^{L}$ is the force on the left arm (N), $\mathbf{B}_1$ is a

viscosity matrix (0, 10; 0, 0) ($N \cdot s \cdot m^{-1}$), and $\boldsymbol{v}^{R}$ is the velocity of the right handle ($m \cdot s^{-1}$). Again, force fields were applied to the left arm only. We set $\mathbf{B}_1$ so that the forward-backward component of $\boldsymbol{f}^{L}$ was always zero, to simplify evaluation of the movement error (i.e., the lateral deviation of the handle at peak velocity). To cancel out the biomechanical effect of the force direction on the lateral deviation of the movement of the left hand, the direction of the force field was reversed for half of the participants so that $\mathbf{B}_1 = (0, -10; 0, 0)$ ($N \cdot s \cdot m^{-1}$). The sign of the movement error due to this reversed force field was reversed, and the results were then averaged across all 8 participants. The relationship between the magnitude of the force field to the left arm and the movement direction of the right arm is shown in Fig. A.2.1B.

Experiment A2. Eight participants attempted to adapt to multiple force fields similar to those of Experiment A1 while always moving both arms forward (i.e., 0º in Fig. A.2.1B). A square was presented as a visual cue for the force fields associated with the 8 different positions of the right arm used in Experiment A1, but the participants were asked to move both arms forward. The force field was derived as follows: $\boldsymbol{f}^{L} = \mathbf{B}_2\boldsymbol{v}^{R}$, where $\mathbf{B}_2 = (0, 10\sin\theta_c; 0, 0)$ ($N \cdot s \cdot m^{-1}$) and θ_c is the direction of the cue for the force field. As in Experiment A1, the direction of the force field was reversed for half of the participants by setting $\mathbf{B}_2 = (0, -10\sin\theta_c; 0, 0)$ ($N \cdot s \cdot m^{-1}$). The relationship between the magnitude of the force field to the left arm and the spatial position of the visual cue is shown in Fig. A.2.1B.

Data acquisition. Data on the motion of the manipulanda were recorded at a sampling rate of 500 Hz. Handle velocity data were low-pass filtered using a 4^{th}-order Butterworth filter with a cutoff frequency of 8 Hz. The lateral deviation of each handle trajectory at the peak velocity from a straight line between the starting position and target was quantified, and the difference between this value and that of the baseline session was used as the movement error.

Statistical tests. In Experiments A1 and A2, the error reduction from the early (1^{st}–5^{th}) to the late (36^{th}–40^{th}) learning trials and the aftereffects in the 1^{st}–5^{th} washout trials was tested for each movement direction using a paired t-test with Bonferroni's correction. The significance level was set to $P < 0.05$.

A.2.2 Results and Discussion

Participants moved their left arm to a single forward target while moving their right arm to 1 of 8 peripheral targets presented randomly (Fig. A.2.1B). Thus, the same left arm movement was exposed to varying force fields depending on the movement direction of the right arm. The entire results of Experiment A1 are shown in Fig. A.2.2A. As expected, movement error gradually decreased in the presence of the force fields. In 5 of 6 force-field directions, the reduction in errors from the early (1^{st}–5^{th} trials) to the late (36^{th}–40^{th}) trials was significant ($P < 0.05$). In addition, the aftereffect was modulated by the movement direction of the right arm. Significant aftereffects were also observed in all 6 directions ($P < 0.05$). Additionally, in the remaining 2 directions in which no force field was applied, no significant aftereffect was observed. Thus, at least 3 different force fields were actually learned in Experiment A1.

To further examine whether the aftereffect was a smooth cosine function of right arm movement direction θ or a categorical function of 2 conflicting and null force fields, we compared the goodness of fit between the following two models: a cosine function (aftereffect = $a \cos\theta + b$) and a signum function (aftereffect = $a \operatorname{sgn}(\cos\theta) + b$). The adjusted R^2 calculated for each model using the bootstrap technique (1,000 bootstrapped samples were synthesized for each model) was significantly larger ($P < 0.001$ by Wilcoxon rank sum test) for the cosine model ($R^2 = 0.807$) than for

the signum model (R^2 = 0.795), indicating that the cosine tuning of the aftereffect was more plausible.

Movement of the right arm could be argued to function as a strong cognitive cue to switch internal models. Indeed, despite some debate (Gupta and Ashe, 2007), several studies have shown that different motor memories can be constructed using cognitive cues (Osu et al., 2004; Cothros et al., 2009). If this has occurred in the present study, participants could also adapt to multiple force fields without overt movement of the opposite arm toward different directions. Contrary to this expectation, another 8 participants who attempted to adapt to similar multiple force fields while moving both arms forward with visual cues for each force field (Experiment A2) did not show evidence of simultaneous learning (Fig. A.2.2B). These results cannot be explained by the difference in the kinematics of the left hand (see Fig. A.2.3).

Taken together, spatial location of visual cue itself is unlikely to explain the result of the present experiment, as well as the result of studies presented in the main body of this thesis (Chapter 3 and 4).

Figures

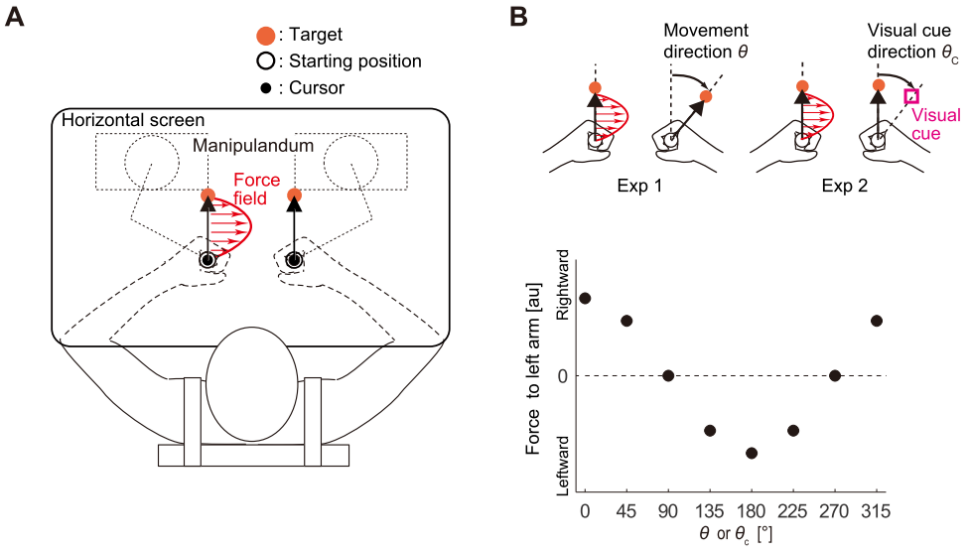

Figure A.2.1. Motor learning task with concurrent movement of the opposite arm.

A, Bimanual reaching task in which participants were trained to adapt a reaching movement with the left arm to a velocity-dependent force field while concurrently moving the right arm. The left arm always moved in the forward direction, while the movement direction of the right arm varied in Experiment A1. ***B***, The amplitude of the force field to the left arm was modulated in a cosine fashion according to the movement direction of the right arm θ (Experiment A1) or the direction of visual cue θ_C (Experiment A2). Note that the right arm always made the same forward movement in the visual cue condition (Experiment A2). Forward direction corresponds to 0º.

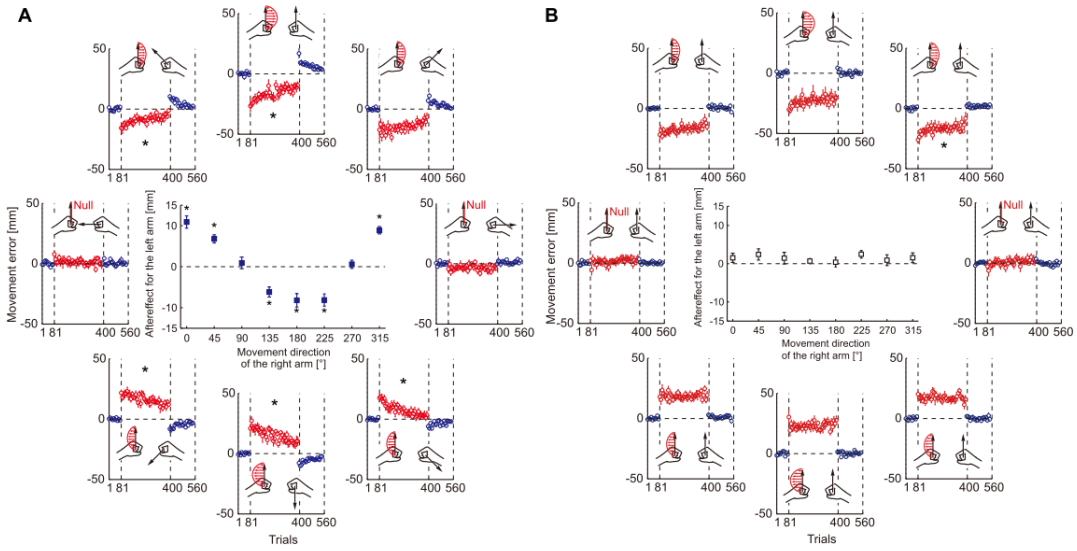

Figure A.2.2. Simultaneous adaptations to multiple force fields.

A, ***B***, Trial-dependent profiles of the movement error of the left arm for Experiments A1 (***A***) and A2 (***B***). Data are presented as mean values ± SE. Peripheral plots represent the trial-dependent error profiles (force field trials are shown as red circles and null-force-field trials as blue circles). The positions of the panels correspond to the 8 movement directions of the right arm (***A***) and the visual cue direction (***B***). The center panel indicates the relationship between the aftereffect error in the 1st–5th washout trials and the movement direction of the right arm (***A***) and the visual cue direction (***B***). The asterisks in the peripheral panels and center panels indicate, respectively, a significant reduction of the movement error (1st–5th trials vs. 36th–40th trials) and a significant aftereffect ($P < 0.05$).

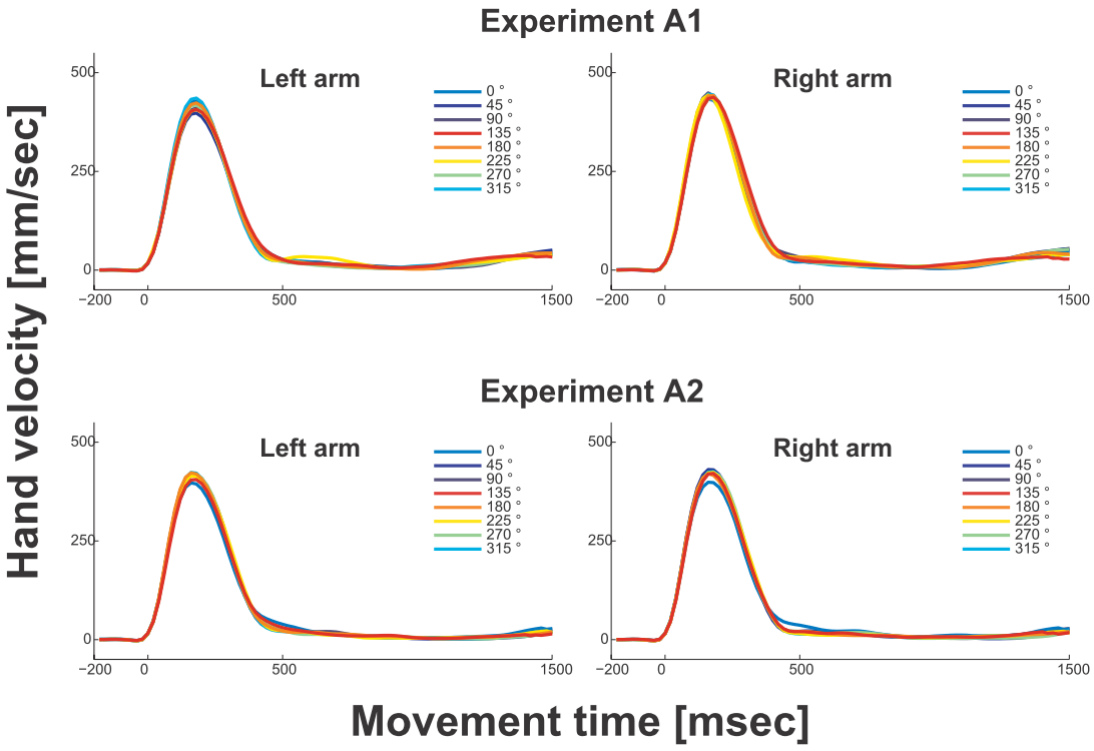

Figure A.2.3. **Kinematics of Reaching Movements**

Velocity profiles of the left and right handles under all experimental conditions of the baseline session are shown (Experiments A1, A2). The velocity profiles were averaged across all participants for each experiment and aligned with the movement onset time as time zero. The color of the lines indicates the movement direction of the right arm. A two-way ANOVA performed using the arm (left or right) and the movement direction of the right arm as factors revealed that there was no significant effect of the arm on the movement onset time (defined as the time at which the movement velocity of the hand first exceeded 10% of its peak value from the Go cue) ($P > 0.05$) and that there was no significant effect of the movement direction of the right arm on the peak velocity of the left arm ($P > 0.05$).

References

Adkins DL, Boychuk J, Remple MS, Kleim JA (2006) Motor training induces experience-specific patterns of plasticity across motor cortex and spinal cord. J Appl Physiol 101:1776-1782.

Ahmadi-Pajouh MA, Towhidkhah F, Shadmehr R (2012) Preparing to reach: selecting an adaptive long-latency feedback controller. J Neurosci 32:9537-9545.

Ahmed AA, Wolpert DM, Flanagan JR (2008) Flexible representations of dynamics are used in object manipulation. Curr Biol 18:763-768.

Aizawa H, Bianco IH, Hamaoka T, Miyashita T, Uemura O, Concha ML, Russell C, Wilson SW, Okamoto H (2005) Laterotopic representation of left-right information onto the dorso-ventral axis of a zebrafish midbrain target nucleus. Curr Biol 15:238-243.

Andersen RA, Mountcastle VB (1983) The influence of the angle of gaze upon the excitability of the light-sensitive neurons of the posterior parietal cortex. J Neurosci 3:532-548.

Andersen RA, Essick GK, Siegel RM (1985) Encoding of spatial location by posterior parietal neurons. Science 230:456-458.

Annett M (1985) Left, right, hand and brain: the right shift theory: Lawrence Erlbaum Associates.

Arce F, Novick I, Mandelblat-Cerf Y, Vaadia E (2010) Neuronal correlates of memory formation in motor cortex after adaptation to force field. J Neurosci 30:9189-9198.

Armstrong CA, Oldham JA (1999) A comparison of dominant and non-dominant hand strengths. J Hand Surg Br 24:421-425.

Asanuma H, Okuda O (1962) Effects of transcallosal volleys on pyramidal tract cell activity of cat. J Neurophysiol 25:198-208.

Asanuma H, Rosén I (1972) Topographical organization of cortical efferent zones projecting to distal forelimb muscles in the monkey. Exp Brain Res 14:243-256.

Atkeson CG (1989) Learning arm kinematics and dynamics. Annu Rev Neurosci 12:157-183.

Avanzino L, Teo JT, Rothwell JC (2007) Intracortical circuits modulate transcallosal inhibition in humans. J Physiol 583:99-114.

Avesar D, Gulledge AT (2012) Selective serotonergic excitation of callosal projection neurons. Front Neural Circ 6.

Bastian AJ, Martin TA, Keating JG, Thach WT (1996) Cerebellar ataxia: Abnormal control of interaction torques across multiple joints. J Neurophysiol 76:492-509.

Bays PM, Wolpert DM (2006) Actions and consequences in bimanual interaction are represented in different coordinate systems. J Neurosci 26:7121-7126.

Bays PM, Wolpert DM (2007) Computational principles of sensorimotor control that minimize

uncertainty and variability. J Physiol 578:387-396.

Bays PM, Wolpert DM, Flanagan JR (2005) Perception of the consequences of self-action is temporally tuned and event driven. Curr Biol 15:1125-1128.

Beck JM, Latham PE, Pouget A (2011) Marginalization in neural circuits with divisive normalization. J Neurosci 31:15310-15319.

Beidelman TO (1961) Right and left hand among the Kaguru - A note on symbolic classification. Africa 31:250-257.

Bennett S (1993) A History of Control Engineering: 1930-1955: Peter Peregrinus.

Berniker M, Kording KP (2008) Estimating the sources of motor errors for adaptation and generalization. Nat Neurosci 11:1454-1461.

Bernstein NA (1967) The co-ordination and regulation of movements: Pergamon Press.

Bhushan N, Shadmehr R (1999) Computational nature of human adaptive control during learning of reaching movements in force fields. Biol Cybern 81:39-60.

Bianco IH, Carl M, Russell C, Clarke JD, Wilson SW (2008) Brain asymmetry is encoded at the level of axon terminal morphology. Neural Dev 3:9.

Bizzi E, Cheung VC, d'Avella A, Saltiel P, Tresch M (2008) Combining modules for movement. Brain Res Rev 57:125-133.

Blakemore SJ, Goodbody SJ, Wolpert DM (1998) Predicting the consequences of our own actions: the role of sensorimotor context estimation. J Neurosci 18:7511-7518.

Blakemore SJ, Frith CD, Wolpert DM (1999) Spatio-temporal prediction modulates the perception of self-produced stimuli. J Cogn Neurosci 11:551-559.

Blakemore SJ, Wolpert D, Frith C (2000) Why can't you tickle yourself? Neuroreport 11:R11-16.

Bloom JS, Hynd GW (2005) The role of the corpus callosum in interhemispheric transfer of information: excitation or inhibition? Neuropsychol Rev 15:59-71.

Botev ZI, Grotowski JF, Kroese DP (2010) Kernel density estimation via diffusion. Ann Stat 38:2916-2957.

Bouisset S, Zattara M (1987) Biomechanical study of the programming of anticipatory postural adjustments associated with voluntary movement. J Biomech 20:735-742.

Bouisset S, Do MC (2008) Posture, dynamic stability, and voluntary movement. Neurophysiol Clin 38:345-362.

Boussaoud D, Jouffrais C, Bremmer F (1998) Eye position effects on the neuronal activity of dorsal premotor cortex in the macaque monkey. J Neurophysiol 80:1132-1150.

Bradshaw JL, Rogers LJ (1996) Tool use and the evolutionary development of manual asymmetry. In: Manual asymmetries in motor performance, pp 33-54. New York: CRC Press.

Brashers-Krug T, Shadmehr R, Bizzi E (1996) Consolidation in human motor memory. Nature 382:252-255.

Brayanov JB, Press DZ, Smith MA (2012) Motor memory is encoded as a gain-field combination of intrinsic and extrinsic action representations. J Neurosci 32:14951-14965.

Brown C, Magat M (2011) Cerebral lateralization determines hand preferences in Australian parrots. Biol Lett 7:496-498.

Buonomano DV, Merzenich MM (1998) Cortical plasticity: from synapses to maps. Annu Rev Neurosci 21:149-186.

Burish MJ, Stepniewska I, Kaas JH (2008) Microstimulation and architectonics of frontoparietal cortex in common marmosets (Callithrix jacchus). J Comp Neurol 507:1151-1168.

Byrne RA, Kuba MJ, Meisel DV, Griebel U, Mather JA (2006a) Octopus arm choice is strongly influenced by eye use. Behav Brain Res 172:195-201.

Byrne RA, Kuba MJ, Meisel DV, Griebel U, Mather JA (2006b) Does Octopus vulgaris have preferred arms? J Comp Psychol 120:198-204.

Carson RG (2005) Neural pathways mediating bilateral interactions between the upper limbs. Brain Res Rev 49:641-662.

Carson RG, Goodman D, Chua R, Elliott D (1993) Asymmetries in the regulation of visually guided aiming. J Mot Behav 25:21-32.

Casey BJ, Thomas KM, Welsh TF, Badgaiyan RD, Eccard CH, Jennings JR, Crone EA (2000) Dissociation of response conflict, attentional selection, and expectancy with functional magnetic resonance imaging. Proc Natl Acad Sci U S A 97:8728-8733.

Chance FS, Abbott LF, Reyes AD (2002) Gain modulation from background synaptic input. Neuron 35:773-782.

Chang SW, Snyder LH (2012) The representations of reach endpoints in posterior parietal cortex depend on which hand does the reaching. J Neurophysiol 107:2352-2365.

Chao ZC, Nagasaka Y, Fujii N (2010) Long-term asynchronous decoding of arm motion using electrocorticographic signals in monkeys. Front Neuroeng 3:3.

Chen R (2004) Interactions between inhibitory and excitatory circuits in the human motor cortex. Exp Brain Res 154:1-10.

Chen XY, Pillai S, Chen Y, Wang Y, Chen L, Carp JS, Wolpaw JR (2007) Spinal and supraspinal effects of long-term stimulation of sensorimotor cortex in rats. J Neurophysiol 98:878-887.

Chen Y, Chen L, Wang Y, Wolpaw JR, Chen XY (2011) Operant conditioning of rat soleus H-reflex oppositely affects another H-reflex and changes locomotor kinematics. J Neurosci 31:11370-11375.

Cheung VC, d'Avella A, Bizzi E (2009a) Adjustments of motor pattern for load compensation via modulated activations of muscle synergies during natural behaviors. J Neurophysiol 101:1235-1257.

Cheung VC, Piron L, Agostini M, Silvoni S, Turolla A, Bizzi E (2009b) Stability of muscle synergies for

voluntary actions after cortical stroke in humans. Proc Natl Acad Sci U S A 106:19563-19568.

Cisek P (2008) A remarkable facilitating effect of parietal damage. Neuron 58:7-9.

Cisek P, Kalaska JF (2005) Neural correlates of reaching decisions in dorsal premotor cortex: specification of multiple direction choices and final selection of action. Neuron 45:801-814.

Cisek P, Crammond DJ, Kalaska JF (2003) Neural activity in primary motor and dorsal premotor cortex in reaching tasks with the contralateral versus ipsilateral arm. J Neurophysiol 89:922-942.

Clarac F (2005a) The History of Reflexes Part 1: From Descartes to Pavlov. In: IBRO History of Neuroscience.

Clarac F (2005b) The History of Reflexes Part 2: From Sherrington to 2004. In: IBRO History of Neuroscience.

Collinger JL, Wodlinger B, Downey JE, Wang W, Tyler-Kabara EC, Weber DJ, McMorland AJ, Velliste M, Boninger ML, Schwartz AB (2012) High-performance neuroprosthetic control by an individual with tetraplegia. Lancet.

Coltz JD, Johnson MT, Ebner TJ (1999) Cerebellar Purkinje cell simple spike discharge encodes movement velocity in primates during visuomotor arm tracking. J Neurosci 19:1782-1803.

Cothros N, Wong JD, Gribble PL (2006) Are there distinct neural representations of object and limb dynamics? Exp Brain Res 173:689-697.

Cothros N, Wong J, Gribble PL (2009) Visual cues signaling object grasp reduce interference in motor learning. J Neurophysiol 102:2112-2120.

Coulthard EJ, Nachev P, Husain M (2008) Control over conflict during movement preparation: role of posterior parietal cortex. Neuron 58:144-157.

Crenna P, Frigo C (1991) A motor programme for the initiation of forward-oriented movements in humans. J Physiol 437:635-653.

Criscimagna-Hemminger S, Shadmehr R (2008) Consolidation patterns of human motor memory. J Neurosci 28:9610-9618.

Criscimagna-Hemminger S, Donchin O, Gazzaniga M, Shadmehr R (2003) Learned dynamics of reaching movements generalize from dominant to nondominant arm. J Neurophysiol 89:168-176.

Criscimagna-Hemminger SE, Bastian AJ, Shadmehr R (2010) Size of error affects cerebellar contributions to motor learning. J Neurophysiol 103:2275-2284.

Crook JM, Eysel UT (1992) GABA-induced inactivation of functionally characterized sites in cat visual cortex (area 18): effects on orientation tuning. J Neurosci 12:1816-1825.

Crook JM, Eysel UT, Machemer HF (1991) Influence of GABA-induced remote inactivation on the orientation tuning of cells in area 18 of feline visual cortex: a comparison with area 17. Neuroscience 40:1-12.

Crook JM, Kisvárday ZF, Eysel UT (1998) Evidence for a contribution of lateral inhibition to orientation tuning and direction selectivity in cat visual cortex: reversible inactivation of functionally

characterized sites combined with neuroanatomical tracing techniques. Eur J Neurosci 10:2056-2075.

Crosby CA, Wehbé MA, Mawr B (1994) Hand strength: normative values. J Hand Surg Am 19:665-670.

d'Avella A, Portone A, Lacquaniti F (2011) Superposition and modulation of muscle synergies for reaching in response to a change in target location. J Neurophysiol 106:2796-2812.

d'Avella A, Portone A, Fernandez L, Lacquaniti F (2006) Control of fast-reaching movements by muscle synergy combinations. J Neurosci 26:7791-7810.

Della-Maggiore V, Malfait N, Ostry DJ, Paus T (2004) Stimulation of the posterior parietal cortex interferes with arm trajectory adjustments during the learning of new dynamics. J Neurosci 24:9971-9976.

Descartes R, Hall TS (1972) Treatise of man: Harvard University Press.

Di Lazzaro V, Oliviero A, Profice P, Insola A, Mazzone P, Tonali P, Rothwell JC (1999) Direct demonstration of interhemispheric inhibition of the human motor cortex produced by transcranial magnetic stimulation. Exp Brain Res 124:520-524.

Diedrichsen J (2007) Optimal task-dependent changes of bimanual feedback control and adaptation. Curr Biol 17:1675-1679.

Diedrichsen J (2012) Motor coordination. Scholarpedia 7:12309.

Diedrichsen J, Shadmehr R, Ivry RB (2010) The coordination of movement: optimal feedback control and beyond. Trends Cogn Sci 14:31-39.

Diedrichsen J, Wiestler T, Krakauer JW (2012) Two Distinct Ipsilateral Cortical Representations for Individuated Finger Movements. Cereb Cortex.

Diedrichsen J, Hashambhoy Y, Rane T, Shadmehr R (2005) Neural correlates of reach errors. J Neurosci 25:9919-9931.

Diedrichsen J, Verstynen T, Hon A, Lehman SL, Ivry RB (2003) Anticipatory adjustments in the unloading task: Is an efference copy necessary for learning? Exp Brain Res 148:272-276.

Dimitriou M, Franklin DW, Wolpert DM (2012) Task-dependent coordination of rapid bimanual motor responses. J Neurophysiol 107:890-901.

Dizio P, Lackner JR (1995) Motor adaptation to Coriolis force perturbations of reaching movements: endpoint but not trajectory adaptation transfers to the nonexposed arm. J Neurophysiol 74:1787-1792.

Dominici N, Ivanenko YP, Cappellini G, d'Avella A, Mondì V, Cicchese M, Fabiano A, Silei T, Di Paolo A, Giannini C, Poppele RE, Lacquaniti F (2011) Locomotor primitives in newborn babies and their development. Science 334:997-999.

Donchin O, Francis J, Shadmehr R (2003) Quantifying generalization from trial-by-trial behavior of adaptive systems that learn with basis functions: theory and experiments in human motor control. J Neurosci 23:9032-9045.

Donchin O, Gribova A, Steinberg O, Bergman H, Vaadia E (1998) Primary motor cortex is involved in bimanual coordination. Nature 395:274-278.

Donchin O, Rabe K, Diedrichsen J, Lally N, Schoch B, Gizewski ER, Timmann D (2012) Cerebellar regions involved in adaptation to force field and visuomotor perturbation. J Neurophysiol 107:134-147.

Dosenbach NU, Visscher KM, Palmer ED, Miezin FM, Wenger KK, Kang HC, Burgund ED, Grimes AL, Schlaggar BL, Petersen SE (2006) A core system for the implementation of task sets. Neuron 50:799-812.

Duda RO, Hart PE, Stork DG (2001) Pattern classification: Wiley.

Duff SV, Sainburg RL (2007) Lateralization of motor adaptation reveals independence in control of trajectory and steady-state position. Exp Brain Res 179:551-561.

Duque J, Mazzocchio R, Dambrosia J, Murase N, Olivier E, Cohen LG (2005) Kinematically specific interhemispheric inhibition operating in the process of generation of a voluntary movement. Cereb Cortex 15:588-593.

Duque J, Murase N, Celnik P, Hummel F, Harris-Love M, Mazzocchio R, Olivier E, Cohen LG (2007) Intermanual Differences in movement-related interhemispheric inhibition. J Cogn Neurosci 19:204-213.

Eccles JC (1982) The synapse: from electrical to chemical transmission. Annu Rev Neurosci 5:325-339.

Egner T, Hirsch J (2005) Cognitive control mechanisms resolve conflict through cortical amplification of task-relevant information. Nat Neurosci 8:1784-1790.

Eisenberg M, Shmuelof L, Vaadia E, Zohary E (2010) Functional organization of human motor cortex: directional selectivity for movement. J Neurosci 30:8897-8905.

Eisenberg M, Shmuelof L, Vaadia E, Zohary E (2011) The representation of visual and motor aspects of reaching movements in the human motor cortex. J Neurosci 31:12377-12384.

Eldred E, Granit R, Merton PA (1953) Supraspinal control of the muscle spindles and its significance. J Physiol 122:498-523.

Elliott D, Lyons J, Chua R, Goodman D, Carson RG (1995) The influence of target perturbation on manual aiming asymmetries in right-handers. Cortex 31:685-697.

Elliott DE, Roy EA (1996) Manual Asymmetries in Motor Performance: CRC PressINC.

Eriksen CW (1995) The flankers task and response competition: A useful tool for investigating a viriety of cognitive problems. Visual Cognition 2:101-118.

Ethier C, Brizzi L, Darling WG, Capaday C (2006) Linear summation of cat motor cortex outputs. J Neurosci 26:5574-5581.

Evarts EV (1968) Relation of pyramidal tract activity to force exerted during voluntary movement. J Neurophysiol 31:14-27.

Fahle M (2005) Perceptual learning: specificity versus generalization. Curr Opin Neurobiol 15:154-160.

Feingold J, Desrochers TM, Fujii N, Harlan R, Tierney PL, Shimazu H, Amemori K, Graybiel AM (2012) A system for recording neural activity chronically and simultaneously from multiple cortical and subcortical regions in nonhuman primates. J Neurophysiol 107:1979-1995.

Ferbert A, Priori A, Rothwell JC, Day BL, Colebatch JG, Marsden CD (1992) Interhemispheric inhibition of the human motor cortex. J Physiol 453:525-546.

Fetz EE (1969) Operant conditioning of cortical unit activity. Science 163:955-958.

Fetz EE, Finocchio DV (1971) Operant conditioning of specific patterns of neural and muscular activity. Science 174:431-435.

Finch M (2004) Triathlon Training: Human Kinetics.

Fincham JM, Carter CS, van Veen V, Stenger VA, Anderson JR (2002) Neural mechanisms of planning: a computational analysis using event-related fMRI. Proc Natl Acad Sci U S A 99:3346-3351.

Flash T, Hogan N (1985) The coordination of arm movements: an experimentally confirmed mathematical model. J Neurosci 5:1688-1703.

Flowers K (1975) Handedness and controlled movement. Br J Psychol 66:39-52.

Franklin DW, Wolpert DM (2011) Computational mechanisms of sensorimotor control. Neuron 72:425-442.

Franklin S, Wolpert DM, Franklin DW (2012) Visuomotor feedback gains upregulate during the learning of novel dynamics. J Neurophysiol 108:467-478.

Franz EA, Waldie KE, Smith MJ (2000) The effect of callosotomy on novel versus familiar bimanual actions: a neural dissociation between controlled and automatic processes? Psychol Sci 11:82-85.

Frey SH (2008) Tool use, communicative gesture and cerebral asymmetries in the modern human brain. Philos Trans R Soc Lond B Biol Sci 363:1951-1957.

Fujii S, Kudo K, Ohtsuki T, Oda S (2010) Intrinsic constraint of asymmetry acting as a control parameter on rapid, rhythmic bimanual coordination: a study of professional drummers and nondrummers. J Neurophysiol 104:2178-2186.

Gandolfo F, Mussa-Ivaldi F, Bizzi E (1996) Motor learning by field approximation. Proc Natl Acad Sci U S A 93:3843-3846.

Gandolfo F, Li C, Benda B, Schioppa C, Bizzi E (2000) Cortical correlates of learning in monkeys adapting to a new dynamical environment. Proc Natl Acad Sci U S A 97:2259-2263.

Ganguly K, Carmena JM (2009) Emergence of a stable cortical map for neuroprosthetic control. PLoS Biol 7:e1000153.

Ganguly K, Carmena JM (2010) Neural correlates of skill acquisition with a cortical brain-machine interface. J Mot Behav 42:355-360.

Ganguly K, Dimitrov DF, Wallis JD, Carmena JM (2011) Reversible large-scale modification of cortical networks during neuroprosthetic control. Nat Neurosci 14:662-667.

Ganguly K, Secundo L, Ranade G, Orsborn A, Chang EF, Dimitrov DF, Wallis JD, Barbaro NM, Knight

RT, Carmena JM (2009) Cortical representation of ipsilateral arm movements in monkey and man. J Neurosci 29:12948-12956.

Gentner R, Gorges S, Weise D, aufm Kampe K, Buttmann M, Classen J (2010) Encoding of motor skill in the corticomuscular system of musicians. Curr Biol 20:1869-1874.

Georgopoulos AP, Caminiti R, Kalaska JF (1984) Static spatial effects in motor cortex and area 5: quantitative relations in a two-dimensional space. Exp Brain Res 54:446-454.

Georgopoulos AP, Schwartz AB, Kettner RE (1986) Neuronal population coding of movement direction. Science 233:1416-1419.

Georgopoulos AP, Kalaska JF, Caminiti R, Massey JT (1982) On the relations between the direction of two-dimensional arm movements and cell discharge in primate motor cortex. J Neurosci 2:1527-1537.

Ghirlanda S, Enquist M (2007) How training and testing histories affect generalization: a test of simple neural networks. Philos Trans R Soc Lond B Biol Sci 362:449-454.

Ghosh S, Porter R (1988) Morphology of pyramidal neurones in monkey motor cortex and the synaptic actions of their intracortical axon collaterals. J Physiol 400:593-615.

Giszter SF, Mussa-Ivaldi FA, Bizzi E (1993) Convergent force fields organized in the frog's spinal cord. J Neurosci 13:467-491.

Goble DJ, Brown SH (2008) The biological and behavioral basis of upper limb asymmetries in sensorimotor performance. Neurosci Biobehav Rev 32:598-610.

Gonzalez Castro LN, Monsen CB, Smith MA (2011) The binding of learning to action in motor adaptation. PLoS Comput Biol 7:e1002052.

Graziano MS, Taylor CS, Moore T (2002) Complex movements evoked by microstimulation of precentral cortex. Neuron 34:841-851.

Graziano MS, Aflalo TN, Cooke DF (2005) Arm movements evoked by electrical stimulation in the motor cortex of monkeys. J Neurophysiol 94:4209-4223.

Green AM, Kalaska JF (2011) Learning to move machines with the mind. Trends Neurosci 34:61-75.

Guertin P (2008) Can the spinal cord learn and remember? ScientificWorldJournal 8:757-761.

Guiard Y (1987) Asymmetric division of labor in human skilled bimanual action: the kinematic chain as a model. J Mot Behav 19:486-517.

Haas G, Diener HC, Rapp H, Dichgans J (1989) Development of feedback and feedforward control of upright stance. Dev Med Child Neurol 31:481-488.

Habas C, Kamdar N, Nguyen D, Prater K, Beckmann CF, Menon V, Greicius MD (2009) Distinct cerebellar contributions to intrinsic connectivity networks. J Neurosci 29:8586-8594.

Hanajima R, Ugawa Y, Machii K, Mochizuki H, Terao Y, Enomoto H, Furubayashi T, Shiio Y, Uesugi H, Kanazawa I (2001) Interhemispheric facilitation of the hand motor area in humans. J Physiol 531:849-859.

Harris CM, Wolpert DM (1998) Signal-dependent noise determines motor planning. Nature 394:780-784.

Hayashi M, Saito D, Aramaki Y, Asai T, Fujibayashi Y, Sadato N (2008) Hemispheric asymmetry of frequency-dependent suppression in the ipsilateral primary motor cortex during finger movement: a functional magnetic resonance imaging study. Cereb Cortex 18:2932-2940.

Hirashima M, Nozaki D (2012) Distinct motor plans form and retrieve distinct motor memories for physically identical movements. Curr Biol 22:432-436.

Hirashima M, Yamane K, Nakamura Y, Ohtsuki T (2008) Kinetic chain of overarm throwing in terms of joint rotations revealed by induced acceleration analysis. J Biomech:2874-2883.

Hobert O, Johnston RJ, Jr., Chang S (2002) Left-right asymmetry in the nervous system: the Caenorhabditis elegans model. Nat Rev Neurosci 3:629-640.

Hochberg LR, Bacher D, Jarosiewicz B, Masse NY, Simeral JD, Vogel J, Haddadin S, Liu J, Cash SS, van der Smagt P, Donoghue JP (2012) Reach and grasp by people with tetraplegia using a neurally controlled robotic arm. Nature 485:372-375.

Hogan N, Bizzi E, Mussa-Ivaldi FA, Flash T (1987) Controlling multijoint motor behavior. Exerc Sport Sci Rev 15:153-190.

Holdefer RN, Miller LE (2002) Primary motor cortical neurons encode functional muscle synergies. Exp Brain Res 146:233-243.

Hollerbach JM, Flash T (1982) Dynamic interactions between limb segments during planar arm movement. Biol Cybern 44:67-77.

Hopkins WD (1996) Chimpanzee handedness revisited: 55 years since Finch (1941). Psychonomic Bull Rev 3:449-457.

Hopkins WD, Russell JL (2004) Further evidence of a right hand advantage in motor skill by chimpanzees (Pan troglodytes). Neuropsychologia 42:990-996.

Houk JC (1979) Regulation of stiffness by skeleto-motor reflexes. Ann Rev Physiol 41:99-114.

Howard IS, Ingram JN, Wolpert DM (2010) Context-dependent partitioning of motor learning in bimanual movements. J Neurophysiol 104:2082-2091.

Howard IS, Ingram JN, Franklin DW, Wolpert DM (2012) Gone in 0.6 seconds: the encoding of motor memories depends on recent sensorimotor states. J Neurosci 32:12756-12768.

Hunt GR, Corballis MC, Gray RD (2001) Laterality in tool manufacture by crows - Neural processing and not ecological factors may influence 'handedness' in these birds. Nature 414:707-707.

Hwang EJ, Donchin O, Smith MA, Shadmehr R (2003) A gain-field encoding of limb position and velocity in the internal model of arm dynamics. PLoS Biol 1:209-220.

Imamizu H, Miyauchi S, Tamada T, Sasaki Y, Takino R, Pütz B, Yoshioka T, Kawato M (2000) Human cerebellar activity reflecting an acquired internal model of a new tool. Nature 403:192-195.

Ingham NJ, McAlpine D (2005) GABAergic inhibition controls neural gain in inferior colliculus neurons sensitive to interaural time differences. J Neurosci 25:6187-6198.

Ingram JN, Howard IS, Flanagan JR, Wolpert DM (2011) A single-rate context-dependent learning process underlies rapid adaptation to familiar object dynamics. PLoS Comput Biol 7:e1002196.

Irlbacher K, Brocke J, Mechow JV, Brandt SA (2007) Effects of GABA(A) and GABA(B) agonists on interhemispheric inhibition in man. Clin Neurophysiol 118:308-316.

Ito M (1989) Long-term depression. Annu Rev Neurosci 12:85-102.

Izawa J, Criscimagna-Hemminger SE, Shadmehr R (2012a) Cerebellar contributions to reach adaptation and learning sensory consequences of action. J Neurosci 32:4230-4239.

Izawa J, Pekny SE, Marko MK, Haswell CC, Shadmehr R, Mostofsky SH (2012b) Motor learning relies on integrated sensory inputs in ADHD, but over-selectively on proprioception in autism spectrum conditions. Autism Res 5:124-136.

Jackson A, Spinks RL, Freeman TC, Wolpert DM, Lemon RN (2002) Rhythm generation in monkey motor cortex explored using pyramidal tract stimulation. J Physiol 541:685-699.

Jackson CP, Miall RC (2008) Contralateral manual compensation for velocity-dependent force perturbations. Exp Brain Res 184:261-267.

Jarosiewicz B, Chase SM, Fraser GW, Velliste M, Kass RE, Schwartz AB (2008) Functional network reorganization during learning in a brain-computer interface paradigm. Proc Natl Acad Sci U S A 105:19486-19491.

Jeeves MA, Silver PH, Milne AB (1988) Role of the corpus-callosum in the development of a bimanual motor skill. Developmental Neuropsychology 4:305-323.

Johansen-Berg H, Della-Maggiore V, Behrens TE, Smith SM, Paus T (2007) Integrity of white matter in the corpus callosum correlates with bimanual co-ordination skills. Neuroimage 36 Suppl 2:T16-21.

Johansson RS, Westling G (1988) Programmed and triggered actions to rapid load changes during precision grip. Exp Brain Res 71:72-86.

Johansson RS, Theorin A, Westling G, Andersson M, Ohki Y, Nyberg L (2006) How a lateralized brain supports symmetrical bimanual tasks. PLoS Biol 4:e158.

Kalaska JF, Cohen DA, Hyde ML, Prud'homme M (1989) A comparison of movement direction-related versus load direction-related activity in primate motor cortex, using a two-dimensional reaching task. J Neurosci 9:2080-2102.

Kamitani Y, Tong F (2005) Decoding the visual and subjective contents of the human brain. Nat Neurosci 8:679-685.

Kandel E, Schwartz J, Jessell T (2000) Principles of Neural Science, Fourth Edition: McGraw-Hill Companies,Incorporated.

Kasuga S, Nozaki D (2011) Cross talk in implicit assignment of error information during bimanual visuomotor learning. J Neurophysiol 106:1218-1226.

Kawakami R, Shinohara Y, Kato Y, Sugiyama H, Shigemoto R, Ito I (2003) Asymmetrical allocation of

NMDA receptor epsilon2 subunits in hippocampal circuitry. Science 300:990-994.

Kawato M (1989) Adaptation and learning in control of voluntary movement by the central nervous system. Adv Robotics 3:229–249.

Kawato M, Gomi H (1992) The cerebellum and VOR/OKR learning models. Trends Neurosci 15:445-453.

Kawato M, Wolpert D (1998) Internal models for motor control. Novartis Found Symp 218:291-304; discussion 304-297.

Kennerley SW, Diedrichsen J, Hazeltine E, Semjen A, Ivry RB (2002) Callosotomy patients exhibit temporal uncoupling during continuous bimanual movements. Nat Neurosci 5:376-381.

Kitazawa S (2002) Neurobiology: ready to unlearn. Nature 416:270-273.

Kitazawa S, Kohno T, Uka T (1995) Effects of delayed visual information on the rate and amount of prism adaptation in the human. J Neurosci 15:7644-7652.

Kubánek J, Miller KJ, Ojemann JG, Wolpaw JR, Schalk G (2009) Decoding flexion of individual fingers using electrocorticographic signals in humans. J Neural Eng 6:066001.

Lackner JR, Dizio P (1994) Rapid adaptation to Coriolis force perturbations of arm trajectory. J Neurophysiol 72:299-313.

Lal R, Friedlander MJ (1990) Effect of passive eye position changes on retinogeniculate transmission in the cat. J Neurophysiol 63:502-522.

Landry P, Labelle A, Deschênes M (1980) Intracortical distribution of axonal collaterals of pyramidal tract cells in the cat motor cortex. Brain Res 191:327-336.

Lee H, Gunraj C, Chen R (2007) The effects of inhibitory and facilitatory intracortical circuits on interhemispheric inhibition in the human motor cortex. J Physiol 580:1021-1032.

Lee JY, Schweighofer N (2009) Dual adaptation supports a parallel architecture of motor memory. J Neurosci 29:10396-10404.

Letzkus P, Ribi WA, Wood JT, Zhu H, Zhang SW, Srinivasan MV (2006) Lateralization of olfaction in the honeybee Apis mellifera. Curr Biol 16:1471-1476.

Li C, Padoa-Schioppa C, Bizzi E (2001) Neuronal correlates of motor performance and motor learning in the primary motor cortex of monkeys adapting to an external force field. Neuron 30:593-607.

Louie K, Grattan LE, Glimcher PW (2011) Reward value-based gain control: divisive normalization in parietal cortex. J Neurosci 31:10627-10639.

Magat M, Brown C (2009) Laterality enhances cognition in Australian parrots. Proc Biol Sci 276:4155-4162.

Mandelblat-Cerf Y, Novick I, Paz R, Link Y, Freeman S, Vaadia E (2011) The neuronal basis of long-term sensorimotor learning. J Neurosci 31:300-313.

Marr D (1983) Vision: A Computational Investigation into the Human Representation and Processing of Visual Information: Henry Holt and Company.

Marsden CD, Merton PA, Morton HB (1971) Servo action and stretch reflex in human muscle and its apparent dependence on peripheral sensation. J Physiol 216:21P-22P.

Marsden CD, Merton PA, Morton HB (1972) Servo action in human voluntary movement. Nature 238:140-143.

Marsden CD, Merton PA, Morton HB (1976) Stretch reflex and servo action in a variety of human muscles. J Physiol 259:531-560.

Massion J (1984) Postural changes accompanying voluntary movements. Normal and pathological aspects. Hum Neurobiol 2:261-267.

Massion J, Ioffe M, Schmitz C, Viallet F, Gantcheva R (1999) Acquisition of anticipatory postural adjustments in a bimanual load-lifting task: normal and pathological aspects. Exp Brain Res 128:229-235.

Meunier S, Kwon J, Russmann H, Ravindran S, Mazzocchio R, Cohen L (2007) Spinal use-dependent plasticity of synaptic transmission in humans after a single cycling session. J Physiol 579:375-388.

Meyer BU, Röricht S, Gräfin von Einsiedel H, Kruggel F, Weindl A (1995) Inhibitory and excitatory interhemispheric transfers between motor cortical areas in normal humans and patients with abnormalities of the corpus callosum. Brain 118 (Pt 2):429-440.

Miall RC, Weir DJ, Wolpert DM, Stein JF (1993) Is the cerebellum a smith predictor? J Mot Behav 25:203-216.

Mieschke PE, Elliott D, Helsen WF, Carson RG, Coull JA (2001) Manual asymmetries in the preparation and control of goal-directed movements. Brain Cogn 45:129-140.

Miklosi A, Andrew RJ (1999) Right eye use associated with decision to bite in zebrafish. Behav Brain Res 105:199-205.

Miyawaki Y, Uchida H, Yamashita O, Sato MA, Morito Y, Tanabe HC, Sadato N, Kamitani Y (2008) Visual image reconstruction from human brain activity using a combination of multiscale local image decoders. Neuron 60:915-929.

Mochizuki H, Huang YZ, Rothwell JC (2004a) Interhemispheric interaction between human dorsal premotor and contralateral primary motor cortex. J Physiol 561:331-338.

Mochizuki H, Terao Y, Okabe S, Furubayashi T, Arai N, Iwata NK, Hanajima R, Kamakura K, Motoyoshi K, Ugawa Y (2004b) Effects of motor cortical stimulation on the excitability of contralateral motor and sensory cortices. Exp Brain Res 158:519-526.

Moritz CT, Perlmutter SI, Fetz EE (2008) Direct control of paralysed muscles by cortical neurons. Nature 456:639-642.

Morton SM, Lang CE, Bastian AJ (2001) Inter- and intra-limb generalization of adaptation during catching. Exp Brain Res 141:438-445.

Mussa-Ivaldi FA, Bizzi E (2000) Motor learning through the combination of primitives. Philos Trans R

Soc Lond B Biol Sci 355:1755-1769.

Mussa-Ivaldi FA, Giszter SF, Bizzi E (1994) Linear combinations of primitives in vertebrate motor control. Proc Natl Acad Sci U S A 91:7534-7538.

Mutha PK, Sainburg RL (2009) Shared Bimanual Tasks Elicit Bimanual Reflexes During Movement. J Neurophysiol 102:3142-3155.

Nakano S, Stillman B, Horvitz HR (2011) Replication-coupled chromatin assembly generates a neuronal bilateral asymmetry in C. elegans. Cell 147:1525-1536.

Needham R (1967) Right and left in Nyoro symbolic classification. Africa 37:425-452.

Netz J, Ziemann U, Hömberg V (1995) Hemispheric asymmetry of transcallosal inhibition in man. Exp Brain Res 104:527-533.

Ni Z, Gunraj C, Nelson AJ, Yeh IJ, Castillo G, Hoque T, Chen R (2009) Two phases of interhemispheric inhibition between motor related cortical areas and the primary motor cortex in human. Cereb Cortex 19:1654-1665.

Nichols TR, Houk JC (1973) Reflex compensation for variations in mechanical properties of a muscle. Science 181:182-184.

Nitsche MA, Seeber A, Frommann K, Klein CC, Rochford C, Nitsche MS, Fricke K, Liebetanz D, Lang N, Antal A, Paulus W, Tergau F (2005) Modulating parameters of excitability during and after transcranial direct current stimulation of the human motor cortex. J Physiol 568:291-303.

Nozaki D, Scott S (2009) Multi-compartment model can explain partial transfer of learning within the same limb between unimanual and bimanual reaching. Exp Brain Res 194:451-463.

Nozaki D, Kurtzer I, Scott S (2006) Limited transfer of learning between unimanual and bimanual skills within the same limb. Nat Neurosci 9:1364-1366.

Oda S, Moritani T (1995) Movement-related cortical potentials during handgrip contractions with special reference to force and electromyogram bilateral deficit. Eur J Appl Physiol Occup Physiol 72:1-5.

Ohki Y, Johansson RS (1999) Sensorimotor interactions between pairs of fingers in bimanual and unimanual manipulative tasks. Exp Brain Res 127:43-53.

Ohki Y, Edin BB, Johansson RS (2002) Predictions specify reactive control of individual digits in manipulation. J Neurosci 22:600-610.

Oliveira FT, Diedrichsen J, Verstynen T, Duque J, Ivry RB (2010) Transcranial magnetic stimulation of posterior parietal cortex affects decisions of hand choice. Proc Natl Acad Sci U S A 107:17751-17756.

Olshausen BA, Field DJ (1996) Emergence of simple-cell receptive field properties by learning a sparse code for natural images. Nature 381:607-609.

Osu R, Hirai S, Yoshioka T, Kawato M (2004) Random presentation enables subjects to adapt to two opposing forces on the hand. Nat Neurosci 7:111-112.

Oswald AM, Schiff ML, Reyes AD (2006) Synaptic mechanisms underlying auditory processing. Curr Opin Neurobiol 16:371-376.

Overduin SA, d'Avella A, Roh J, Bizzi E (2008) Modulation of muscle synergy recruitment in primate grasping. J Neurosci 28:880-892.

Overduin SA, d'Avella A, Carmena JM, Bizzi E (2012) Microstimulation activates a handful of muscle synergies. Neuron 76:1071-1077.

Padoa-Schioppa C, Li CS, Bizzi E (2002) Neuronal correlates of kinematics-to-dynamics transformation in the supplementary motor area. Neuron 36:751-765.

Padoa-Schioppa C, Li C, Bizzi E (2004) Neuronal activity in the supplementary motor area of monkeys adapting to a new dynamic environment. J Neurophysiol 91:449-473.

Palmer LM, Schulz JM, Murphy SC, Ledergerber D, Murayama M, Larkum ME (2012) The cellular basis of GABA(B)-mediated interhemispheric inhibition. Science 335:989-993.

Perez MA, Cohen LG (2009) Interhemispheric inhibition between primary motor cortices: what have we learned? J Physiol 587:725-726.

Peters M, Durding BM (1978) Handedness measured by finger tapping: a continuous variable. Can J Psychol 32:257-261.

Petersen P, Petrick M, Connor H, Conklin D (1989) Grip strength and hand dominance: challenging the 10% rule. Am J Occup Ther 43:444-447.

Pistohl T, Schulze-Bonhage A, Aertsen A, Mehring C, Ball T (2012) Decoding natural grasp types from human ECoG. Neuroimage 59:248-260.

Poggio T, Girosi F (1990) Regularization algorithms for learning that are equivalent to multilayer networks. Science 247:978-982.

Poggio T, Bizzi E (2004) Generalization in vision and motor control. Nature 431:768-774.

Pouget A, Sejnowski TJ (1997) Spatial transformations in the parietal cortex using basis functions. J Cogn Neurosci 9:222-237.

Pouget A, Dayan P, Zemel R (2000) Information processing with population codes. Nat Rev Neurosci 1:125-132.

Pruszynski JA, Kurtzer I, Nashed JY, Omrani M, Brouwer B, Scott SH (2011) Primary motor cortex underlies multi-joint integration for fast feedback control. Nature 478:387-390.

Rack PMH, Westbury DR (1969) Effects of length and stimulus rate on tension in isometric cat soleus muscle. J Physiol 204:443-&.

Rack PMH, Westbury DR (1974) Short-range stiffness of active mammalian muscle and its effect on mechanical properties. J Physiol 240:331-350.

Rakic P, Yakovlev PI (1968) Development of the corpus callosum and cavum septi in man. J Comp Neurol 132:45-72.

Richardson AG, Lassi-Tucci G, Padoa-Schioppa C, Bizzi E (2008) Neuronal activity in the cingulate

motor areas during adaptation to a new dynamic environment. J Neurophysiol 99:1253-1266.

Ridding MC, Brouwer B, Nordstrom MA (2000) Reduced interhemispheric inhibition in musicians. Exp Brain Res 133:249-253.

Rogers LJ, Vallortigara G (2008) From Antenna to Antenna: Lateral Shift of Olfactory Memory Recall by Honeybees. PloS One 3.

Roh J, Cheung VC, Bizzi E (2011) Modules in the brain stem and spinal cord underlying motor behaviors. J Neurophysiol 106:1363-1378.

Rokni U, Steinberg O, Vaadia E, Sompolinsky H (2003) Cortical representation of bimanual movements. J Neurosci 23:11577-11586.

Roy TA, Ruff CB, Plato CC (1994) Hand dominance and bilateral asymmetry in the structure of the second metacarpal. Am J Phys Anthropol 94:203-211.

Sainburg RL (2010) Lateralization of Goal-Directed Movement. In: Vision and Goal-Directed Movement, pp 219-288. Illinois, US: Human Kinetics.

Salinas E, Sejnowski TJ (2001) Gain modulation in the central nervous system: where behavior, neurophysiology, and computation meet. Neuroscientist 7:430-440.

Schabowsky CN, Hidler JM, Lum PS (2007) Greater reliance on impedance control in the nondominant arm compared with the dominant arm when adapting to a novel dynamic environment. Exp Brain Res 182:567-577.

Schaefer SY, Haaland KY, Sainburg RL (2007) Ipsilesional motor deficits following stroke reflect hemispheric specializations for movement control. Brain 130:2146-2158.

Scheidt RA, Reinkensmeyer DJ, Conditt MA, Rymer WZ, Mussa-Ivaldi FA (2000) Persistence of motor adaptation during constrained, multi-joint, arm movements. J Neurophysiol 84:853-862.

Schlaug G, Jäncke L, Huang Y, Staiger JF, Steinmetz H (1995) Increased corpus callosum size in musicians. Neuropsychologia 33:1047-1055.

Schlerf J, Ivry RB, Diedrichsen J (2012) Encoding of Sensory Prediction Errors in the Human Cerebellum. J Neurosci 32:4913-4922.

Schmitz C, Assaiante C (2002) Developmental sequence in the acquisition of anticipation during a new co-ordination in a bimanual load-lifting task in children. Neurosci Lett 330:215-218.

Schmitz C, Martin N, Assaiante C (2002) Building anticipatory postural adjustment during childhood: a kinematic and electromyographic analysis of unloading in children from 4 to 8 years of age. Exp Brain Res 142:354-364.

Scott SH (2003) The role of primary motor cortex in goal-directed movements: insights from neurophysiological studies on non-human primates. Curr Opin Neurobiol 13:671-677.

Seeley WW, Menon V, Schatzberg AF, Keller J, Glover GH, Kenna H, Reiss AL, Greicius MD (2007) Dissociable intrinsic connectivity networks for salience processing and executive control. J Neurosci 27:2349-2356.

Serrien DJ, Ivry RB, Swinnen SP (2006) Dynamics of hemispheric specialization and integration in the context of motor control. Nat Rev Neurosci 7:160-166.

Shadmehr R (2004) Generalization as a behavioral window to the neural mechanisms of learning internal models. Hum Mov Sci 23:543-568.

Shadmehr R, Mussa-Ivaldi FA (1994) Adaptive representation of dynamics during learning of a motor task. J Neurosci 14:3208-3224.

Shadmehr R, Wise SP (2005) The computational neurobiology of reaching and pointing: a foundation for motor learning: MIT Press.

Shadmehr R, Krakauer JW (2008) A computational neuroanatomy for motor control. Exp Brain Res 185:359-381.

Shergill SS, Bays PM, Frith CD, Wolpert DM (2003) Two eyes for an eye: the neuroscience of force escalation. Science 301:187.

Sherrington CS (1906) The Integrative action of the nervous system: Yale University Press.

Sherrington CS (1965) Inhibition as a Coordinative Factor. In: Nobel Lectures, Physiology or Medicine 1922-1941. Amsterdam: Elsevier Publishing Company.

Shimoda K, Nagasaka Y, Chao ZC, Fujii N (2012) Decoding continuous three-dimensional hand trajectories from epidural electrocorticographic signals in Japanese macaques. J Neural Eng 9:036015.

Shinohara Y, Hosoya A, Yamasaki N, Ahmed H, Hattori S, Eguchi M, Yamaguchi S, Miyakawa T, Hirase H, Shigemoto R (2012) Right-hemispheric dominance of spatial memory in split-brain mice. Hippocampus 22:117-121.

Simon JR, Wolf JD (1963) Choice reaction-time as a function of angular stimulus-response correspondence and age. Ergonomics 6:99-105.

Sing GC, Joiner WM, Nanayakkara T, Brayanov JB, Smith MA (2009) Primitives for motor adaptation reflect correlated neural tuning to position and velocity. Neuron 64:575-589.

Sisti HM, Geurts M, Gooijers J, Heitger MH, Caeyenberghs K, Beets IAM, Serbruyns L, Leemans A, Swinnen SP (2012) Microstructural organization of corpus callosum projections to prefrontal cortex predicts bimanual motor learning. Learning & Memory 19:351-357.

Smith MA, Ghazizadeh A, Shadmehr R (2006) Interacting adaptive processes with different timescales underlie short-term motor learning. PLoS Biol 4:e179.

Solgi M, Liu T, Weng J (2013) A computational developmental model for specificity and transfer in perceptual learning. J Vis 13.

Soteropoulos DS, Perez MA (2011) Physiological changes underlying bilateral isometric arm voluntary contractions in healthy humans. J Neurophysiol 105:1594-1602.

Soteropoulos DS, Edgley SA, Baker SN (2011) Lack of evidence for direct corticospinal contributions to control of the ipsilateral forelimb in monkey. J Neurosci 31:11208-11219.

Sridharan D, Levitin DJ, Menon V (2008) A critical role for the right fronto-insular cortex in switching between central-executive and default-mode networks. Proc Natl Acad Sci U S A 105:12569-12574.

Stagg CJ, Bachtiar V, Johansen-Berg H (2011a) The role of GABA in human motor learning. Curr Biol 21:480-484.

Stagg CJ, Best JG, Stephenson MC, O'Shea J, Wylezinska M, Kincses ZT, Morris PG, Matthews PM, Johansen-Berg H (2009) Polarity-sensitive modulation of cortical neurotransmitters by transcranial stimulation. J Neurosci 29:5202-5206.

Stagg CJ, Bestmann S, Constantinescu AO, Moreno LM, Allman C, Mekle R, Woolrich M, Near J, Johansen-Berg H, Rothwell JC (2011b) Relationship between physiological measures of excitability and levels of glutamate and GABA in the human motor cortex. J Physiol 589:5845-5855.

Stout D (2011) Stone toolmaking and the evolution of human culture and cognition. Philos Trans R Soc Lond B Biol Sci 366:1050-1059.

Stout D, Chaminade T (2012) Stone tools, language and the brain in human evolution. Philos Trans R Soc Lond B Biol Sci 367:75-87.

Stout D, Toth N, Schick K, Chaminade T (2008) Neural correlates of Early Stone Age toolmaking: technology, language and cognition in human evolution. Philos Trans R Soc Lond B Biol Sci 363:1939-1949.

Strick PL (2002) Stimulating research on motor cortex. Nat Neurosci 5:714-715.

Sun T, Walsh CA (2006) Molecular approaches to brain asymmetry and handedness. Nat Rev Neurosci 7:655-662.

Swinnen SP (2002) Intermanual coordination: from behavioural principles to neural-network interactions. Nat Rev Neurosci 3:348-359.

Swinnen SP, Wenderoth N (2004) Two hands, one brain: cognitive neuroscience of bimanual skill. Trends Cogn Sci 8:18-25.

Tanaka H, Sejnowski TJ, Krakauer JW (2009) Adaptation to visuomotor rotation through interaction between posterior parietal and motor cortical areas. J Neurophysiol 102:2921-2932.

Tapley SM, Bryden MP (1985) A group test for the assessment of performance between the hands. Neuropsychologia 23:215-221.

Tcheang L, Bays PM, Ingram JN, Wolpert DM (2007) Simultaneous bimanual dynamics are learned without interference. Exp Brain Res 183:17-25.

Theorin A, Johansson RS (2007) Zones of bimanual and unimanual preference within human primary sensorimotor cortex during object manipulation. Neuroimage 36 Suppl 2:T2-T15.

Theorin A, Johansson RS (2010) Selection of prime actor in humans during bimanual object manipulation. J Neurosci 30:10448-10459.

Thompson AK, Chen XY, Wolpaw JR (2009) Acquisition of a simple motor skill: task-dependent adaptation plus long-term change in the human soleus H-reflex. J Neurosci 29:5784-5792.

Thompson AK, Chen XY, Wolpaw JR (2012) Soleus H-reflex operant conditioning changes the H-reflex recruitment curve. Muscle Nerve.

Thoroughman KA, Shadmehr R (1999) Electromyographic correlates of learning an internal model of reaching movements. J Neurosci 19:8573-8588.

Thoroughman KA, Shadmehr R (2000) Learning of action through adaptive combination of motor primitives. Nature 407:742-747.

Ting LH, Macpherson JM (2005) A limited set of muscle synergies for force control during a postural task. J Neurophysiol 93:609-613.

Todor JI, Doane T (1977) Handedness classification: preference versus proficiency. Percept Mot Skills 45:1041-1042.

Todor JI, Kyprie PM (1980) Hand differences in the rate and variability of rapid tapping. J Mot Behav 12:57-62.

Todor JI, Cisneros J (1985) Accommodation to increased accuracy demands by the right and left hands. J Mot Behav 17:355-372.

Todorov E, Jordan MI (2002) Optimal feedback control as a theory of motor coordination. Nat Neurosci 5:1226-1235.

Toga AW, Thompson PM (2003) Mapping brain asymmetry. Nat Rev Neurosci 4:37-48.

Tresch MC, Saltiel P, Bizzi E (1999) The construction of movement by the spinal cord. Nat Neurosci 2:162-167.

Udupa K, Ni Z, Gunraj C, Chen R (2010) Effect of long interval interhemispheric inhibition on intracortical inhibitory and facilitatory circuits. J Physiol 588:2633-2641.

Ugawa Y, Hanajima R, Kanazawa I (1993) Interhemispheric facilitation of the hand area of the human motor cortex. Neurosci Lett 160:153-155.

Ung RV, Imbeault MA, Ethier C, Brizzi L, Capaday C (2005) On the potential role of the corticospinal tract in the control and progressive adaptation of the soleus h-reflex during backward walking. J Neurophysiol 94:1133-1142.

Vallortigara G (2006) The evolutionary psychology of left and right: costs and benefits of lateralization. Dev Psychobiol 48:418-427.

van der Fits IB, Klip AW, van Eykern LA, Hadders-Algra M (1998) Postural adjustments accompanying fast pointing movements in standing, sitting and lying adults. Exp Brain Res 120:202-216.

van der Knaap LJ, van der Ham IJ (2011) How does the corpus callosum mediate interhemispheric transfer? A review. Behav Brain Res 223:211-221.

Van Opstal AJ, Hepp K, Suzuki Y, Henn V (1995) Influence of eye position on activity in monkey superior colliculus. J Neurophysiol 74:1593-1610.

Viallet F, Massion J, Massarino R, Khalil R (1992) Coordination between posture and movement in a bimanual load lifting task: putative role of a medial frontal region including the supplementary motor area. Exp Brain Res 88:674-684.

Wagner MJ, Smith MA (2008) Shared internal models for feedforward and feedback control. J Neurosci 28:10663-10673.

Wainscott SK, Donchin O, Shadmehr R (2005) Internal models and contextual cues: encoding serial order and direction of movement. J Neurophysiol 93:786-800.

Wang J, Sainburg RL (2004) Interlimb transfer of novel inertial dynamics is asymmetrical. J Neurophysiol 92:349-360.

Wang W, Chan SS, Heldman DA, Moran DW (2010) Motor cortical representation of hand translation and rotation during reaching. J Neurosci 30:958-962.

Wang Y, Pillai S, Wolpaw JR, Chen XY (2009) H-reflex down-conditioning greatly increases the number of identifiable GABAergic interneurons in rat ventral horn. Neurosci Lett 452:124-129.

White O, Diedrichsen J (2010) Responsibility assignment in redundant systems. Curr Biol 20:1290-1295.

Wiestler T, McGonigle DJ, Diedrichsen J (2011) Integration of sensory and motor representations of single fingers in the human cerebellum. J Neurophysiol 105:3042-3053.

Williams J, Spurlock G, McGuffin P, Mallet J, Nöthen MM, Gill M, Aschauer H, Nylander PO, Macciardi F, Owen MJ (1996) Association between schizophrenia and T102C polymorphism of the 5-hydroxytryptamine type 2a-receptor gene. European Multicentre Association Study of Schizophrenia (EMASS) Group. Lancet 347:1294-1296.

Wilson D (1891) The right hand: left-handedness: Macmillan.

Wolpaw JR (1987) Operant conditioning of primate spinal reflexes: the H-reflex. J Neurophysiol 57:443-459.

Wolpaw JR, O'Keefe JA (1984) Adaptive plasticity in the primate spinal stretch reflex: evidence for a two-phase process. J Neurosci 4:2718-2724.

Wolpaw JR, Lee CL (1989) Memory traces in primate spinal cord produced by operant conditioning of H-reflex. J Neurophysiol 61:563-572.

Wolpaw JR, Tennissen AM (2001) Activity-dependent spinal cord plasticity in health and disease. Annu Rev Neurosci 24:807-843.

Wolpert DM, Kawato M (1998) Multiple paired forward and inverse models for motor control. Neural Netw 11:1317-1329.

Wolpert DM, Ghahramani Z, Jordan MI (1995) An internal model for sensorimotor integration. Science 269:1880-1882.

Wolpert DM, Miall RC, Kawato M (1998) Internal models in the cerebellum. Trends Cogn Sci 2:338-347.

Wolpert DM, Diedrichsen J, Flanagan JR (2011) Principles of sensorimotor learning. Nat Rev Neurosci 12:739-751.

Wolpert L (2003) Causal belief and the origins of technology. Philos Transact A Math Phys Eng Sci 361:1709-1719.

Woodworth RS (1899) The accuracy of voluntary movement. Psychol Rev 3:1-114.

Wu Y, Kawakami R, Shinohara Y, Fukaya M, Sakimura K, Mishina M, Watanabe M, Ito I, Shigemoto R (2005) Target-cell-specific left-right asymmetry of NMDA receptor content in schaffer collateral synapses in epsilon1/NR2A knock-out mice. J Neurosci 25:9213-9226.

Xiao J, Padoa-Schioppa C, Bizzi E (2006) Neuronal correlates of movement dynamics in the dorsal and ventral premotor area in the monkey. Exp Brain Res 168:106-119.

Xu T, Yu X, Perlik AJ, Tobin WF, Zweig JA, Tennant K, Jones T, Zuo Y (2009) Rapid formation and selective stabilization of synapses for enduring motor memories. Nature 462:915-919.

Yajima Y, Hayashi Y (1990) GABAergic inhibition upon auditory response properties of neurons in the dorsal cochlear nucleus of the rat. Exp Brain Res 81:581-588.

Yanagisawa T, Hirata M, Saitoh Y, Goto T, Kishima H, Fukuma R, Yokoi H, Kamitani Y, Yoshimine T (2011) Real-time control of a prosthetic hand using human electrocorticography signals. J Neurosurg 114:1715-1722.

Yanagisawa T, Hirata M, Saitoh Y, Kishima H, Matsushita K, Goto T, Fukuma R, Yokoi H, Kamitani Y, Yoshimine T (2012) Electrocorticographic control of a prosthetic arm in paralyzed patients. Ann Neurol 71:353-361.

Yokoi A, Hirashima M, Nozaki D (2011) Gain field encoding of the kinematics of both arms in the internal model enables flexible bimanual action. J Neurosci 31:17058-17068.

Zatorre RJ, Fields RD, Johansen-Berg H (2012) Plasticity in gray and white: neuroimaging changes in brain structure during learning. Nat Neurosci 15:528-536.

Ziemann U, Hallett M (2001) Hemispheric asymmetry of ipsilateral motor cortex activation during unimanual motor tasks: further evidence for motor dominance. Clin Neurophysiol 112:107-113.